Experimental characterization of water sorption and transport properties of polymer electrolyte membranes for fuel cells

Libeth Maldonado Sánchez

Université de Lorraine
Ecole doctorale EMMA – Energie, Mécanique, Matériaux
Centre National de la Recherche Scientifique – CNRS
Région Lorraine

THESE

présentée pour l'obtention du titre de

Docteur de l'Université de Lorraine

spécialité : Mécanique et Energétique

par

Libeth Maldonado Sánchez

Directeur de thèse: Olivier Lottin

Experimental characterization of water sorption and transport properties of polymer electrolyte membranes for fuel cells

Caractérisation expérimentale des propriétés de sorption de l'eau et de transport des membranes de piles à combustible

---

Soutenance publique prévue le 26 Novembre 2012 devant le jury constitué de:

Rapporteurs:	M. Lionel Flandin	Professeur, LEPMI-LMOPS, Le Bourget-du Lac
	Mme. Sandrine Lyonnard	Chercheur, CEA, Grenoble
Examinateurs:	Mme. Deborah Jones	Directrice de Recherche, CNRS, Montpellier
	M. Edward M. Sabolsky	Professeur, West Virginia University, USA
	M. Jean-Christophe Perrin	Maître de Conférences, LEMTA-UL, Nancy
	M. Olivier Lottin	Professeur, LEMTA-UL, Nancy
	M. Jérôme Dillet	Ingénieur de Recherche, LEMTA-UL, Nancy

Laboratoire d'Energétique et de Mécanique Théorique et Appliquée – LEMTA
UMR 7563 CNRS Université de Lorraine
54500 Vandoeuvre lès Nancy, France.

Introduction

Proton exchange membrane fuel cells (PEMFCs) are considered as one of the most promising energy conversion systems for powering all kind of vehicles. In the recent years, the focus was put on the fuel cells applications since they promise to be a solution to the energy problems. However, their main components (proton exchange membrane, gas diffusion electrodes, bipolar plates, etc) are still the object of intense fundamental and technological research, especially for durability and cost issues. One of the most interesting challenges to be addressed concerns the proton exchange membrane, which is the heart of the fuel cell.

The most commonly used proton exchange membranes in fuel cells are perfluorosulfonic acid (PFSA) membranes. These membranes are composed of a polytetrafluoroethylene backbone and perfluorinated pendant side chains terminated by sulfonic ionic (-RSO_3-) functional groups responsible for its good proton conductivity and water sorption properties when exposed to liquid water or to a humid environment. The adsorbed water serves as a transport medium for protons and gives the membrane good ionic conductivity properties during the operation of the PEMFC. Among the PFSA membranes, the most studied and commercially successful is Nafion®, an ionomer developed and manufactured by DuPont de Nemours & Co since 1960s.

The properties of Nafion membranes used in polymer electrolyte fuel cells are important for the performance and durability, the ionic conductivity and the mechanical response representing their most important ones.

A large quantity of research articles has been devoted to the characterization of Nafion membrane properties: water uptake, water diffusion, ionic conductivity and mechanical properties. However, the direct comparison between literature results is hardly possible because the ranges of experimental conditions (relative humidity and temperature) are often limited and differ from one author to the other. Moreover, the pre-treatments applied to the membrane are sometimes extremely different since no standardization of these protocols has been defined. Though, several studies have demonstrated that Nafion properties can be sensitive to pre-treatments, and more specifically to its thermal history.

Starting from these observations, we decided to characterize sorption, proton conductivity, water self-diffusion and the mechanical properties of Nafion using simple and reproducible experimental protocols described in Chapter 2. Our primary objective is to make available a wide range of experimental data (presented in Chapter 3) that can be used either for simulation or modelling of processes in PEMFC or with a more fundamental objective, in view of getting a deeper understanding on the thermodynamics of sorption and transport phenomena in Nafion.

The literature also shows that the Nafion properties can present certain instabilities when exposed to constant relative humidity and temperature conditions over long periods of time. These instabilities are manifested by a decrease of the water sorption, associated with a drop of the proton conductivity and an increase of the rigidity of the polymer. This long-term exposure effect has been named "hygrothermal aging" and a mechanism based on the formation of sulfonic anhydrides (RSO_2-O-SO_2R) was proposed to explain it. In Chapter 4, we extend this study by exploring a wide range of aging conditions on membranes with different pre-treatments.

For some fuel cell applications (*e.g.* automotive), the lifetime of Nafion is shorter at high temperature because of phenomena such as shrinkage and swelling induced by hydration/dehydration cycles. As a consequence, numerous attempts have been made to develop alternative membranes operating at temperatures higher than 80°C. These membranes must demonstrate good proton conductivity and thermo-mechanical stability with a limited gas humidification. The Nafion-zirconia composite (prepared by *in-situ* growth of inorganic nanoparticles of zirconium dioxide (ZrO_2) in Nafion membrane) developed by the Functional Ceramics Group at West Virginia University, USA, is a possible candidate as an alternative proton exchange membrane. In Chapter 5, we present preliminary fuel cell tests with composite membrane carried out at high temperature and low relative humidity at West Virginia University. We observed from the results that incorporating nanoparticles does not improve the fuel cell voltage nor the conductivity of the membranes. Based on these statements, we performed systematic water sorption, proton conductivity, and stress-strain measurements on Nafion/zirconia composite membranes. Our primary objective is to understand why these Nafion composite membranes do not perform better than the original ones, especially at high temperature and low relative humidity.

Acknowledgements

This thesis would not have been possible without the guidance and the help of several individuals who in one way or another contributed and extended their valuable assistance in the preparation and completion of this study.

It is with immense gratitude that I acknowledge the support and help of my PhD director Professor Olivier Lottin and my advisor Assistant Professor Jean-Christophe Perrin, who have been guiding my research work during these years. I have learned from them not only the knowledge on PEMFC, but also the most critical thinking towards scientific research.

The former and current group members of the fuel cell group, in particular Engineer Jérôme Dillet for his unconditional help and precise advices in the assembly of the conductivity cell, Engineer Sébastien Leclerc for his invaluable assistance in doing the nuclear magnetic resonance measurements, and Assistant Professor Gaël Maranzana for his support and inspiring ideas.

Professor Stéphane André, in charge of the thermomechanics and rheology of polymer materials group, for his scientific contributions and his assistance at the rheology facilities.

Former students: Elise Souaillat, Pierre-Alain Dandonneau, Pierre Guiganti, and Hacene Si Hadj Mohand for their contributions to this work.

I would also like to thank all the members of LEMTA for their friendliness and kindness. A special thank to Edith Lang for her unlimited assistance and generosity.

Dr. Edward Sabolsky, Professor at West Virginia University in USA, for his collaboration that benefits my vision of scientific research.

I owe my greatest gratefulness to my mom, Ana Rosa, whose eternal love and guiding light are always present from above, regardless the time or the sky.

I want to thank my dad, Ramón, for his unconditional encouragement, guidance and support from the initial to the final of this journey. Nothing I learned is without my parent's help.

Though being apart for years, to my sister Rosalba and my little nice Camelia, who kept supporting and caring about me during my PhD experience. Thanks.

I am heartily thankful to James, who has accompanied, delighted, and motivated me during my PhD life. This project and my time in France have been fulfilled with beautiful and unforgettable moments because of him.

Lastly, I offer my regards and blessings to all of those from Venezuela and France who supported me in any respect throughout the project.

I have been blessed to have the opportunity to complete this journey in such a beautiful country.

Contents

Chapter 1

Literature review on the properties of Proton Exchange Membranes

In this chapter, an overview of fuel cells and proton exchange membrane fuel cells (PEMFCs) is presented, followed by a review of the current electrolyte membranes. The important properties of Nafion membranes are then described in relation with the morphology of the polymer. The influence of the membrane pre-treatment and aging is discussed. Finally, Nafion-based composite membranes, possible alternative to perfluorosulfonic acid (PFSA) electrolyte membranes, are presented at the end of the chapter.

1 Fuel cells

Fuel cells offer the promise of low-polluting, highly efficient energy conversion, with devices designed to generate power as long as fuel is supplied. In their most general form, fuel cells use hydrogen and oxygen from air to produce water and electricity. With the goal of using environmentally friendly primary energy sources that do not rely on fossil fuels, fuel cells have become the leading candidate to replace internal combustion engines. Fuel cells first came out as onboard power supplies for spaceships. After evolving for several decades, fuel cells become now available for some transport and portable applications. Nowadays, hundredth of fuel cells powered test vehicles and tenth of hydrogen fuelling stations are already in use all over the world [1, 2, 3, 4, 5].

Fuel cell powered systems have important advantages compared to other potential energy converters (*e.g.* electric vehicles) such as their independence from the electric grid [5, 6, 7]. Moreover, the hydrogen fuel has a higher energy mass density than lithium or alkaline batteries do.

Hydrogen can be produced starting from traditional fossil fuels, biomass, solar or wind power [1]. Along with all the other kinds of renewable energy sources, fuel cells can contribute to resolving the energy and global warming issues. Table 1.1 lists the type of fuel cells classified by their electrolyte and operating temperature [5, 8, 9].

Table 1.1: Different types of fuel cells.

Fuel cells	Electrolyte (working temperature)	Fuels	Applications
Alkaline fuel cell (AFC)	Aqueous KOH (< 100°C)	Hydrogen	Spaceships Electricity storage
Proton exchange membrane fuel cell (PEMFC)	Polymer membranes (< 0°C – 80°C)	Hydrogen	Vehicles Portable devices
Direct methanol fuel cell (DMFC)	Polymer membranes (60 – 100°C)	Methanol	Portable devices
Solid oxide fuel cell (SOFC)	Ion conducting ceramics (600 – 1000°C)	Reformed hydrocarbons	Stationary power systems Power plants
Phosphoric acid fuel cell (PAFC)	Liquid H_3PO_4 (175 – 200°C)	Hydrogen	Stationary power systems Vehicles
Molten carbonate fuel cell (MCFC)	Metal carbonates (600 – 1000°C)	Natural gas Biogas Coal	Power plants

1.1 Basic principles of fuel cells

Fuel cells are electrochemical cells in which the free enthalpy (Gibbs energy) of the electrochemical reaction between a fuel, such as hydrogen, and an oxidant, such as oxygen is converted into electrical energy [1, 2, 3, 4, 5, 6, 7, 8, 9]. The free enthalpy change of an electrochemical reaction $\overline{\Delta g_f}$ is related to the cell thermodynamic voltage of the cell (E), *via*:

$$\overline{\Delta g_f} = -nFE \qquad \text{Eq 1}$$

where n is the number of electrons involved in the reaction and F is the Faraday constant. The theoretical voltage of the cell is equal to the difference between the thermodynamic equilibrium potential of the two electrochemical half reactions occurring at each electrode (cathode, E_c and anode, E_a), in the absence of a current flow:

$$E = E_c - E_a \qquad \text{Eq 2}$$

For the case of a hydrogen/oxygen fuel cell, the anode half reaction is the direct oxidation of hydrogen and the cathode reaction is the oxygen reduction. The overall reaction is:

$H_2 + 1/2\ O_2 \longrightarrow H_2O$ with $\overline{\Delta g_f^0}$ = – 237 kJ/mol Eq 3

The equilibrium cell voltage in standard conditions is:

$$E_0 = \frac{-\overline{\Delta g_f^0}}{nF} = 1.23\,\mathrm{V} \qquad \text{Eq 4}$$

The current work focuses on polymer electrolyte membrane fuel cells (PEMFCs). This type of fuel cell usually operates at moderate temperatures, around 80°C – 90°C, and uses a polymer-based electrolyte membrane (PEM) to separate hydrogen and air and to conduct protons from the anode to the cathode. The basic principles of PEMFC are presented in the following section.

1.2 Principles of the proton exchange membrane fuel cell

PEM fuel cells are considered today as the most promising means for powering all kind of vehicles and some portable devices. Theoretically, PEM fuel cells can reach at least twice the efficiency of internal combustion engines with much less pollutant emissions [10]. Moreover, the high energy mass density of hydrogen makes PEMFCs more appealing than battery systems [3]. In addition, PEM fuel cells are suitable for the automotive industry thanks to its high power density (in term of the volume of the fuel cell).

Figure 1.1 shows the main components of a PEM fuel cell. The heart of the fuel cell consists of two electrodes and an electrolyte, forming the membrane electrodes assembly (MEA). During operation, hydrogen is supplied to the anode, while the oxidant (*e.g.* oxygen or air) is supplied to the cathode. At the anode, hydrogen molecules are split into protons and electrons thanks to a catalyst. The electrons pass though the external circuit, while protons flow through the electrolyte and react with oxygen at the cathode.

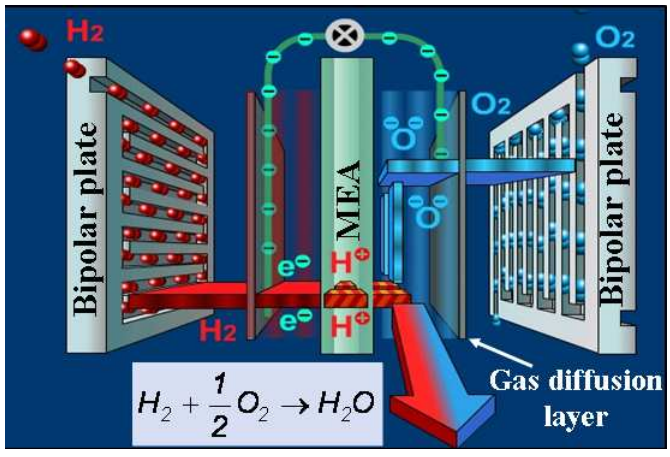

Figure 1.1: Principle of the proton exchange membrane fuel cell.

The electrochemical reactions occurring at each electrode of a PEM fuel cell are recalled below [5]:

At the anode, hydrogen is oxidized to liberate two electrons and two protons:

$$H_2 \longrightarrow 2\,H^+ + 2\,e^- \qquad \text{Eq 5}$$

At the cathode, oxygen is reduced:

$$1/2\,O_2 + 2\,H^+ + 2\,e^- \longrightarrow H_2O \qquad \text{Eq 6}$$

Which gives the overall reaction:

$$H_2 + 1/2\,O_2 \longrightarrow H_2O \qquad \text{Eq 7}$$

The catalyst (usually platinum, Pt) is used under the form of carbon supported nanoparticles. These nanoparticles must have two conducting pathways: an electronic pathway offered by the carbon support to the current collector, and a protonic pathway, offered by the ionomer (in the catalyst layer) to the electrolyte [11].

Up to now, the best polymer membranes for PEM fuel cells are perfluorosulfonic acid (PFSA) membranes because of their high ionic conductivity and chemical stability in reducing and oxidizing environments. The most currently used material is Nafion®, commercialized by DuPont de Nemours & Co. for about 40 years. The main issue with these PFSA membranes is the need of a high hydration to obtain a good ionic conductivity: as a consequence the operation temperature of fuel cells is limited around 80 °C – 90°C [12]. The structure and the properties of Nafion® are described in Section 2.

An assemblage is required between the two conducting electrodes and the proton exchange membrane. This membrane electrode assembly (MEA) is part of the basic unit of the PEM fuel cell to maintain a good three-phase interface between the reactant gases, electrical conductivity (catalyst), and ion conductivity (ion conducting polymer).

In addition to a membrane and two electrodes, MEA also includes gas diffusion layers (GDLs), the GDLs are generally porous gas diffusion layers located between the electrodes and the bipolar plates to ensure the supply of the reactant gases to the active zones where the metal catalyst (usually platinum) is in contact with the ionic and electronic conductor. They also facilitate the residual water from the MEA and heat conduction toward the bipolar plates [12].

The bipolar plates have to collect and conduct the current from the anode to the cathode side. These current-collector plates also serve as flow fields for the reactant gases. In addition, they often have to carry a cooling fluid through the fuel cell stack to control the fuel cell temperature

[9]. Generally, graphite is used to make the bipolar plates because this material is light, conductive, and not prone to corrosion in the fuel cell environment. However, graphite being extremely difficult to machine, most of the fuel cell makers develop metal or composite bipolar plates.

Sealing gaskets are placed between the bipolar plates and the MEA to prevent gas and coolant leakage. The typical sealing materials utilized in PEM fuel cells are fluorine rubber, ethylene propylene diene monomer rubber, and silicone [13].

The elements that form the PEMFC system are the object of intense fundamental and technological research, especially because of durability and low cost requirements [11, 12, 14]. A review of the main technical challenges is presented in the following section.

1.3 Technical challenges

Despite the fact that PEM fuel cells are very promising, they face a number of technical challenges such as hydrogen storage, water management and the need to reduce the cost and to improve the durability of their components [8, 9, 15, 16].

Most PEM fuel cell systems use hydrogen as fuel. Therefore a large-scale production and distribution infrastructure has to be developed to supply this hydrogen to the end-users. There are delicate engineering issues concerning hydrogen storage, mostly for onboard usage. Most of the time, hydrogen is stored in pure form, either liquefied or pressurized. Several metal hydrides have shown promising properties in term of storage capacity, without the energy losses associated with high pressure on liquid storage. However, these materials are limited by the slow kinetics of adsorption or desorption of hydrogen [17, 18].

To be commercially competitive, the cost of fuel cell vehicles should be comparable to that of traditional vehicles. Today, the estimated cost of a 1 kW fuel cell system is around 51 USD $ [19], which is far more expensive than internal combustion engines or even battery-powered engines. One of the main cost issue arises from the large amount of platinum ($\sim$ 1 mg/cm^2) used for catalytic reactions, in order to improve the total efficiency of the system [15]. It is difficult to reduce the Pt loading since it would cause an increase of the activation losses in the electrodes and a decrease of the cell performance. However, recent progresses have increased the surface area of Pt and decreased the loading below 0.2 mg/cm^2 [20]. On the other hand, the performance of Pt as catalyst suffers from contaminants in the hydrogen such as carbon monoxide (CO),

hydrogen sulfide (H_2S), and ammonia (NH_3). Currently, most of the hydrogen is produced from reformed natural gas and as a consequence, contaminant gases are present in the product hydrogen if no expensive purification technologies are used. Even a small amount of contaminants can be harmful to the catalyst layer [21]. Other issues such as corrosion of the catalyst carbon support and sintering of Pt particles also affect the durability of the catalyst layers [22, 23].

One of the most interesting challenges to be addressed in this research work concerns the proton exchange membrane. As mentioned before, the PEM is the heart of the fuel cell and must have a high conductivity and selectivity for proton transport, a good chemical, thermal and mechanical stability to endure the harsh acidic environment and repeated operation cycles. The most used PEM membrane is Nafion®. Though this membrane exhibits a better stability than many alternative electrolyte polymers, Nafion® shows gradual chemical and physical degradation over a period of operation [8, 14, 24]. For this type of membranes, the degree of hydration strongly influences the physical and the mechanical properties: the proton conductivity is dramatically enhanced by hydration, and the mechanical properties of the membrane are directly linked to the water sorption. As a consequence, degradation and aging phenomena occurring in the PEM membranes represent critical issues to improve the performance and lifetime of fuel cell system.

It is widely accepted that a sufficient water content is necessary to maintain a good proton conductivity of Nafion membrane [25, 26, 27, 28]. This creates difficulties in the water management during fuel cell operation. Water management includes the control of water and gas flows in the fuel cell system, in particular in the gas diffusion layers. Multiple channels are machined into the bipolar plate to ensure sufficient distribution of fuel and oxygen (or air) to the reaction on the electrodes, and to facilitate the flow of product water. Water that accumulates at the cathode has to be removed quickly, otherwise it will block the path of oxygen, which is called “flooding” [29, 30]. As a result, the current density of the fuel cell will decrease (see Figure 1.2).

The temperature is also an important parameter that may bring difficulties for supplying water to the fuel cell. The working temperature of a PEM fuel cell is usually maintained around 80°C - 90°C. At higher temperatures, the PEM membrane dehydrates, loses its conductivity properties and may suffer from mechanical damage [31]. On the other hand, higher working temperatures are favorable to the kinetics of the electrochemical reactions and may improve the tolerance of platinum (Pt) to contaminants. Various solutions to increase the membrane working temperature under low humidity conditions have been proposed and numerous studies have

been performed on the fabrication and characterization on new electrolyte materials [32, 33, 34, 35, 36, 37, 38, 39, 40, 31, 41]. The following section describes a wide selection of electrolyte materials that are suitable for PEMFC systems.

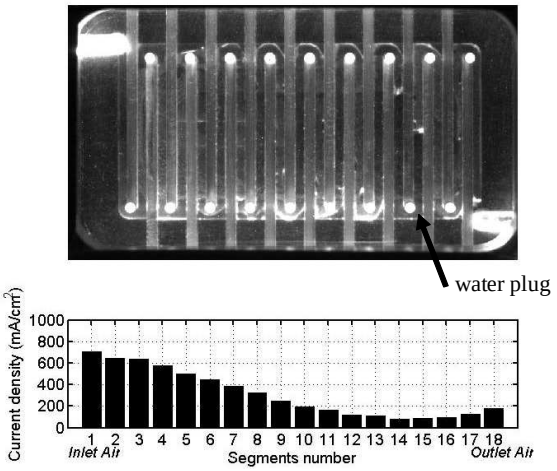

Figure 1.2: Top: formation and evolution of water plug in the air channel (cathode side) of a segmented fuel cell. Bottom: the corresponding local current densities [42].

1.4 Proton exchange membranes for fuel cells

Today, the development of new membranes is the object of intense research. The synthesis of new membranes can be achieved by varying the chemistry of polymers and/or by making processes, such as extrusion, casting, impregnation, radiation grafting or plasma polymerisation [43, 44, 45]. Membranes are classified according to their chemical composition and working temperatures. Some of them are briefly presented in this section.

1.4.1 Perfluorosulfonic acid (PFSA) membranes

As mentioned above, PFSA membranes are the most used electrolytes in PEMFC. PFSA membranes such as Nafion® are composed of a polytetrafluoroethylene (PTFE) backbone and perfluorinated pendant side chains terminated by sulfonic ionic functional groups [46]. Other PFSA based membranes from Fumatech, Dow Chemical, and Asahi Glass are also used and investigated. The main variations among the four types of membranes are in their pendant side chain lengths [32, 47]. The membranes developed by Dow Chemical differ from Nafion® by a shorter side chain carrying the sulfonic group with a lower equivalent weight (the number of grams of dry polymer per mole of sulfonic acid groups). As a result, their ionic conductivity and water holding capacity are slightly higher than that of Nafion® but their mechanical stability is limited. Flemion® membranes, developed by Asahi Glass, and Fumapen® membranes, developed

by Fumatech, differ from Nafion® by a lower equivalent weight; however the three types of membranes contain a long side chain.
More details about this type of membranes (especially about Nafion) are given in Section 2.

1.4.2 Non-fluorinated membranes

The most important group of non-fluorinated membranes developed for fuel cell applications are based on aromatic hydrocarbons. These membranes present a promising alternative to Nafion for elevated temperature applications (150-200°C), because of their low cost, their processability, their numerous chemical formulations, and their mechanical, thermal and oxidative stability [31]. Aromatic hydrocarbons can be incorporated directly into the backbone of a hydrocarbon polymer or they can be polymers modified with large side groups in the backbone to render them suitable for conduction of protons [37]. The aromatic rings offer the possibility of electrophilic as well as nucleophilic substitution. In this category, several chemical structures are considered: sulphonated polybenzimidazoles (sPBI), sulphonated polyetheretherketones (sPEEK), sulphonated polyetherketone (sPEK), and sulphonated polyimide (sPI) are some of the membranes being developed. Their rates of sulfonation [34, 35] and their reticulated-crosslinked structure [48] limit their swelling but ensure their mechanical stability.

1.4.3 Polymer blends membranes

The solubility of two polymers can be efficiently improved by favoring specific interactions between the polymer chains, such as ionic interaction, hydrogen bonding, or ion-dipole interactions, which also tends to crosslink the blend and modify mechanical and swelling properties. Ionically crosslinked polymer blends are prepared by associating a sulfonated polymer with a basic polymer, followed by acid washing to regenerate the protonic material [36]. Often, the blend is composed of an acid and a basic polymer and is then called acid–base polymer. The interactions between acid and base polymers, such as ionic cross-linking (electrostatic forces) and hydrogen bonding bridges, contribute to the control of membrane swelling without a decrease in flexibility. Therefore, the resulting membranes will have elevated working temperatures (120–200°C), low water sorption, reduced cross-over, high electrochemical properties, good thermal stability and high mechanical flexibility and strength [41].

1.4.4 Anhydrous polymer membranes

Extensive studies on polybenzimidazole (PBI) doped with phosphoric acid (H_3PO_4) for use in PEMFCs operating at elevated temperature (120–200°C) have been carried out [38, 39]. PBI is a

basic polymer with excellent mechanical and chemical stability in this temperature range and H_3PO_4 is a weak acid that supports conductivity in anhydrous conditions by forming a hydrogen-bonded network. Furthermore, the PBI-H_3PO_4 membrane is cheaper than Nafion. Water molecules favor proton conductivity by enhancing the dissociation of the acid and increasing the number of charge carriers. This result can be achieved without external humidification through diffusion of water produced at the cathode. Several challenges associated with the development of reliable PBI-based PEMFCs have been identified, such as adsorption of phosphate anions on the catalyst, high corrosion rate of the amorphous carbon catalyst support, dissolution and sintering of catalyst particles at high temperature and accelerated degradation of the MEA due to open circuit voltage in the no-load state [49].

1.4.5 Composite membranes

Composite membranes consist in the dispersion of solid acid particles (*e.g.* zirconium phosphate (ZrP)) and/or of inorganic particles (*e.g.* hygroscopic oxides, clays, zeolites, and mineral acids) into the polymer matrix [12, 40]. As an example, the solid acid particles (*i.e.* ZrP) provide extra proton sources into the polymer matrix due to their Brønsted acidity. Moreover, the inorganic particles (*i.e.* ZrO_2) play a key role in holding water within the Nafion membrane (refer to Section 5).

In general, composite membranes are of great interest as possible alternative to PFSA membranes because of their ability to donate protons, their thermal stability to temperatures above 180 °C, and their hygroscopic and hydrophilic character.

Despite all the efforts in the development of alternative membranes, Nafion and PFSA are still considered as the best polymer electrolyte membranes for fuel cells thanks to their good transport properties and chemical and mechanical stability. In the next section, we present and discuss the most important properties of Nafion, based on the results of the studies published in the literature.

2 Generalities on Nafion® membranes

This material was developed and commercialized as ion-exchange membranes by DuPont de Nemours & Co in the late 1960's under the trade name of Nafion® to be used as electrolyte polymer separator in electrochemical devices such as chlor-alkali electrolysers or hydrogen/oxygen (H_2/O_2) fuel cells [50]. For fuel cells applications, Nafion has a good balance of properties of interest, such as ionic conductivity, chemical stability, and mechanical endurance.

These properties are strongly related to the chemical structure and morphology of the membrane.

2.1 Chemical structure and morphology

Nafion is a Perfluorosulfonated ionomer (PFSI) composed of a polytetrafluoroethylene (PTFE) backbone with fluoro-ether pendant side chains ending in sulfonic ionic groups ($-SO_3^-H^+$) which chemical structure is shown in Figure 1.3.

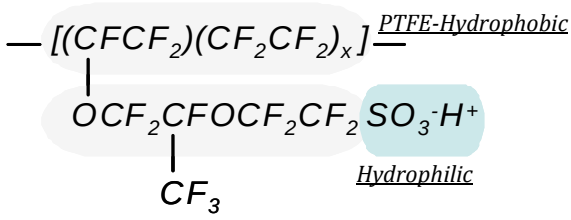

Figure 1.3: Chemical structure of Nafion® 1100 EW, X=6.6 [46].

The amount of polymer per mole of sulfonic acid groups, defined as the equivalent weight (EW), is approximately 1100 grams [46]. The larger the EW, the fewer the number of sulfonic acid groups in the membrane. The equivalent weight is also related to the ion exchange capacity (IEC) of the membrane by the equation EW= 1000/IEC [46]. Nafion membranes are named according to a combination of their equivalent weight and thickness. In the case of Nafion® N115, the equivalent weight is 1100 g/equivalent and its thickness is 0.0053" (inches). NRE 212 (0.002"), N117 (0.007"), N1135 (0.0035"), and N1110 (0.010") present almost the same EW as N115. Commercially available Nafion 1100EW solutions in alcohol are used for recasting membranes and for impregnating the gas diffusion layers (GDLs) before hot-pressing. Nafion produced nowadays is considered as chemically stabilized by DuPont de Nemours & Co [43], the ends of the main PTFE chains being protected against radical attacks.

As seen previously in Figure 1.3, the molecular structure of Nafion is characterized by two regions: the hydrophobic region, which corresponds to the polytetrafluoroethylene (PTFE) matrix, and the hydrophilic region, around the sulfonic ionic groups. These two features explain the sorption, the transport, and the mechanical properties of Nafion, once the membrane is hydrated: the hydrophilic groups make the membrane adsorb water when it is immerged in a solution or exposed to a humid environment, then the adsorbed water helps to separate the two regions in Nafion and to create the pathways in the ionic region where the protons travel. On the other hand, the hydrophobic groups confer the membrane its morphological stability and its good mechanical endurance due to the semi-crystalline and amorphous structure of PTFE [12].

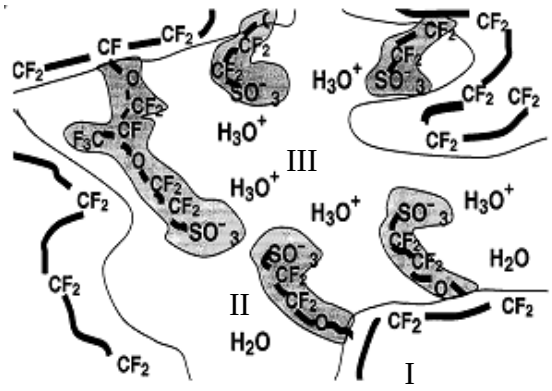

Figure 1.4: Phase separation in Nafion® from Yeager and Steck [51].

Yeager and Steck [51] divided these phase-separated domains into three regions (Figure 1.4). The authors defined the fluorocarbon (hydrophobic) matrix as region I. The intermediate region, containing the side-chains, a smaller amount of adsorbed water, some sulfonic groups, and a fraction of the counter-ions, is defined as region II. The ionic clusters, which contain some sulfonic groups, the majority of adsorbed water, and some counter-ions, are defined as region III.

The properties of Nafion membranes being strongly correlated to their morphology, a large number of studies have been devoted to the fine characterization of their structure at all the relevant length-scales, from the molecular scale up to the micron [50, 52, 53, 54, 55, 56, 57, 58, 59, 60, 61, 62, 63, 64, 65, 66]. Based on these studies, several structural models have been proposed in the literature.

One typical model was proposed in the earliest 1980's by Gierke *et al.* [55]. This model describes the membrane as a network of hydrated ionic clusters, interconnected by nanochannels where the protons can travel. When the amount of water increases in the system, these ionic clusters swell, percolate, and grow as a fusion process (Figure 1.5).

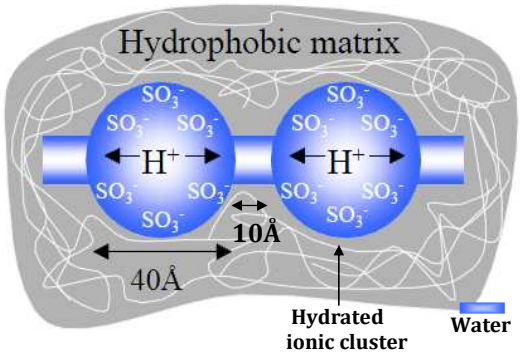

Figure 1.5: Structure of Nafion® from Gierke et al. [55].

The structure of Nafion may vary significantly depending on the hydration level. Another structural model was suggested by Gebel [50]. The author describes the changes in the morphology of Nafion at different hydration stages up to dissolution. The dry membranes consist in isolated ionic clusters, which grow as a function of the hydration following three successive stages: first, water stays into isolated clusters. The second phase consists in the interconnection of these clusters at a medium hydration level. Finally, an inversion of the structure happens for a water volume fraction of approximately 0.6. The membrane is then

described at high hydration level as a network of connected fluorocarbon polymeric aggregates dispersed in water.

More recently, improved models suggest the presence of elongated structures within the Nafion formed by fluorocarbon polymer chains aggregates. In Figure 1.6, the structure proposed by Rubatat *et al.* [57] is composed of an assembly of elongated polymer packets of about 800Å (80nm) in length and 10Å in diameter resulting from the aggregation of the polymer PTFE chains.

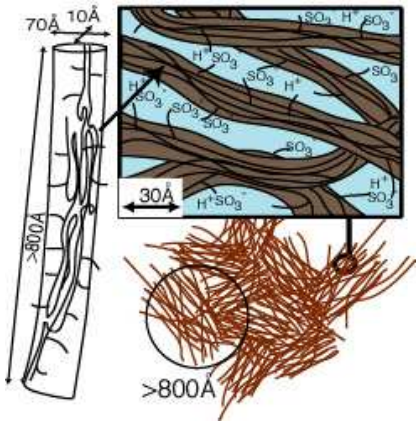

Figure 1.6: Structure of Nafion® at different length scales from Rubatat et al. [57].

However, several difficulties still exists in defining the right morphological model of Nafion membranes over a large range of water fraction and at different length scales. This is due mostly to the random structure of the ionomer, the complexity of co-organized semi-crystalline matrix and ionic domains, dependence on the fabrication process, thermal history, and the large number of morphological variations with water swelling [46].

In this study, we consider a simple model, similar to that proposed by Gierke *et al*. for the interpretation of the physical properties of Nafion N115 and NRE212 and their variations with relative humidity, temperature and time.

2.2 Pre-treatment

Before the characterization of Nafion properties, it is first important to follow a pre-treatment protocol in order to prepare the membrane in a well-defined reference state.

Several pre-treatments have been proposed in the literature. For example, the membrane prepared in the acid form ($-RSO_3H$), may be present in several states: as-received (untreated) state typical of end product, expanded state after successive conditioning stages in boiled acids and water, shrunk state achieved by drying at temperatures close to the glass transition temperature (> 100°C), and normal or reference state (it includes conditioning and drying at low temperature). In addition, Nafion can be prepared in different ionic forms ($-RSO_3^-M^+$, where M^+

is the exchangeable cation), by boiling in hydroxides (*e.g.* LiOH, NaOH and KOH) or different salt solutions (*e.g.* LiCl, $CsCO_3$ and KCO_3).

2.2.1 Conditioning

First, a cleaning treatment is applied in order to remove all organic and inorganic impurities. Then, the membranes are chemically treated with acid solutions at high temperature to exchange the membrane in the acidic form ($-RSO_3H$).

Table 1.2 describes four conditioning protocols from the literature. It must be noted that there is no standardization of these different pre-treatments.

Table 1.2: Different conditioning treatments from literature.

Yoshida *et al.* [67]	Legras *et al.* [68]	Hensley *et al.* [69]	Majsztrik *et al.* [70]
N117	N117	N117, N115, N112, N111	N112, N115, N1110, N1123
- Boiling in 3wt% H_2O_2,1 h	- Boiling in 0.75M HNO_3, 2 h	- Soaking in warm water, 24 h	- Boiling in H_2O_2, 1 h
- Boiling in DI_w, 1 h	- Washed in DI_w until neutral water	- Refluxing in 3wt% H_2O_2, 2 h	- Rinsing in boiling DI_w, 20 min
- Boiling in 1M H_2SO_4,1 h		- Refluxing in 1M HNO_3, 4 h	- Boiling in 1M H_2SO_4, 1 h
- Boiling in DI_w, 1 h		- Refluxing in 3 fresh charges of water, 4 h	- Rinsing in boiling DI_w, 20 min

M: mol/litre; DI_w: distilled water

2.2.2 Drying

The conditioning is followed by a drying treatment in order to remove must of the remaining water, and to shrink the expanded porous structure (due to the conditioning treatment). The critical parameters involved in this pre-treatment are due to:

- drying temperature (30°C to 110°C), *e.g.* drying at 70°C, 2 h [70],
- drying time (1 h to 24 h),
- vacuum system, *e.g.* vacuum drying at 110°C, 16 h [67].

The important number of parameters used in the different pre-treatments protocols result in a dispersion of the data in the literature and it is generally difficult to find a clear explanation of the effects of those pre-treatments on Nafion properties and on structural changes.

In this study, we chose to pre-treat as-received Nafion N115 and NRE212 membranes prior to their characterization. Our protocol includes a conditioning treatment (cleaning and acidification), and a heat treatment (drying) of the membrane (see Chapter 2, Section 1).

This protocol ensures that the SO_3^- groups are acidified with an H^+ counter-ion. Most of all, it prepares the membrane in a well-defined reference state before characterization. New (as-received) membranes sometimes show a brown color caused by the adsorption of impurities when they are in contact with the atmospheric air and their properties might be altered. In this case, our protocol returns the membrane back to the initial state.

2.3 Physical properties

As mentioned earlier, the hydrated structure of Nafion® membranes confer them adequate properties for fuel cell operation. The hydrophobic domain gives the membrane some mechanical strength and prevents the ionomer from dissolving, while the hydrophilic domain hydrates considerably the membrane and provides efficient water transport and a high ionic conductivity. The mechanical properties of the membrane, as well as its sorption and transport properties strongly depend on the external conditions in term of relative humidity (RH) and temperature (T). To a lesser extent, the different conditioning and heat treatments applied to the membrane samples before their characterization also play an important role. These pre-treatments slightly change the membrane properties and are warily responsible for the scattering of the published data.

The objective of this section is to extract a large number of data from literature on water sorption, proton conductivity, water-self diffusion and mechanical properties of Nafion membranes. We will then compare the different results as a function of the different pre-treatments. Finally, this bibliographic study will confirm how difficult it is to obtain reliable data about Nafion properties.

2.3.1 Water sorption

Water sorption in Nafion membranes is defined as the amount of water adsorbed by the membrane in equilibrium with vapor or liquid water at a given temperature. It is generally expressed as the number of water molecules per sulfonic acid site: $\lambda = n[H_2O] / n[SO_3^-]$ and it is also expressed as water uptake or water mass fraction: $c = m_{H20}/m_{dry\ Nafion}$.

Sorption isotherm

The sorption isotherms of Nafion membrane in the acidic form exhibit different behaviors as shown in Figure 1.7. The shape of the sorption isotherm is generally associated with three sorption mechanisms: the dissociation of the acid group SO_3H ($\lambda \sim 2$-3) is called the Langmuir contribution, the adsorption of tightly bound water ($\sim 4 < \lambda < \sim 10$) corresponds to Henry's law

and the aggregation of water molecules (clustering, λ > ~10) can be described by the Flory-Huggins theory [71].

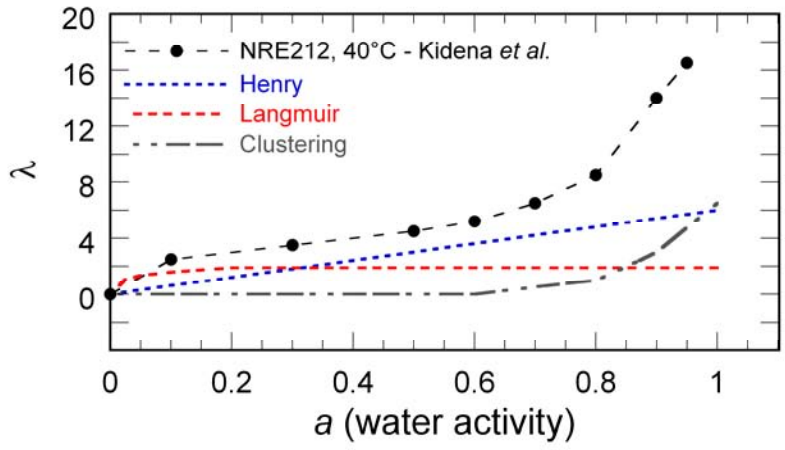

Figure 1.7: Sorption isotherm of Nafion NRE212 at 40°C, adapted from Kidena et al. [71]. The curve can be decomposed into three contributions: Henry, Langmuir and Clustering.

Other models have also been used in the literature to describe the sorption phenomena in Nafion. The BET (Brunauer-Emmett-Teller) equation for example has been exploited by Takata *et al*. [72], whereas the GAB (Guggenheim-Anderson-De Boer) and the Zimm-Lundberg equations have been proposed by Tsonos *et al.* [73].

2.3.1.1 Thermodynamic models

Several authors introduced thermodynamic parameters into the sorption models in order to better understand the sorption phenomena, explain the temperature dependence of water uptake and understand the presence of two thermodynamically stable water states when the membrane is in equilibrium with saturated vapor (RH = 1) and with liquid water (Schroeder's paradox). For example, Futerko and Hsing [74] added two parameters to their Flory-Huggins model: the Flory interaction parameter (χ) and the constant *K*. The parameter χ corresponds to the molecular interaction between the membrane and the water while the parameter *K* corresponds to the equilibrium constant for the proton transfer reaction: $-SO_3H + H_2O \Leftrightarrow -SO_3^- + H_3O^+$.

The authors express these two parameters using two temperature-dependent expressions that explain the temperature dependence of water sorption in saturated vapor and water uptake in liquid water. The model shows an increase of the liquid water uptake with temperature and a decrease of the water uptake in saturated conditions with temperature. Moreover, the authors deduced that, at low temperature, the water uptake of membranes in contact with saturated vapor is higher than with liquid water. They suggested that the structures of the hydrated

membranes are different in the two cases, *i.e.*, that they in fact represent distinct thermodynamic states.

Tsonos *et al.* [73] added the same Flory parameter χ to their thermodynamic model. The authors confronted the model to the experimental data and showed that the parameter χ is an increasing function of the water activity up to RH = 0.79, which means a decrease of the water-membrane interactions. χ decreases at higher water activity (RH >0.79), which traduces an increase of the water-membrane interactions.

None of the two mentioned models, however, took in consideration the elastic contributions or even the stress-relaxation process [52] inside the membrane when it is in equilibrium with water. This property is known to influence the equilibrium swelling and water sorption mechanism [75, 76, 77]. Among the authors who have considered the Young modulus of the membrane in their work, we can mention the thermodynamic model proposed by Choi *et al*. [75]. The authors considered in their work two models: the Flory-Huggins and the Freger's elastic models. They analyzed the osmotic pressure inside the membrane by the swelling pressure in the matrix of the membrane caused by the sorbed water and, in terms of Young modulus effect.

In addition, Eikerling and Berg [78] proposed a more comprehensive thermodynamic model in order to interpret the ionomer architecture during water sorption and the swelling of a single pore of the membrane. The authors incorporated in the model a microscopic swelling parameter related to the charge density at the pore walls of the membrane. The authors took into consideration the effects of the capillary pressure, the osmotic pressure, the shape of the pores, the distribution of the charged groups at the pore walls, the dielectric properties of water in the pores, the proton distribution effect, and the microscopic elastic properties of the polymer matrix.

2.3.1.2 Water sorption from literature (water vapor)

Numerous data on water sorption in Nafion membranes have been presented in the literature. Table 1.3 and Table 1.4 report the water sorption values (λ) and as well as the different membrane pre-treatment procedures used by the different authors.

Table 1.3: Reported water sorption in Nafion membranes from literature.

Author	Nafion	Pre-treatments	Method	T(°C)	RH	λ
Rieke and Vanderborgh 1987[79]	1100 EW	HNO_3, 3*M*, *b*, 1 h DI_w, *b*, 1 h DI_w, *a*, 20 psi, 123°C, 2 h	Gravimetric method	30 50 75 95	1 1 1 1	15 9 6 11
Zawodzinski *et al.* 1991[80]	N117	H_2O_2, *b*/DI_w, *r* H_2SO_4, *b* DI_w, *r* *vd*, 105°C	Gravimetric method membranes equilibrated with solutions of lithium chloride	30 30 30 30	0.37 0.51 0.8 0.97	*3 *3.8 *7 *13.2
Morris and Sun1993[81]	N117	HNO_3, *b* DI_w, *b* *vd*, 0.01-1Pa, 150°C, 24 h	Cahn microbalance Solutions of lithium chloride Immersion in water	25 50 100	1 1 1	13.5 16.7 23.1
Hinatsu *et al.* 1994[82]	N117	H_2O_2, *b* DI_w, *r* H_2SO_4. 1*M*, *b*/DI_w, *r* *vd*, 105°C, 2-3 h	Gravimetric method	80 80 80 80 80	0.1 0.3 0.6 0.8 1	*1 *2.5 *4 *6 *9.6
Gates and Newman 2000[83]	N117	H_2O_2. 3wt%, *b*, 1 h DI_w, *b*, 1 H_2SO_4. 0.5*M*, *b*, 1 h DI_w, *b*, 1 h *vd*, 105°C, 1 h	Gravimetric method	 60 60 60 60	*P* (x10^2 Pa) 50 80 100 200	 *3.1 *4 *4.5 *8.3
Tsonos *et al.* 2000[73]	($SO_3^-K^+$) 1190 EW	Not reported	Gravimetric method membranes equilibrated with saturated salt solutions	40 40 40	0.32 0.8 1	*1 *2 *8
Choi *et al.* 2005[75]	1100 EW	Not reported	Tapered element oscillating microbalance (TEOM)	25 25 25 25 25	0.1 0.3 0.75 0.8 1	*1.9 *3.0 *6 *7 *14
Jalani *et al.* 2005[84]	N112	H_2O_2. 3wt%, *b*, 30 min H_2SO_4. 0.5*M*, *h*, 60°C, 30 min DI_w, *h*, 60°C, 1 h *d*, RT	Tapered element oscillating microbalance (TEOM)	30 30 30 30 30 30 50	0.05 0.2 0.6 0.8 0.9 1 1	*1.9 *3 *5 *6.5 *9 *14 *13.5
		As received (untreated)		80 90 30	1 1 0.9	*15.4 *16.5 *10.75
		t, vd, 30°C		30	0.9	*12.5
		t, vd, 110°C, 24 h		30	0.9	*10.5
		t, hp, 170°C		30	0.9	*9

b: boiling; *a*: autoclave; *r*: rinsing; *vd*: vacuum drying; *h*: heating; *d*: drying; *hp*: hot pressing; DI_w: distilled water; RT: room temperature; *t*: treated; *P*: pressure; *M*: mol/litre; * values read from published isotherm curves.

Table 1.4: Reported water sorption in Nafion membranes from literature (continued).

Author	Nafion	Pre-treatments	Method	T(°C)	RH	λ
Onishi *et al.* 2007[85]	N117	H_2O_2. 3wt%, *b,* 1 h, DI_w, *b*, 1 h H_2SO_4. 0.5*M*, *b*, 1 h DI_w, *b*, 1 h *d*, 30°C	Gravimetric method and conductivity equations	30 50 65 80	1 1 1 1	25.3 24.6 23.8 22.2
		Idem, with *h,* 108°C, RH = 0.2, 30 min *d*, 30°C		5 18 30 50 65 80	1 1 1 1 1 1	*15 *15 *16 *18 *20 *21
Alberti *et al.* 2009[86]	N117	H_2O_2. 3wt%, *b,* 1 h H_2SO_4. 0.5*M*, *b*, 1 h DI_w, *b*, 1 h *d*, 120°C, 15 h	Gravimetric method	50 80 100 120 140	0.99 0.99 0.99 0.99 0.99	11.5 14 20 28 57
Mangiagli *et al.* 2009[87]	NRE212	As received (untreated) DI_w, *s*, RT, 24 h *d,* 30°C, 15 min	Dynamic vapor sorption analyzer (DVS)	30 30 30 30 30 30 30	0.01 0.12 0.26 0.42 0.60 0.78 0.88	*0.2 *1.1 *2 *3 *4.2 *6 *7.5
Kidena *et al.* 2010[71]	NRE212	H_2SO_4. 2*M*, *h*, 80°C, 2 h DI_w, *h*, 80°C, 2 h *d*, 80°C, 1 h	Isothermal adsorption measurement system and impedance analyzer	40 40 40 40 40 40 80 80 80 80 80 80	0.10 0.30 0.60 0.80 0.90 0.95 0.10 0.30 0.60 0.80 0.90 0.95	*2.5 *3.5 *5.2 *8.5 *14 *16.5 *2 *3 *4.8 *7.3 *8.5 *9

b: boiling; *h*: heating; *d*: drying; *s*: storing; DI_w: distilled water; RT: room temperature; *M*: mol/litre; * values read from published isotherm curves.

As seen from Table 1.3 and Table 1.4, the sorption data present certain discrepancies. These differences can be the result of changes in the Nafion microstructure caused by the different pre-treatments and, in particular, the different thermal history of the membrane. They can also come from the differences in the equivalent weight EW, the synthesis method (dispersion casting or extrusion), the different thicknesses, or the effect of the external conditions (relative humidity and temperature) that can be sometimes difficult to control. These points are discussed below.

Thermal history

As mentioned earlier, the sorption data from literature cannot be compared to each other without taking into account certain parameters such as the pre-treatment history. For example, the hydration is lower in a membrane that was dried at temperatures higher than 100°C (see Table 1.3), as shown by Zawodzinski *et al*. (T_{dry} = 105°C, λ = 13.2) and by Morris and Sun (T_{dry} = 150°C, λ = 13.5) at RH = 1 and at 30°C. Other authors such as Hinatsu *et al*. [82], Alberti *et al*. [86, 88] and Evans *et al*. [89] confirmed these statements. In addition to that, we observe that the hydration is higher for a membrane that was not dried, as shown by Onishi *et al*. (λ = 25.3) in the same conditions.

Other authors showed using infrared spectroscopy that a number of water molecules remains in the membrane even after intense drying treatments [90, 91, 92, 93]. For example, Korzeniewski *et al*. [92] estimated that 3 water molecules per sulfonic site remained after drying 24 hours at 110°C. This value is significantly different from the value given by Ludvigsson *et al*. [93] (λ = 1, after drying under vacuum at room temperature). These examples show that the sorption curve might start with an initial λ value different than zero, depending on the drying conditions. In addition, the shape of the sorption curves may differ according to the authors because of the different pre-treatments used [27, 74, 75].

The acidification pre-treatment also represents an important factor for the water sorption capacity. In Table 1.4, Mangiagli *et al.* [87] showed lower lambda values for membranes NRE212 that were not treated before the measurements (λ = 7.5 at RH = 0.88 and T = 30°C). These values are compared to those of treated N117 obtained by Zawodzinski *et al*. [80] (T_{dry} = 105°C, λ = 10), in the same conditions. As mentioned in the pre-treatment section, cleaning and acidifying the "as-received" membranes make sure that all the polluting traces left in the membranes disappear and that all the SO_3^- groups are totally acidified with H^+ counter-ion.

The "Schroeder's paradox effect" (defined as the difference in water content between immersion in saturated water vapor and in liquid water) was reported in several studies [70, 83, 94, 95, 96, 97]. Most of the authors measured a higher sorption capacity in liquid phase than in vapor phase, but a more recent study demonstrated that Schroeder's paradox may originate in Nafion from the effect of pre-drying on the morphology of the polymer, a too short equilibration time and/or a humidification air that may not have been at 100% [85].

Synthesis of membranes

The water sorption values obtained from two different synthesized membranes such as dispersion casted NRE212 and extruded N115, with thicknesses of 0.002" and 0.005", respectively, present discrepancies. It has been observed that NRE212 present higher lambda values than that of N115 (as shown in Chapter 3).

Temperature effect

The water sorption capacity may also be influenced by temperature. For example, in Table 1.3 Rieke and Vanderborgh [79] showed that the water sorption decreases as the temperature increases: λ = 15 (30°C), 9 (50°C), 6 (75°C), 11 (95°C), at RH = 1. Similar results were presented by Kidena *et al.* [71] (Table 1.4): λ = 16.5 (40°C) and 9 (80°C), at RH = 0.95. In addition, Broka and Ekdunge [98] observed a decrease of the lambda value at RH = 0.1 that was dramatic in the region 25-50°C and less pronounced above 50°C. The authors however, did not give an explanation for this behavior.

Other studies reported that the water sorption increases as the temperature increases, as shown by Morris *et al.* [81]: λ = 13.5 (25°C), 16.7 (50°C), 23.1 (100°C), at RH = 1, and by Onashi *et al.* [85]: λ = 15 (18°C), 16 (30°C), 18 (50°C), 20 (65°C), 21 (80°C), at RH = 1. Jalani *et al*. [99] also measured a lower vapor sorption capacity at 25°C than at 90°C (Table 1.4).

As shown by the literature data [71, 72, 79, 81, 85, 98, 99], the effect of temperature on the sorption properties of Nafion is not clear and it is not possible, at the present time, to know whether the sorption capacity is a decreasing or an increasing function of T.

2.3.1.3 Water sorption from literature (liquid water)

As for water sorption in water vapor, there exist numerous data in the literature on sorption in liquid water. Table 1.5 shows some reported values.

Table 1.5: Water sorption of Nafion membranes in liquid water from literature.

Author	Nafion	Pre-treatments	T(°C)	λ
Springer *et al.* 1991 [100]	N117	*d*, 30°C	30	22
		N-form (normal - *d*, 80°C)	30	17
Zawodzinski *et al.* 1993 [27]	N117	*vd*, 25°C, P_2O_5	27 to 94	21
		vd, 105°C, 1 h	27	12
			65	14
			80	16
Hinatsu *et al.* 1994[82]	N117	E-form (expanded - *b*)	25	22
		N-form (normal - *d*, 80°C)	25	13
		S-form (shrunken - *d*, 105°C)	25	11
Onishi *et al.* 2007[85]	N117	E-form (expanded - *b*)	30	23
		S-form (shrunken - *d*, 105°C)	30	13
		h, 108°C, RH = 0.2, *c*, 30°C	30	16
Peron *et al.* 2010[101]	NR211	As received (untreated)	25	*12
			100	*28
		vd, 80°C, 15 h	25	*12
			100	*28

d: dry; *vd*: vacuum dry; *h*: heating; *c*: cooling; P_2O_5: phosphorus pentoxide (desiccant); * values read from published curves.

Thermal history

As shown in Table 1.5, the sorption data present certain discrepancies mostly due to the different applied pre-treatments. For example, Zawodzinski *et al.* [27] proposed to dry the cleaned Nafion at room temperature (25°C) or 105°C before immersing in water. It was observed that the samples that were dried at room temperature adsorb almost two times more water than the samples that were dried at elevated temperatures: T_{dry} = 25°C, λ = 21 (27°C) and T_{dry} = 105°C, λ = 12 (27°C).

On the other hand, Hinatsu *et al*. [82] proposed three different pre-treatments: the conditioned (cleaned and acidified) Nafion, the dried Nafion at 80°C and the shrunk Nafion at 105°C. The authors observed that the conditioned membranes adsorb significantly more water than those that were previously dried. In addition, the water content after drying at 105°C was less than that after drying at 80°C, indicating a significantly greater degree of shrinkage of the microstructure at 105°C than at 80°C. The three pre-treatment procedures define the three general forms of perfluorosulfonic acid membranes, classified by Yeo and Yeager [102] in 1985, as: "E-form" (expanded form), "N-form" (normal form), and "S-form" (shrunken form).

In general, these pre-treatment effects are thought to be related to the formation and breakup of hydrated ion clusters in the membranes. The high water content of conditioned (boiled) membranes is thought to be the result of the development of an open structure caused by the

formation of large ionic clusters. Drying membranes at elevated temperatures results in pore shrinkage and reorientation of the side chains. These phenomena are reversible: the membrane can return to its initial state after exposure to water at elevated temperatures.

Temperature effect

It is shown in Table 1.5 that the temperature at which water sorption is measured influences the sorption capacity only if treated Nafion has been dried at temperatures higher than 30°C, as shown by Zawodzinski *et al*. [27]: T_{dry} > 30°C, λ = 12 (27°C), 14 (65°C) and 16 (80°C). When Nafion is dried at T_{dry} < 30°C, the water sorption capacity is almost constant as a function of temperature: λ = 21 (27°C) and λ = 21 (94°C). Similar results have been presented by Hinatsu *et al*. [82]: T_{dry} = 105°C, λ = 11(30°C), 15 (60°C), 18 (80°C) and 22 (100°C) (see Figure 1.8).

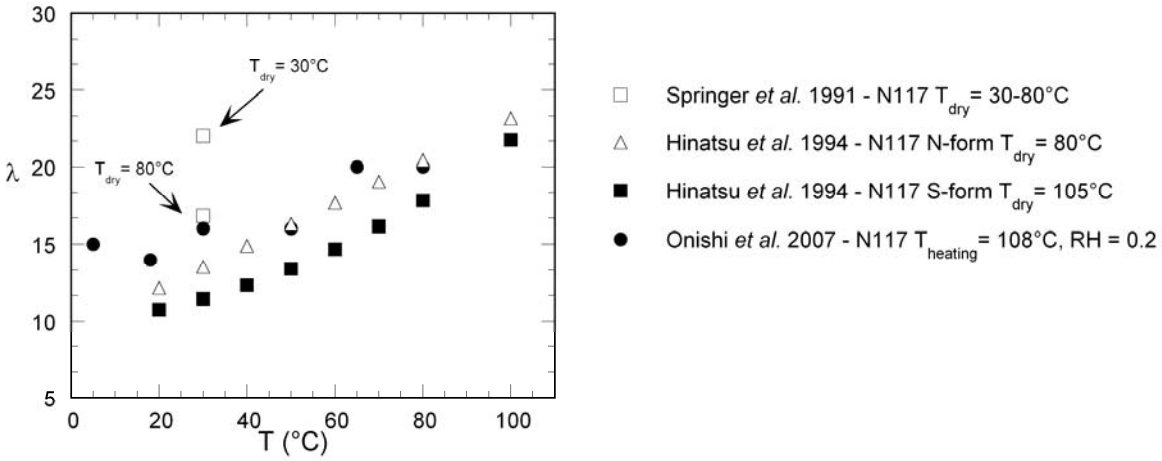

Figure 1.8: Water sorption of treated Nafion as a function of the measuring temperature and for different drying temperatures.

As observed, the different results on water sorption of Nafion in liquid water are consistent from one author to the other.

2.4 Water and proton transport

The mass transport in Nafion membranes plays a fundamental role during the operation of fuel cells. Transport mechanisms across the membrane are of different nature; they include electro-osmosis, water diffusion, and proton transport. These mechanisms are coupled to each other and described by parameters that all depend on water content.

Water can be transported through the membrane when the fuel cell is under operation *via* different processes [28, 80]:

- Electro-osmosis: the water molecules are dragged by the protons from the anode to the cathode.
- Water back-diffusion: the transport occurs because of a gradient of water concentration between the cathode and the anode.
- Thermo-osmosis: the transport occurs under the influence of a gradient of temperature [103].
- Hydraulic permeation: the transport occurs because of a gradient of pressure [70].

When the membrane is characterized *ex-situ*, adsorbed water is at thermodynamic equilibrium. In this study, we characterize water and protons transport by measuring the water self-diffusion coefficient (Ds) and the proton conductivity (σ), respectively.

2.4.1 Water diffusion

This property can be evaluated by various methods. Pulsed-field gradient nuclear magnetic resonance (PFGNMR) is used to measure the water self-diffusion in Nafion at the micrometric scale [104, 105]. Water diffusion can also be evaluated from proton conductivity data, from dynamic water uptake measurements, or deduced from steady-state water permeation experiments [80, 81, 106].
It is important to highlight that the last three methods evaluate the water diffusivity averaged over large distances inside the membrane. As a consequence, they may give a diffusion coefficient that can be significantly different from the self-diffusion coefficient obtained locally by PFGNMR.

The method to choose will depend on the property of interest. For example, experiments based on water permeation and water uptake can give general information about diffusion through the membrane. These measurements will depend mostly on the equilibrium water uptake. However, the nuclear magnetic resonance (NMR) measurements performed at the micrometer scale can give some information on the evolution of the water diffusion caused by any structural changes in the Nafion after different pre-treatments or in different external conditions (RH and T).

The typical evolution of the water-self diffusion coefficient (Ds) determined by PFGNMR in Nafion membranes is displayed on Figure 1.9, as a function of λ. It must be noted that at the highest water content, the self-diffusion of water in Nafion is about 4 times slower than the diffusion of free water (Ds = 2.5×10^{-5} cm^2/s at 25°C). This effect is due to the tortuosity of the diffusion path in the membrane structure, caused by the presence of the side chains and the backbone of the polymer.

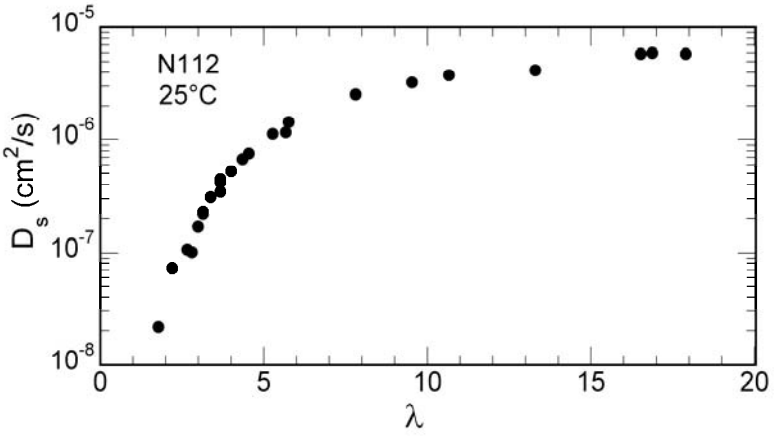

Figure 1.9: Water self-diffusion coefficient in Nafion N112 at 25°C, adapted from Perrin [104].

Table 1.6 and Table 1.7 show reported water diffusion coefficients in Nafion from NMR, conductivity and dynamic water uptake measurements.

Table 1.6: Water diffusion coefficients in Nafion membranes from literature.

Author	Nafion	Method	T (°C)	λ	RH	Ds (10^{-6} cm^2/s)
Zawodzinski *et al.* 1991[80]	N117	PFGNMR	30	2	-	0.6
			30	3	-	1.2
			30	4	-	2.1
			30	6	-	3.7
			30	9	-	4.4
			30	14	-	5.8
			30	22	-	*7
		Proton Conductivity	30	3	-	*2
			30	6	-	*6
			30	9	-	*8
			30	14	-	*12
			30	22	-	*18
Kreuer 1997[105]	N117	PFGNMR	60	5	-	* 0.1
			60	10	-	*1
Morris and Sun 1993[81]	N117	Dynamic water uptake	25	2	-	*0.05
			50	2	-	*0.15
			100	1	-	*0.05
Rivin *et al.* [106]2001	N117	Dynamic water uptake	32	-	0.05	0.007
		Permeation	32		0.4	0.67
			32		0.6	1.4
			32		0.8	1.9
			32		1	2.3
			32		liquid	3.1

* values read from published curves.

Table 1.7. Water diffusion coefficients in Nafion membranes from literature (continued).

Author	Nafion	Method	T (°C)	λ	RH	Ds (10^{-6} cm^2/s)
Perrin 2006[104]	N112	PFGNMR	25	2.8	-	0.1
			25	3.7	-	0.3
			25	7.8	-	2.5
			25	16.5	-	5.9
Kidena *et al.* 2010[71]	NR-212	PFGNMR	40	-	0.4	*2
			40	-	0.6	*3.5
			40	-	0.8	*5.5
			80	-	0.4	*3.25
			80	-	0.6	*6.4
			80	-	0.8	*10.4
		Proton Conductivity	40	-	0.4	*3.6
			80	-	0.4	*7.5

* values read from published curves.

We can observe from Table 1.6 and Table 1.7 that the water diffusion coefficient strongly increases as a function of water content. It is generally accepted that the water diffusion coefficient follows an Arrhenius law as a function of temperature [104].

2.4.2 Proton transport

The overall proton transport mechanism first involves the dissociation of the acid groups $-SO_3H$. Then, the dissociated protons become mobile enough to be transported in the water medium within the membrane *via* various transport mechanisms. Paddison and Paul [107] showed that at least two or three water molecules per sulfonic acid group are required to enable the dissociation.

Zawodzinski *et al*. [27] proposed a simple, qualitative, description of the proton transport in Nafion as a function of water content: at low hydration ($\lambda \sim 2$-3), the proton transport is slow because there are few water molecules to help the dissociation and solvation of the sulfonic acid groups. These water molecules are strongly attached to the polymer matrix, resulting in a significant resistance to the transport of hydronium ions (H_3O^+). When the hydration level increases ($\lambda \sim 4$-14), there is enough loosely bound water and the transport greatly increases. When the hydration level further increases ($\lambda > 14$), the water behaves almost as bulk water, which helps the transport of proton.

Choi *et al*. [108] proposed a model for proton transport similar to this quantitative model and based on three transport mechanisms: the proton hopping mechanism (or surface diffusion), the Grotthuss diffusion (or structural diffusion), and the mass diffusion (or vehicular mechanism)

[109]. In the proton hopping, the mechanism of transport occurs along the pores surface of the membrane and the proton hops from one ionic cluster to the adjacent one. In the Grotthuss mechanism, the proton transport occurs in the pore filled with bulk-like water and the proton hops from one water molecule to the adjacent one. In the mass diffusion mechanism, the hydronium ions (H_3O^+) are the carriers of protons, and both water and protons diffuse with a similar diffusion coefficient.

In this study, we characterize the transport of protons by measuring the proton conductivity. This macro property governs proton mobility trough a membrane, and adequate connections throughout the water domain lead to high proton conductivity because of the high diffusivity of water. The typical proton conductivity (σ) of a fully hydrated Nafion membrane is about 0.1 Siemens/cm (S/cm) at room temperature, and about 0.15 S/cm at 80°C. The increase in conductivity with water content is represented in Figure 1.10.

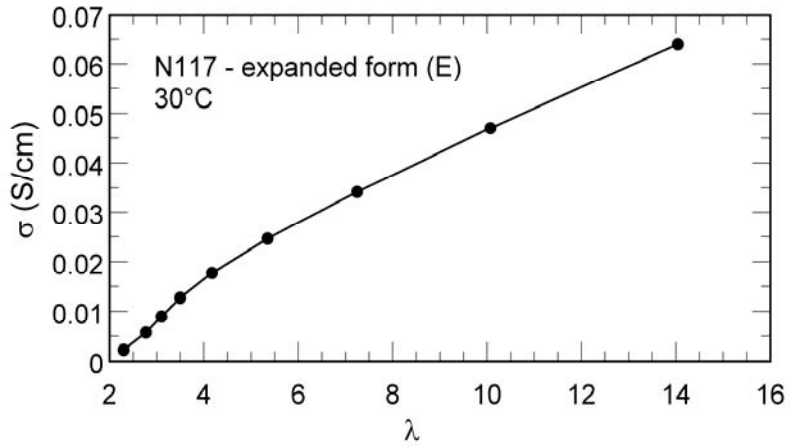

Figure 1.10: Evolution of the proton conductivity of Nafion N117 at 30°C as a function of water content, adapted from Sone et al. [110].

Proton conductivity is usually measured using AC impedance spectroscopy (see Chapter 2: Experimental Protocols).

Proton conductivity measurements are very common in the literature about Nafion and, as for water uptake, different experimental conditions and/or membrane pre-treatments are applied before or during the measurements. As a result, a wide range of experimental values can be found for the same experimental conditions (RH, T or λ, T). Table 1.8 and Table 1.9 report some of the available literature values.

Table 1.8: Reported proton conductivity of Nafion membranes from literature.

Author	Nafion	Pre-treatments	Method	T(°C)	RH	σ (S/cm) vapor	σ (S/cm) water
Sone *et al.* 1996[110]	N117	E form	4-*p*, AC-*i* 10Hz-100kHz	30	1	**0.064 *IP*	-
		N form		30	1	**0.040 *IP*	-
		S form		30	1	**0.023 *IP*	-
		FS form		30	1	**0.018 *IP*	-
Slade *et al.* 2002[111]	N117	H_2O_2. 2wt%, *h*, 80°C, 2 h	4-*p*, DC-*i* *hy*, H_2SO_4	25	-	-	*0.16 *TP*
	N115	DI_w, *r*		25	-	-	*0.134 *TP*
	N112	H_2SO_4. 0.5*M*, *s'*, 48 h		25	-	-	*0.08 *TP*
	MEA-N117	DI_w, *r*	*in-situ* PEMFC	25	-	-	*0.113 *TP*
	MEA-N115	H_2SO_4. 0.02*M*, *b*, 1 h		25	-	-	*0.107 *TP*
	MEA-N112	DI_w, *r*		25	-	-	*0.073 *TP*
Silva *et al.* 2004[112]	N117	H_2O_2. 3wt%, *b*/DI_w, *r* HNO_3. 20*wt*%, *b* DI_w, *r*, 1 h	AC-DC-*i* 100-1kHz *hy*, H_2SO_4	25	λ=13	0.048±1 *TP*	-
	N115			25	λ=13	0.033±2 *TP*	-
	N112			25	λ=13	0.023±1 *TP*	-
	N117			65	λ=13	0.079±1 *TP*	-
	N115			65	λ=13	0.045±2 *TP*	-
	N112			65	λ=13	0.031±1 *TP*	-
Casciola *et al.* 2006[113]	N117	untreated	4-*p*, *i*, 100kHz	120	0.9	*0.18 *IP*/0.10 *TP*	-
		h, 120°C, RH = 0.95		120	0.9	0.075 *TP*	-
		h, 120°C, RH = 0.3, *P*, 60kg/cm²		120	0.9	*0.16 *IP*/0.079 *TP*	-
		h, 120°C, RH = 0.95, *P*, 97kg/cm²		120	0.9	*0.061 *IP*/0.013 *TP*	-
Xie *et al.* 2006[114]	N115	not reported	AC-*i*, 100-10MHz 4-*p* wire	22	-	-	0.086 *IP*
			4-*p* strip	22	-	-	0.088 *IP*
			2-*p* strip	22	-	-	0.092 *IP*
Onishi *et al.* 2007[85]	N117	E-form	4-*p*, AC-*i* 1Hz-65kHz	5	-	-	0.085 *IP*
				20	-	-	0.111 *IP*
				30	-	-	0.121 *IP*
				50	-	-	0.160 *IP*
				65	-	-	0.199 *IP*
				80	-	-	0.223 *IP*
		d, 108°C, RH = 0.2, 30min		5	-	-	0.050 *IP*
				18	-	-	0.059 *IP*
				30	-	-	0.078 *IP*
				50	-	-	0.108 *IP*
				65	-	-	0.159 *IP*
				80	-	-	0.185 *IP*

b: boiling ; *r*: rinsing ; *h*: heating; *d*: drying; *hy*: hydrated; DI_w: distilled water; *P*: pressure; *p*: probe; *i*: impedance; *IP*: in-plane measurement; *TP*: through-plane measurement; *s'*: soaked; *M*: mol/litre; * read from published curves; ** calculated from phenomenological equations.

Table 1.9: Reported proton conductivity of Nafion membranes from literature (continued).

Author	Nafion	Pre-treatments	Method	T(°C)	RH	σ (S/cm) vapor	σ (S/cm) water
Alvarez-Gallego and de Heer 2009[115]	N117	H_2O_2. 3wt%, *b*/DI_w, *b* H_2SO_4. 0.5*M*, *b*/DI_w, *s*, 24 h	4-*p*, AC-*i* 1Hz-1MHz	0	-	-	*0.044 *IP*
				25	-	-	*0.076 *IP*
	NR-212	As-received		0	-	-	*0.047 *IP*
		DI_w, *s*, 24 h		25	-	-	*0.077 *IP*
Peron *et al.* 2010[101]	NR-211	As-received		25	-	-	*0.070 *IP*
				60	-	-	*0.125 *IP*
				100	-	-	*0.180 *IP*
		vd, 80°C, 15 h		25	-	-	*0.070 *IP*
				60	-	-	*0.140 *IP*
				100	-	-	*0.180 *IP*
Kidena *et al.* 2010[71]	NR-212	H_2SO_4. 2*M*, *h*, 80°C, 2 h DI_w, *h*, 80°C, 2 h *d*, 80°C, 1 h	4-*p*, AC-*i* 10Hz-100kHz	40	0.6	*0.025 *IP*	-
				40	0.9	*0.125 *IP*	-
				60	0.6	*0.05 *IP*	-
				60	0.9	*0.14 *IP*	-
				80	0.6	*0.065 *IP*	-
				80	0.9	*0.17 *IP*	-

b: boiling ; *r*: rinsing ; *h*: heating; *d*: drying; *vd*: vacuum dry; DI_w: distilled water; *p*: probe; *i*: impedance; *IP*: in-plane measurement; *M*: mol/litre; * read from published curves.

As seen from the tables, there are some discrepancies in the conductivity results. These discrepancies are strongly related to the different pre-treatments (thermal history), the external conditions (RH and T), the characterization methods, and the direction along which the conductivity is measured: in-plane or through-plane.

Thermal history

Sone *et al*. [110] demonstrated changes in Nafion conductivity as a function of the drying treatment. The authors determined that conductivity in saturated vapor condition was higher when Nafion was conditioned in water and in acid, that is to say in its expanded (*E*) form (σ = 0.064 S/cm). Then, the proton conductivity decreased in Nafion dried at 80°C [referred to as the normal (*N*) form (σ = 0.040 S/cm)], at 105°C [the shrunken (*S*) form (σ = 0.023 S/cm)], and at 120°C [the further-shrunken (*FS*) form (σ = 0.018 S/cm)]. As stated by the authors, this evolution may be caused by the collapse of water channels or clusters when the membrane was dried at higher temperature. For the membrane to achieve high sorption capacity and high conductivity after such thermal effect, it is necessary to expand the collapsed channels by boiling in water.

Temperature effect

Most of the authors agree on the fact that the proton conductivity of Nafion increases with temperature and follows an Arrhenius law [105]. The activation energy (E_a) obtained from the different measurements is variable in the range 8-15 kJ/mol, depending on the hydration of the membrane [112, 116, 117]. In heat-treated Nafion, however, Sone *et al*. [110] presented conductivity values that decreased from 20°C to 45°C (σ = 0.054 to 0.036 S/cm) and then increased up to 80°C (σ = 0.057 S/cm) at RH = 1. According to the authors, the variations of the proton conductivity with respect to temperature were explained by a change in water uptake and the effects of temperature on σ were very moderate (E_a < 2 kJ/mol for 45 < T < 80°C). On the other hand, Rieke and Vanderborgh [79] presented conductivity values that increased from room temperature to 50°C (σ = 0.06 to 0.113 S/cm), and then decreased from 50°C to 90°C (σ = 0.113 to 0.081 S/cm) at RH = 1. Again, these variations were explained by a change of water content with temperature.

2.5 Mechanical properties (Young modulus)

The mechanical properties of Nafion membranes play an important role in fuel cell operation and durability. They are directly linked to water uptake and temperature [118]. High stresses are created as the membrane swells from water adsorption and shrinks by changes in temperature and membrane water content during fuel cell operation. Moreover, these swelling-induced stresses may cause the mechanical failure of the membrane, either by formation of pin holes or delamination of the membrane from the electrode material.

In general, there exist several standard tests to measure the mechanical properties of Nafion membranes. However, the tensile test, in which a membrane is pulled to failure in a relatively short period of time, is one of the most useful. During this test, the Nafion sample is elongated in uniaxial tension at a constant rate, the load necessary to produce a given elongation being measured as a dependent variable. Then, the load-elongation (stress versus strain) curve is plotted from the results [119] and the Young modulus, E, correspond to the initial slope (Figure 1.11).

Earlier studies [118, 120] have demonstrated that different pre-treatments and external conditions (RH and T) can lead to structural changes in Nafion, and therefore different stress-strain responses, as shown in Figure 1.11.

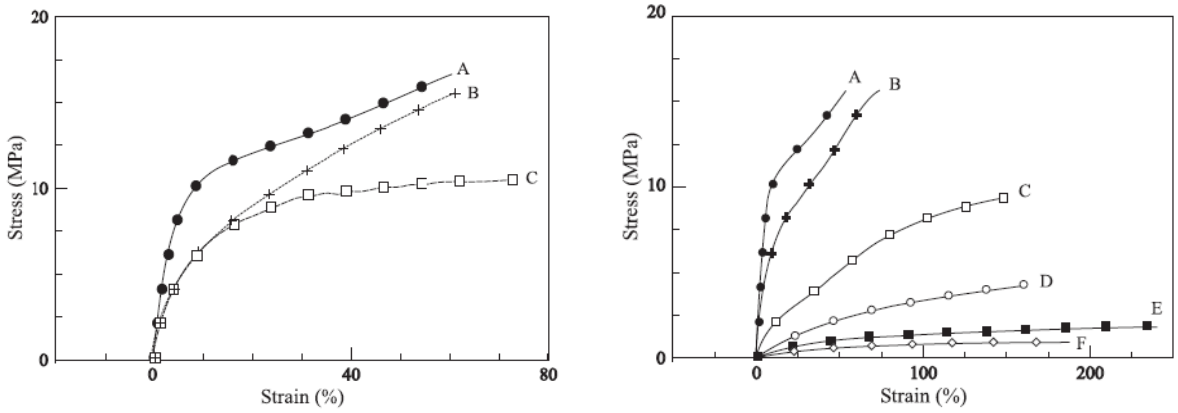

Figure 1.11: Left: experimental conditions effect on Nafion N117 strain-stress curves: (A) as-received, (B) soaked in water – 24 h, and (C) soaked in boiling water – 1 h. Right: temperature effect on as-received N117: (A) 25°C, (B) 60°C, (C) 120°C, (D) 150°C, (E) 180°C. Figures reproduced from Kawano et al. [118].

These plots show that the elastic modulus of Nafion decreases strongly with the temperature and varies significantly as a function of the applied pre-treatments. This large decrease in elastic modulus may be interpreted in the framework of the model of Eisenberg [121]. The author provided an explanation of this effect by analyzing the critical temperature (Tc) of the membrane: as the temperature is increased above a critical temperature without water adsorbance (T ~ 90°C), the sulfonic acid clusters become miscible in the PTFE matrix, reducing the elastic modulus. On the other hand, the author observed that, by adding a small quantity of water into the clusters ($\lambda < 3$), it solvates the sulfonic acid groups and creates strong hydrogen bonds within the clusters, providing crosslinks which stiffen Nafion, increase the hydrogen binding energy and thus the elastic modulus. However, as the water content increases further ($\lambda > 3$), the remaining sulfonic acid group are solvated and they act like flexible joints giving a stronger but more flexible interaction, which decreases the elastic modulus and the yield stress. This is what is called "Plasticization" from the literature [122].

Other studies show that the mechanical properties of perfluorosulfonic acid (PFSA) membranes are influenced by membrane pre-treatment, hydration, and temperature. For example, Kusoglu *et al*. [123] reported a diminution of the Young modulus in Nafion N112 membranes as a function of temperature and relative humidity (Figure 1.12). In addition, Tang *et al*. [124] and Solasi *et al*. [125] reported similar results with Nafion® N111 and Nafion N112, respectively.

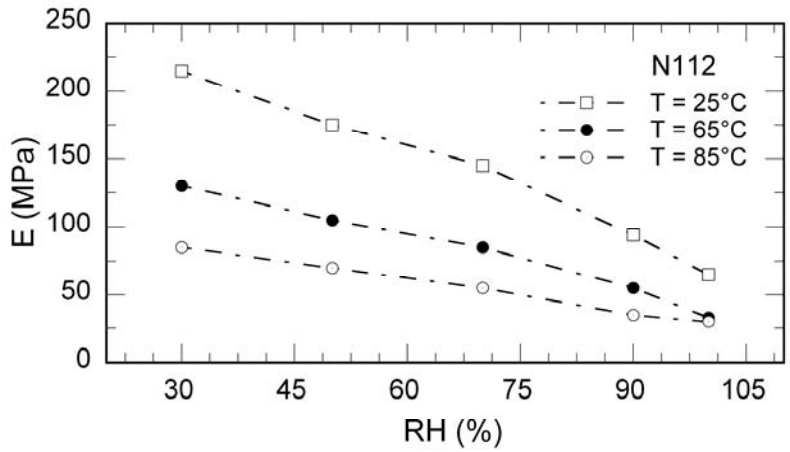

Figure 1.12: Young modulus of Nafion N112 at different temperatures, adapted from Kusoglu et al. [123].

Despite the vast literature on water sorption, proton conductivity, and modeling of ionomer structure, the relationship between these properties and the mechanical properties are still not well understood. In addition, there is no comprehensive information about the viscoelastic properties of Nafion membranes, particularly in conditions relevant to fuel cell operation: elevated temperature and humidity. Table 1.10 and Table 1.11 report a summary of the Young modulus of Nafion taken from the literature.

Table 1.10. Reported Young modulus of Nafion membranes from literature.

Authors	**Membrane**	**Method**	**Membrane condition**	**T(°C)**	**E (MPa)**
Werner *et al.* 1996[126]	N117	Strain rate: 0.20/min in machine direction	*d*, 200°C	25	**100
			Humidified	25	**50
Kawano *et al*. 2002[118]	N117	Preload force: 0.005N Soak time: 1 min Force ramp rate: 0.500N/min Upper force: 18.00 N	As-received (untreated)	27	*islope*= 2
				60	*islope*= 1.47
				90	*islope*= 0.44
				120	*islope*= 0.05
				150	*islope*= 0.03
				180	*islope*= 0.02
			d, 70°C, 24 h	27	*islope*= 2.10
				60	*islope*= 1.76
				90	*islope*= 0.80
				120	*islope*= 0.13
				150	*islope*= 0.04
				180	*islope*= 0.02
Kundu *et al*. 2005[127]	Solution cast N117	Preload force: 0.1N Strain rate: 0.001/min Strain: 0.015-0.024	Water soaked	80	*45
	Solution cast N112		Water soaked	80	*35

d: drying; ** slope calculated from published curves; *islope*: initial slope (MPa/strain); * read from published curves.

Table 1.11: Reported Young modulus of Nafion membranes from literature (continued).

Authors	Membrane	Method	Membrane condition	T(°C)	E (MPa)
Fujimoto *et al.* 2005[128]	N117	Strain rate: 0.17/min	Ambient	25	200
			Water soaked	25	52
Liu *et al.* 2006[129]	N117 H_2SO_4. 0.5*M*, *b*, 2 h DI_w, *b*, 2 h *vd*, 70°C	Strain rate: 0.7/min	RH = 0.4	23	270 ± 4
		Strain rate: 0.3/min	RH = 0.4	23	253 ± 7
		Strain rate: 0.12/min	RH = 0.4	23	256 ± 18
		Strain rate: 0.07/min	RH = 0.4	23	263 ± 10
		Strain rate: 0.025/min	RH = 0.4	23	250 ± 5
Satterfield and Benziger 2009[120]	N115 H_2O_2. 3wt%, *b*, 1 h DI_w, *b*, 20 min H_2SO_4. 1*M*, *b*, 1 h DI_w, *b*, 20 min *s*, 25°C, RH = 1	Strain rate: 2.28/min	RH = 0.1	23	*215
			RH = 0.3	23	*300
			RH = 1	23	*40
			RH = 0.1	90	*80
			RH= 0.3	90	*95
			RH = 1	90	*58
			RH< 0.1	23	*355
			RH< 0.1	60	*255
			RH< 0.1	90	*60
			RH = 1	23	*110
			RH = 1	60	*75
			RH = 1	90	*60
DuPont 2009[43]	N112, N1135, N115, N117, N1110		RH = 0.5	23	249
			Water soaked	23	114
				100	64
Kusoglu *et al.* 2010[123]	N112 H_2O_2. 3wt%, *b* H_2SO_4. 0.5*M*, *b*, 1 h DI_w, *b*, 1 h; *d*, RT, 24 h		Water soaked	25	*65
				45	*50
				65	*33
				85	*30

d: drying; *b*: boiling; *vd*: vacuum drying; *s*: storing; DI_w: distilled water; RT: room temperature; *M*: mol/litre; * read from published curves.

As seen from the tables, we can observe that the Young (elastic) modulus of Nafion membranes decreases as a function of temperature and water content.

It must also be noted that most of these mechanical values were obtained in a small range of temperatures and with little humidity control, leaving the investigator with a limited choice of external conditions (RH and T).

Other studies related to the stress-strain and the stress-relaxation (the time-dependent decrease in stress under constant strain) behaviors in Nafion membranes were performed by Liu *et al*. [129]. The authors studied this phenomenon in vapor equilibrated Nafion N117 membranes by examining the effects of strain rate and counter-ion type. On the other hands, Majsztrik *et al*. [70] focused on the experimental and theoretical investigation of the time-temperature dependent viscoelastic response of PFSA membranes swollen in various humidity conditions.
Furthermore, Satterfield and Benziger [120] showed an improvement of the mechanical properties (*i.e.* an increase of the elastic modulus, traduced also as rigidity) due to changes in PFSA membrane microstructure, specifically of Nafion-based composite membranes. In general, these composite membranes exhibit higher performances in fuel cells (*i.e.* higher hydration, higher proton conductivity, improved mechanical and thermal stability) at temperatures higher than 100°C (see Section 4).

3 Aging of Nafion® membranes

It is first important to define the terms of durability, aging and degradation:

- Durability: the ability of a PEMFC stack or individual component to resist permanent change in performance over time. Voltage decay leads to a decrease in performance that may be recoverable or reversible [22].
- Aging: the change in the properties of materials under the action of factors (*e.g.* heat, humidity, chemical agents, and mechanical stress) under operation or during storage and treatments.
- Degradation: the decrease of a PEMFC stack or individual component in voltage and quality. Degradation is not recoverable or reversible. For example, the formation of pinholes and cracks within a MEA (mostly due to different water content inside the cells, [130]) has been detected during electrochemical characterization such as open circuit voltage (OCV).

In general, durability is one of the most important characteristics for PEMFCs [22]. For example, the performance of a PEMFC is affected by cycling voltage conditions (as shown in Figure 1.13), degradation of materials (*i.e*. catalyser and bipolar plates) and/or the presence of impurities.

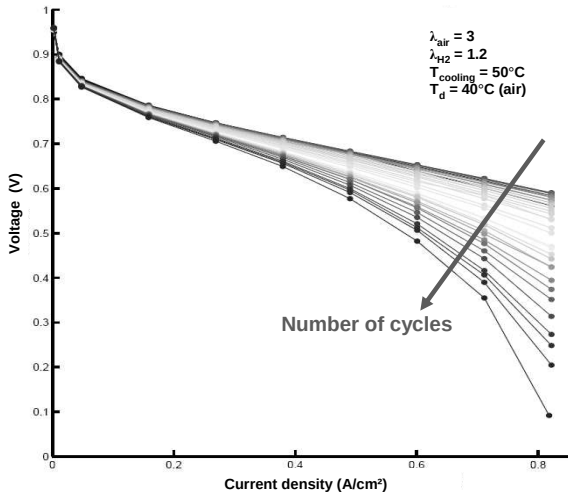

Figure 1.13: Evolution of the polarization curves in a fuel cell system as a function of cycling voltages, reproduced from Lamibrac et al. [131].

In this literature review, we focus on the durability of the proton exchange membranes.

PEM membranes present great physical and mechanical properties and excellent chemical stability. However, their properties can be limited, once exposed to:

In-situ

- Hydration and dehydration cycling.
- Voltage-current cycling.
- Compression and constraints cycling.
- Start/stop cycles.
- Radicals effect generated by the Fenton's reagent.

Ex-situ

- Different pre-treatments (conditioning and heat treatment).
- High temperature (> 100°C).
- Low humidity condition (RH < 0.5).
- Long-term exposure to humidity and temperature.

The durability of Nafion membranes can be evaluated by performing either *in-situ* or *ex-situ* tests. For example, several authors [14, 22, 132, 133, 134, 135] have investigated the chemical degradation of the Nafion membranes *in-situ* in presence of humidity, temperature, cyclic stress, and cyclic current, and *ex-situ* in presence of peroxide/hydroperoxide radicals (Fenton's test). The authors have also used different analytical methods (IR spectroscopy, NMR, chromatography, etc) able to monitor the structural changes in the membrane, to analyse the water produced during fuel cell operation, and to elucidate the different degradation products.

It is important to highlight that *ex-situ* tests are more easily performed because they allow the identification of the degradation products, the determination of their kinetics of formation, and consequently the determination of the involved aging mechanism.

Other authors have investigated *ex-situ* the effect of temperature and humidity on the evolution of the Nafion properties during long periods of time. This particular type of aging is called in the literature [136] "hygrothermal aging effect". When the Nafion is exposed to constant RH and T conditions, the water sorption, the water transport and the mechanical properties were shown to decay (Figure 1.14 (right)). The authors assume that during this hygrothermal aging, a reaction occurs in the Nafion membrane. This reaction was identified as the condensation of the sulfonic groups and the formation of anhydride sulphuric (Figure 1.14 (left)).

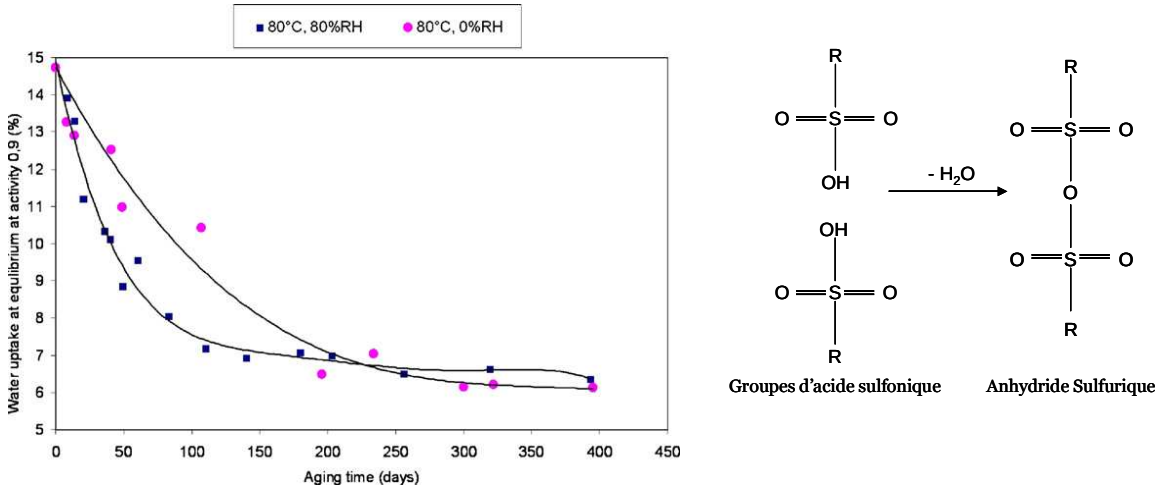

Figure 1.14: Left: Water uptake of Nafion N112 aged at 80°C, RH = 0 and at 80°C, RH = 0.8. Right: Reaction of sulfonic acids condensation. The figures were reproduced from Collette et al. [136].

From an experimental point of view, the hygrothermal aging is simple to study: one only needs to expose Nafion membranes to constant temperature and relative humidity conditions for a long time. Then, the measurement of the water content, the proton conductivity and the mechanical properties as a function of time gives an access to the time evolution of the properties of the membranes.

These types of durability studies can serve as a reference guide for the development of new membranes with a higher stability of their properties.

4 Improved Nafion-based membranes with inorganic nanoparticles

Despite the favorable properties of perfluorosulfonic acid (Nafion-type) membranes in PEMFCs, one of the major issues remains the strong dependence of proton conductivity on water content, limiting the working temperature of the PEMFC to about 90°C. For example, temperatures above 100°C drive off the water, drying out the membrane and reducing its conductivity and the cell performance. Moreover, the lifetime of the Nafion membrane within the cell is shortened at higher temperatures because it becomes softer and can develop tears or holes [122, 137]. Thus, a design goal for new fuel cell membrane materials is their ability to perform well at low humidity and high temperatures.

A promising approach is to modify Nafion® membranes by adding inorganic oxide particles. Their improved performance at low relative humidity and elevated temperature has been largely attributed to increased water retention and water management, high ion exchange capacity, high mechanical durability and robustness, and high proton conductivity [12, 122, 137, 138, 139, 140, 141, 142, 143, 144].

Figure 1.15 shows the increased water retention, the current-voltage and the proton conductivity curves on different Nafion composite membranes when compared to unmodified Nafion membrane.

Different inorganic oxides like silicon dioxide (SiO_2), titanium dioxide (TiO_2), zirconium dioxide (ZrO_2) and aluminium oxide (Al_2O_3) have been proposed for the development of these types of composite membranes. Their hygroscopic nature permits to enhance the water uptake and the water retention of the membrane. The composite membranes can be prepared *via* recasting polymer solution with the inorganic particles or *via in-situ* growth of these particles in a Nafion membrane by sol-gel processing [145, 146, 147].
Today, results on composite membranes are still scattered and inconclusive. Further, the systematic comparisons of these new membranes with unmodified Nafion are made difficult by the large number of inorganic oxide materials and loading combinations, as well as different procedures for composite membrane fabrication and testing [12, 122, 137, 139, 140, 141, 142, 143, 144, 147, 148, 149, 150].

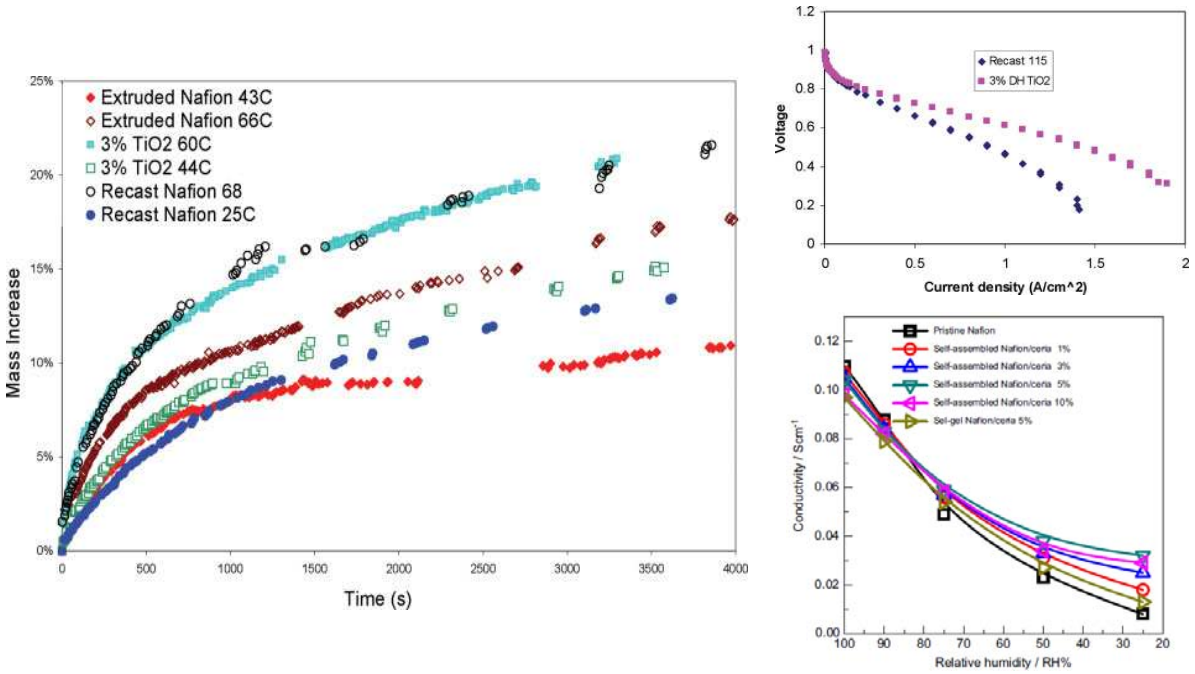

Figure 1.15: Left: Water uptake of Nafion and Nafion/titania composite membranes in saturated water vapor at different temperatures, reprinted from Satterfield et al. [122]. Right (top): current–voltage curve of fully hydrated fuel cells at 80°C with Nafion N115 and Nafion N115/TiO_2 (3 wt % and 21-nm particle) composite membranes, reprinted from Satterfield et al. [122]. Right (bottom): Proton conductivity of Nafion and Nafion/CeO_2 composite membrane as a function of relative humidity, reprinted from Wang et al. [144].

5 Objectives of this work

PEMFCs are currently considered as the most promising systems for powering all kind of vehicles. However, their principal elements (proton exchange membrane, gas diffusion electrode, bipolar plate, etc) are still the object of intense fundamental and technological research especially for durability and cost issues. One of the most interesting challenges to be addressed in this research area concerns the proton exchange membrane (the heart of the fuel cell). The most used PEM membrane is Nafion® because of its high proton conductivity (when properly hydrated), its good chemical and thermal stability, and its mechanical integrity. For these reasons, Nafion is still considered today as the reference material for polymer electrolyte membrane for fuel cells.

As seen in this chapter, there exist a large number of publications focusing on the study of the properties of Nafion membranes. The experimental conditions corresponding to these studies are however discrepant from one author to the other. Moreover, the pre-treatments applied to

the membrane samples are sometimes extremely different since no standardization of the protocol was defined. Several studies have demonstrated that the Nafion material was very sensitive to these pre-treatments and, more specifically, to its thermal history. As a consequence, the data extracted from the literature are dispersed and are sometimes not consistent with each other. As a result, it remains difficult to gather a complete set of water sorption, transport and mechanical data measured on similar Nafion membranes, using a similar pre-treatment and obtained using the same experimental method and protocol.

The first objective of the present work is to collect a large number of experimental data on the most fundamental properties of Nafion membrane, on a broad range of experimental conditions in terms of temperature and relative humidity. These systematic measurements are performed by following simple and reproducible experimental protocols. The detailed protocols and the experimental techniques are described in Chapter 2.

In Chapter 3, we use the obtained results to study the effects of the thermal pre-treatment on the membrane sorption, transport and mechanical properties. Then, the data collected at different temperatures help us analyzing the ambiguity about the temperature dependence of the water sorption in vapor phase.

We have seen from the literature review that the Nafion properties can present certain instabilities when exposed to constant RH and T conditions during a long period of time. This phenomenon was defined as “hygrothermal aging”.
The main objective of the Chapter 4 is to study the long-term evolution of the Nafion properties exposed to constant RH and T conditions. In this chapter we show the results of a systematic characterization of aged Nafion N115 in a wide RH range, at 60°C and 80°C and at different aging time. Our target is:

- to confirm, or not, that the Nafion properties are evolving as a function of time,
- if so, to identify which properties are affected and in which extent,
- to precise in which range of T and RH this hygrothermal aging occurs.

Furthermore, we analyze the reversibility of this phenomenon (when its properties may return to its initial state). The objective is to precise in which range of T and RH this reversibility occurs and if it occurs after immersion in water, in acid solution, or even after cycling the RH conditions.

From an operational point of view, the strong humidification requirements of Nafion membranes limit the operational temperature in PEMFCs to 80°C - 90°C. This strong hydration dependency and low temperature represent critical issues for the performance and durability of

the fuel cell system. The main objective of the last part of this thesis is to characterize alternative membranes as Nafion/zirconia (ZrO_2) composite membranes developed by the Functional Ceramics Group at West Virginia University, USA. The working cooperation between the two laboratories emerged from an assembled research work with Dr. Edward Sabolsky around five years on the processing of new piezoelectric materials for spacecrafts and new ceramic materials for solid oxide fuel cell (SOFC) at NexTech Materials, Ohio, USA.

This study is proposed in Chapter 5. Then, the results will be compared with those of unmodified Nafion in terms of water sorption, proton conductivity and tensile-stress tests. This study will serve as a reference for designing new membranes and/or new PEMFC systems able to work at high temperature and low humidity conditions.

6 References

[1] Winter, U. and Weidner, H., Hydrogen for the Mobility of the Future Results of GM/Opel's Well-to-Wheel Studies in North America and Europe, *Fuel Cells*, Vol. 3, No. 3, 2003, pp. 76–83.

[2] Friedlmeier, G., Friedrich, J., and Panik, F., Test Experiences with the DaimlerChrysler Fuel Cell Electric Vehicle NECAR 4, *Fuel Cells*, Vol. 1, No. 2, 2001, pp. 92–96.

[3] Wieser, C., Novel Polymer Electrolyte Membranes for Automotive Applications - Requirements and Benefits, *Fuel Cells*, Vol. 4, No. 4, 2004, pp. 245–250.

[4] Cropper, M., Fuel Cells for People, *Fuel Cells*, Vol. 4, No. 3, 2004, pp. 236–240.

[5] Carrette, L., Friedrich, K. A., and Stimming, U., Fuel Cells-Fundamentals and Applications, *Fuel Cells*, Vol. 1, No. 1, 2001, pp. 5–39.

[6] de Bruijn, F. A., Dam, V. A. T., and Janssen, G. J. M., Review: Durability and Degradation Issues of PEM Fuel Cell Components, *Fuel Cells*, Vol. 8, No. 1, 2008, pp. 3–22.

[7] EG&G Technical Services, I., *Fuel Cell Handbook*, Department of Energy, Office of Fossil Energy, National Energy Technology Laboratory, West Virginia, USA., 7th ed., 2004.

[8] Okada, O. and Yokoyama, K., Development of Polymer Electrolyte Fuel Cell Cogeneration Systems for Residential Applications, *Fuel Cells*, Vol. 1, No. 1, 2001, pp. 72–77.

[9] Larminie, J. and Dicks, A., *Fuel Cell Systems Explained*, Wiley, New York, USA., 2nd ed., 2003.

[10] Mehta, V. and Cooper, J. S., Review and analysis of PEM fuel cell design and manufacturing, *Journal of Power Sources*, Vol. 114, No. 1, 2003, pp. 32–53.

[11] Scibioh, M., Oh, I.-H., Lim, T.-H., Hong, S.-A., and Ha, H., Investigation of various ionomer-coated carbon supports for direct methanol fuel cell applications, *Applied Catalysis B: Environmental*, Vol. 77, No. 3-4, 2008, pp. 373–385.

[12] Dupuis, A.-C., Proton exchange membranes for fuel cells operated at medium temperatures: Materials and experimental techniques, *Progress in Materials Science*, Vol. 56, No. 3, 2011, pp. 289–327.

[13] Schulze, M., Knöri, T., Schneider, A., and Gülzow, E., Degradation of sealings for PEFC test cells during fuel cell operation, *Journal of Power Sources*, Vol. 127, No. 1-2, 2004, pp. 222–229.

[14] Tang, H., Peikang, S., Jiang, S. P., Wang, F., and Pan, M., A degradation study of Nafion proton exchange membrane of PEM fuel cells, *Journal of Power Sources*, Vol. 170, No. 1, 2007, pp. 85–92.

[15] Arita, M., Technical Issues of Fuel Cell Systems for Automotive Application, *Fuel Cells*, Vol. 2, No. 1, 2002, pp. 10–14.

[16] Barbir, F. and Yazici, S., Status and development of PEM fuel cell technology, *International Journal of Energy Research*, Vol. 32, No. 5, 2008, pp. 369–378.

[17] Corey, R. L., Ivancic, T. M., Shane, D. T., Carl, E. A., Bowman, R. C., Bellosta von Colbe, J. M., Dornheim, M., Bormann, R., Huot, J., Zidan, R., Stowe, A. C., and Conradi, M. S., Hydrogen Motion in Magnesium Hydride by NMR, *Journal of Physical Chemistry C*, Vol. 112, No. 49, 2008, pp. 19784–19790.

[18] Corey, R. L., Shane, D. T., Bowman, R. C., and Conradi, M. S., Atomic Motions in LiBH4 by NMR, *Journal of Physical Chemistry C*, Vol. 112, No. 47, 2008, pp. 18706–18710.

[19] Car manufacturers, Oil, gas, Utilities, Industrial gas companies, NGOs, g., and clean energy organisations, A portfolio of power-trains for Europe: a fact-based analysis - The role of Battery Electric Vehicles, Plug-in Hybrids and Fuel Cell Electric Vehicles, Tech. rep., European Union, 2010.

[20] Debe, M. K., Effect of Electrode Surface Area Distribution on High Current Density Performance of PEM Fuel Cells, *Journal of The Electrochemical Society*, Vol. 159, No. 1, 2012, pp. B53–B66.

[21] Cheng, X., Shi, Z., Glass, N., Zhang, L., Zhang, J., Song, D., Liu, Z.-S., Wang, H., and Shen, J., A review of PEM hydrogen fuel cell contamination: Impacts, mechanisms, and mitigation, *Journal of Power Sources*, Vol. 165, No. 2, 2007, pp. 739–756.

[22] Wu, J., Yuan, X., Martin, J., Wang, H., Zhang, J., Shen, J., Wu, S., and Merida, W., A review of PEM fuel cell durability: Degradation mechanisms and mitigation strategies, *Journal of Power Sources*, Vol. 184, No. 1, 2008, pp. 104–119.

[23] Péron, J., Nedellec, Y., Jones, D. J., and Rozière, J., The effect of dissolution, migration and precipitation of platinum in Nafion®-based membrane electrode assemblies during fuel cell operation at high potential, *Journal of Power Sources*, Vol. 185, No. 2, 2008, pp. 1209–1217.

[24] Healy, J., Hayden, C., Xie, T., Olson, K., Waldo, R., Brundage, M., Gasteiger, H., and Abbott, J., Aspects of the Chemical Degradation of PFSA Ionomers used in PEM Fuel Cells, *Fuel Cells*, Vol. 5, No. 2, 2005, pp. 302–308.

[25] Commer, P., Cherstvy, A., Spohr, E., and Kornyshev, A., The effect of water content on proton transport in polymer electrolyte membranes, *Fuel Cells*, Vol. 2, No. 3-4, 2002, pp. 127–136.

[26] Saito, M., Arimura, N., Hayamizu, K., and Okada, T., Mechanisms of Ion and Water Transport in Perfluorosulfonated Ionomer Membranes for Fuel Cells, *Journal of Physical Chemistry B*, Vol. 108, No. 41, 2004, pp. 16064–16070.

[27] Zawodzinski, Jr., T. A., Derouin, C., Radzinski, S., Sherman, R. J., Smith, V. T., Springer, T. E., and Gottesfeld, S., Water Uptake by and Transport Through Nafion® 117 Membranes, *Journal of the Electrochemical Society*, Vol. 140, No. 4, 1993, pp. 1041–1047.

[28] Zawodzinski, Jr., T. A., Springer, T. E., Davey, J., Jestel, R., Lopez, C., Valerio, J., and Gottesfeld, S., A Comparative Study of Water Uptake By and Transport Through Ionomeric Fuel Cell Membranes, *Journal of the Electrochemical Society*, Vol. 140, No. 7, 1993, pp. 1981–1985.

[29] Bazylak, A., Liquid water visualization in PEM fuel cells: A review, *International Journal of Hydrogen Energy*, Vol. 34, No. 9, 2009, pp. 3845–3857.

[30] Alink, R., Gerteisen, D., and Mérida, W., Investigating the Water Transport in Porous Media for PEMFCs by Liquid Water Visualization in ESEM, *Fuel Cells*, 2011.

[31] Devanathan, R., Recent developments in proton exchange membranes for fuel cells, *Energy & Environmental Science*, 2008, pp. 101–119.

[32] Wakizoe, M., Velev, O. A., and Srinivasan, S., Analysis of proton exchange membrane fuel cell performance with alternate membranes, *Electrochimica Acta*, Vol. 40, No. 3, 1995, pp. 335–344.

[33] Kopitzke, R. W., Linkous, C. A., and Nelson, G. L., Thermal stability of high temperature polymers and their sulfonated derivatives under inert and saturated vapor conditions, *Polymer Degradation and Stability*, Vol. 67, No. 2, 2000, pp. 335–344.

[34] Wang, F., Hickner, M., Kim, Y. S., Zawodzinski, T. A., and McGrath, J. E., Direct polymerization of sulfonated poly(arylene ether sulfone) random (statistical) copolymers: candidates for new proton exchange membranes, *Journal of Membrane Science*, Vol. 197, No. 1-2, 2002, pp. 231–242.

[35] Bae, J. M., Honma, I., Murata, M., Yamamoto, T., Rikukawa, M., and Ogata, N., Properties of selected sulfonated polymers as proton-conducting electrolytes for polymer electrolyte fuel cells, *Solid State Ionics*, Vol. 147, No. 1-2, 2002, pp. 189–194.

[36] Rozière, J. and Jones, D., Non-fluorinated polymer materials for proton exchange membrane fuel cells, *Annual Review of Materials Research*, Vol. 33, 2003, pp. 503–555.

[37] Smitha, B., Sridhar, S., and Khan, A. A., Solid polymer electrolyte membranes for fuel cell applications–a review, *Journal of Membrane Science*, Vol. 259, No. 1-2, 2005, pp. 10–26.

[38] Xiao, L., Zhang, H., Scanlon, E., Ramanathan, L. S., Choe, E.-W., Rogers, D., Apple, T., and Benicewicz, B. C., High-Temperature Polybenzimidazole Fuel Cell Membranes via a Sol-Gel Process, *Chemistry of Materials*, Vol. 17, No. 21, 2005, pp. 5328–5333.

[39] Lobato, J., Cañizares, P., Rodrigo, M. A., Linares, J. J., and Aguilar, J. A., Improved polybenzimidazole films for H3PO4-doped PBI-based high temperature PEMFC, *Journal of Membrane Science*, Vol. 306, No. 1-2, 2007, pp. 47–55.

[40] Navarra, M. A., Croce, F., and Scrosati, B., New, high temperature superacid zirconia-doped Nafion (TM) composite membranes, *Journal of Materials Chemistry*, Vol. 17, No. 30, 2007, pp. 3210–3215.

[41] Ahmad, H., Kamarudin, S. K., Hasran, U. A., and Daud, W. R. W., Overview of hybrid membranes for direct-methanol fuel-cell applications, *International Journal of Hydrogen Energy*, Vol. 35, No. 5, 2010, pp. 2160–2175.

[42] Dillet, J., Lottin, O., Maranzana, G., Didierjean, S., Conteau, D., and Bonnet, C., Direct observation of the two-phase flow in the air channel of a proton exchange membrane fuel cell and of the effects of a clogging/unclogging sequence on the current density distribution, *Journal of Power Sources*, Vol. 195, No. 9, 2010, pp. 2795–2799.

[43] DuPont, http://www.dupont.com/fuelcells/pdf/dfc101.pdf, 2009.

[44] Jiang, Z., Jiang, Z.-j., Yu, X., Meng, Y., and Li, J., Plasma deposition of polymer electrolyte membrane for proton exchange membrane fuel cell (PEMFC) applications, *Surface and Coatings Technology*, Vol. 205, No. 1, 2010, pp. S231–S235.

[45] Chen, J., Li, D., Koshikawa, H., Asano, M., and Maekawa, Y., Crosslinking and grafting of polyetheretherketone film by radiation techniques for application in fuel cells, *Journal of Membrane Science*, Vol. 362, No. 1-2, 2010, pp. 488–494.

[46] Mauritz, K. A. and Moore, R. B., State of Understanding of Nafion, *Chemical Reviews*, Vol. 104, No. 10, 2004, pp. 4535–4586.

[47] Subianto, S., Cavaliere, S., Jones, D. J., and Rozière, J., Effect of side-chain length on the electrospinning of perfluorosulfonic acid ionomers, *Journal of Polymer Science Part A: Polymer Chemistry*, Vol. 51, 2012, pp. 118–128.

[48] Kerres, J., Cui, W., and Junginger, M., Development and characterization of crosslinked ionomer membranes based upon sulfinated and sulfonated PSU crosslinked PSU blend membranes by alkylation of sulfinate groups with dihalogenoalkanes, *Journal of Membrane Science*, Vol. 139, No. 2, 1998, pp. 227–241.

[49] Qi, Z. and Buelte, S., Effect of open circuit voltage on performance and degradation of high temperature PBI-H3PO4 fuel cells, *Journal of Power Sources*, Vol. 161, No. 2, 2006, pp. 1126–1132.

[50] Gebel, G., Structural evolution of water swollen perfluorosulfonated ionomers from dry membrane to solution, *Polymer*, Vol. 41, No. 15, 2000, pp. 5829–5838.

[51] Yeager, H. L. and Steck, A., Cation and Water Diffusion in Nafion Ion Exchange Membranes: Influence of Polymer Structure, *Journal of The Electrochemical Society*, Vol. 128, No. 9, 1981, pp. 1880–1884.

[52] Yeo, S. C. and Eisenberg, A., Physical properties and supermolecular structure of perfluorinated ion-containing (nafion) polymers, *Journal of Applied Polymer Science*, Vol. 21, No. 4, 1977, pp. 875–898.

[53] Komoroski, R. A. and Mauritz, K. A., A sodium-23 nuclear magnetic resonance study of ionic mobility and contact ion pairing in a perfluorosulfonate ionomer, *Journal of the American Chemical Society*, Vol. 100, No. 24, 1978, pp. 7487–7489.

[54] Heitner Wirguin, C., Infra-red spectra of perfluorinated cation-exchanged membranes, *Polymer*, Vol. 20, No. 3, 1979, pp. 371–374.

[55] Gierke, T. D., Munn, G. E., and Wilson, F. C., The morphology in nafion perfluorinated membrane products, as determined by wide- and small-angle x-ray studies, *Journal of Polymer Science: Polymer Physics Edition*, Vol. 19, No. 11, 1981, pp. 1687–1704.

[56] Schmidt Rohr, K. and Chen, Q., Water Nanochannels in Nafion®: Quantitative Scattering Analysis and NMR, Annual progress report, Department of Energy, Ames Laboratory and Dept. of Chemistry. Iowa State University, USA., 2007.

[57] Rubatat, L., Rollet, A. L., Gebel, G., and Diat, O., Evidence of Elongated Polymeric Aggregates in Nafion, *Macromolecules*, Vol. 35, No. 10, 2002, pp. 4050–4055.

[58] Dreyfus, B., Gebel, G., Aldebert, P., Pineri, M., Escoubes, M., and Thomas, M., Distribution of the 'micelles' in hydrated perfluorinated ionomer membranes from SANS experiments, *Journal de physique Paris*, Vol. 51, No. 12, 1990, pp. 1341–1354.

[59] Gebel, G. and Lambard, J., Small-Angle Scattering Study of Water-Swollen Perfluorinated Ionomer Membranes, *Macromolecules*, Vol. 30, No. 25, 1997, pp. 7914–7920.

[60] Kumar, S. and Pineri, M., Interpretation of small-angle x-ray and neutron scattering data for perfluorosulfonated ionomer membranes, *Journal of Polymer Science Part B: Polymer Physics*, Vol. 24, No. 8, 1986, pp. 1767–1782.

[61] Ioselevich, A. S., Kornyshev, A. A., and Steinke, J. H. G., Fine Morphology of Proton-Conducting Ionomers, *Journal of Physical Chemistry B*, Vol. 108, No. 32, 2004, pp. 11953–11963.

[62] Starkweather, H. W., Crystallinity in perfluorosulfonic acid ionomers and related polymers, *Macromolecules*, Vol. 15, No. 2, 1982, pp. 320–323.

[63] Haubold, H. G., Vad, T., Jungbluth, H., and Hiller, P., Nano structure of NAFION: a SAXS study, *Electrochimica Acta*, Vol. 46, No. 10-11, 2001, pp. 1559–1563.

[64] Litt, M. H., Reevaluation of Nafion morphology, Vol. 38, 1997, pp. 80–81.

[65] Rollet, A.-L., Diat, O., and Gebel, G., A New Insight into Nafion Structure, *Journal of Physical Chemistry B*, Vol. 106, No. 12, 2002, pp. 3033–3036.

[66] Rubatat, L., Gebel, G., and Diat, O., Fibrillar Structure of Nafion: Matching Fourier and Real Space Studies of Corresponding Films and Solutions, *Macromolecules*, Vol. 37, No. 20, 2004, pp. 7772–7783.

[67] Yoshida, N., Ishisaki, T., Watakabe, A., and Yoshitake, M., Characterization of Flemion® membranes for PEFC, *Electrochimica Acta*, Vol. 43, No. 24, 1998, pp. 3749–3754.

[68] Legras, M., Hirata, Y., Nguyen, Q. T., Langevin, D., and Métayer, M., Sorption and diffusion behaviors of water in Nation 117 membranes with different counter ions, *Desalination*, Vol. 147, No. 1-3, 2002, pp. 351–357.

[69] Hensley, J. E., Way, J. D., Dec, S. F., and Abney, K. D., The effects of thermal annealing on commercial Nafion® membranes, *Journal of Membrane Science*, Vol. 298, No. 1-2, 2007, pp. 190–201.

[70] Majsztrik, P. W., Satterfield, M. B., Bocarsly, A. B., and Benziger, J. B., Water sorption, desorption and transport in Nafion membranes, *Journal of Membrane Science*, Vol. 301, No. 1-2, 2007, pp. 93–106.

[71] Kidena, K., Ohkubo, T., Takimoto, N., and Ohira, A., PFG-NMR approach to determining the water transport mechanism in polymer electrolyte membranes conditioned at different temperatures, *European Polymer Journal*, Vol. 46, No. 3, 2010, pp. 450–455.

[72] Takata, H., Mizuno, N., Nishikawa, M., Fukada, S., and Yoshitake, M., Adsorption properties of water vapor on sulfonated perfluoropolymer membranes, *International Journal of Hydrogen Energy*, Vol. 32, No. 3, 2007, pp. 371–379.

[73] Tsonos, C., Apekis, L., and Pissis, P., Water sorption and dielectric relaxation spectroscopy studies in hydrated Nafion (-SO3K) membranes, *Journal of Materials Science*, Vol. 35, No. 23, 2000, pp. 5957–5965.

[74] Futerko, P. and Hsing, I.-M., Thermodynamics of Water Vapor Uptake in Perfluorosulfonic Acid Membranes, *Journal of The Electrochemical Society*, Vol. 146, No. 6, 1999, pp. 2049–2053.

[75] Choi, P., Jalani, N. H., and Datta, R., Thermodynamics and Proton Transport in Nafion I. Membrane Swelling, Sorption, and Ion-Exchange Equilibrium, *Journal of The Electrochemical Society*, Vol. 152, No. 3, 2005, pp. E84–E89.

[76] Choi, P., Jalani, N. H., Thampan, T. M., and Datta, R., Consideration of thermodynamic, transport, and mechanical properties in the design of polymer electrolyte membranes for higher temperature fuel cell operation, *Journal of Polymer Science Part B: Polymer Physics*, Vol. 44, No. 16, 2006, pp. 2183–2200.

[77] Satterfield, M. B., *Mechanical and water sorption properties of Nafion and composite Nafion/titanium dioxide membranes for polymer electrolyte membrane fuel cells*, Ph.D. thesis, Princeton University, New Jersey, USA., 2007.

[78] Eikerling, M. and Berg, P., Poroelectroelastic theory of water sorption and swelling in polymer electrolyte membranes, *Soft Matter*, Vol. 7, No. 13, 2011, pp. 5976–5990.

[79] Rieke, P. and Vanderborgh, N., Temperature dependence of water content and proton conductivity in polyperfluorosulfonic acid membranes, *Journal of Membrane Science*, Vol. 32, No. 2-3, 1987, pp. 313–328.

[80] Zawodzinski, Jr., T. A., Neeman, M., Sillerud, L. O., and Gottesfeld, S., Determination of water diffusion coefficients in perfluorosulfonate ionomeric membranes, *Journal of Physical Chemistry*, Vol. 95, No. 15, 1991, pp. 6040–6044.

[81] Morris, D. R. and Sun, X., Water-sorption and transport properties of Nafion 117 H, *Journal of Applied Polymer Science*, Vol. 50, No. 8, 1993, pp. 1445–1452.

[82] Hinatsu, J. T., Mizuhata, M., and Takenaka, H., Water uptake of perfluorosulfonic acid membranes from liquid water and water vapor, *Journal of the Electrochemical Society*, Vol. 141, No. 6, 1994, pp. 1493–1498.

[83] Gates, C. M. and Newman, J., Equilibrium and diffusion of methanol and water in a nafion 117 membrane, *AIChE Journal*, Vol. 46, No. 10, 2000, pp. 2076–2085.

[84] Jalani, N., Choi, P., and Datta, R., TEOM: A novel technique for investigating sorption in proton-exchange membranes, *Journal of Membrane Science*, Vol. 254, No. 1-2, 2005, pp. 31–38.

[85] Onishi, L. M., Prausnitz, J. M., and Newman, J., Water - Nafion Equilibria. Absence of Schroeder's Paradox, *Journal of Physical Chemistry B*, Vol. 111, No. 34, 2007, pp. 10166–10173.

[86] Alberti, G. and Narducci, R., Evolution of Permanent Deformations (or Memory) in Nafion 117 Membranes with Changes in Temperature, Relative Humidity and Time, and Its Importance in the Development of Medium Temperature PEMFCs, *Fuel Cells*, Vol. 9, No. 4, 2009, pp. 410–420.

[87] Mangiagli, P., Ewing, C.S., a. X. K., Wang, Q., and Hickner, M., Dynamic water uptake of flexible polymer networks ion-containing polymer networks, *Fuel Cells*, Vol. 9, No. 4, 2009, pp. 432–438.

[88] Alberti, G., Narducci, R., and Sganappa, M., Effects of hydrothermal/thermal treatments on the water-uptake of Nafion membranes and relations with changes of conformation, counter-elastic force and tensile modulus of the matrix, *Journal of Power Sources*, Vol. 178, No. 2, 2008, pp. 575–583.

[89] Evans, C. E., Noble, R. D., Nazeri Thompson, S., Nazeri, B., and Koval, C. A., Role of conditioning on water uptake and hydraulic permeability of Nafion® membranes, *Journal of Membrane Science*, Vol. 279, No. 1-2, 2006, pp. 521–528.

[90] Ostrowska, J. and Narebska, A., Infrared study of hydration and association of functional groups in a perfluorinated Nafion membrane. - Part 2, *Colloid & Polymer Science*, Vol. 262, No. 4, 1984, pp. 305–310.

[91] Laporta, M., Pegoraro, M., and Zanderighi, L., Perfluorosulfonated membrane (Nafion): FT-IR study of the state of water with increasing humidity, *Physical Chemistry Chemical Physics*, Vol. 1, No. 19, 1999, pp. 4619–4628.

[92] Korzeniewski, C., Snow, D., and Basnayake, R., Transmission infrared spectroscopy as a probe of nafion film structure: Analysis of spectral regions fundamental to understanding hydration effects, *Applied Spectroscopy*, Vol. 60, No. 6, 2006, pp. 599–604.

[93] Ludvigsson, M., Lindgren, J., and Tegenfeldt, J., FTIR study of water in cast Nafion films, *Electrochimica Acta*, Vol. 45, No. 14, 2000, pp. 2267–2271.

[94] Cornet, N., Gebel, G., and De Geyer, A., Existence d'un paradoxe de Schroeder avec la membrane Nafion? étude par diffusion de rayons X aux petits angles, Vol. 8, 1998, pp. 63–68.

[95] Choi, P. and Datta, R., Sorption in proton-exchange membranes. An explanation of Schroeder's paradox, *Journal of the Electrochemical Society*, Vol. 150, No. 12, 2003, pp. E601–E607.

[96] Vallieres, C., Winkelmann, D., Roizard, D., Favre, E., Scharfer, P., and Kind, M., On Schroeder's paradox, *Journal of Membrane Science*, Vol. 278, No. 1-2, 2006, pp. 357–364.

[97] Bass, M. and Freger, V., Hydration of Nafion and Dowex in liquid and vapor environment: Schroeder's paradox and microstructure, *Polymer*, Vol. 49, No. 2, 2008, pp. 497–506.

[98] Broka, K. and Ekdunge, P., Oxygen and hydrogen permeation properties and water uptake of Nafion® 117 membrane and recast film for PEM fuel cell, *Journal of Applied Electrochemistry*, Vol. 27, 1997, pp. 117–123.

[99] Jalani, N. and Datta, R., The effect of equivalent weight, temperature, cationic forms, sorbates, and nanoinorganic additives on the sorption behavior of Nafion®, *Journal of Membrane Science*, Vol. 264, No. 1-2, 2005, pp. 167–175.

[100] Springer, T., Zawodzinski, T., and Gottesfeld, S., Polymer electrolyte fuel cell model, *Journal of the Electrochemical Society*, Vol. 138, No. 8, 1991, pp. 2334–2342.

[101] Péron, J., Mani, A., Zhao, X., Edwards, D., Adachi, M., Soboleva, T., Shi, Z., Xie, Z., Navessin, T., and Holdcroft, S., Properties of Nafion® NR-211 membranes for PEMFCs, *Journal of Membrane Science*, Vol. 356, No. 1-2, 2010, pp. 44–51.

[102] Yeo, R. S. and Yeager, H. L., *Modern Aspects of Electrochemistry N.16*, Vol. 16, Springer, New York, USA., 1985.

[103] Kim, S. and Mench, M. M., Investigation of Temperature-Driven Water Transport in Polymer Electrolyte Fuel Cell: Phase-Change-Induced Flow, *Journal of The Electrochemical Society*, Vol. 156, No. 3, 2009, pp. B353–B362.

[104] Perrin, J.-C., *Etude Expérimentale multi-échelles de la dynamique de l'eau dans les membranes ionomères utilisées en pile à combustible.*, Ph.D. thesis, Université Joseph Fourier, Grenoble I, Grenoble, France., 2006.

[105] Kreuer, K. D., On the development of proton conducting materials for technological applications, *Solid State Ionics*, Vol. 97, No. 1-4, 1997, pp. 1–15.

[106] Rivin, D., Kendrick, C. E., Gibson, P. W., and Schneider, N. S., Solubility and transport behavior of water and alcohols in Nafion®, *Polymer*, Vol. 42, No. 2, 2001, pp. 623–635.

[107] Paddison, S. and Paul, R., The nature of proton transport in fully hydrated Nafion®, *Physical Chemistry Chemical Physics*, Vol. 4, No. 7, 2002, pp. 1158–1163.

[108] Choi, P., Jalani, N. H., and Datta, R., Thermodynamics and Proton Transport in Nafion II. Proton Diffusion Mechanisms and Conductivity, *Journal of The Electrochemical Society*, Vol. 152, No. 3, 2005, pp. E123–E130.

[109] Janssen, G., A Phenomenological Model of Water Transport in a Proton Exchange Membrane Fuel Cell, *Journal of the Electrochemical Society*, Vol. 148, No. 12, 2001, pp. A1313–A1323.

[110] Sone, Y., Ekdunge, P., and Simonsson, D., Proton Conductivity of Nafion 117 as Measured by a Four-Electrode AC Impedance Method, *Journal of The Electrochemical Society*, Vol. 143, No. 4, 1996, pp. 1254–1259.

[111] Slade, S., Campbell, S., Ralph, T., and Walsh, F., Ionic conductivity of an extruded Nafion 1100 EW series of membranes, *Journal of the Electrochemical Society*, Vol. 149, No. 12, 2002, pp. A1556–A1564.

[112] Silva, R. F., De Francesco, M., and Pozio, A., Tangential and normal conductivities of Nafion® membranes used in polymer electrolyte fuel cells, *Journal of Power Sources*, Vol. 134, No. 1, 2004, pp. 18–26.

[113] Casciola, M., Alberti, G., Sganappa, M., and Narducci, R., On the decay of Nafion proton conductivity at high temperature and relative humidity, *Journal of Power Sources*, Vol. 162, No. 1, 2006, pp. 141–145.

[114] Xie, Z., Song, C., Andreaus, B., Navessin, T., Shi, Z., Zhang, J., and Holdcroft, S., Discrepancies in the measurement of ionic conductivity of PEMs using two- and four-probe AC impedance spectroscopy, *Journal of the Electrochemical Society*, Vol. 153, No. 10, 2006, pp. E173–E178.

[115] Alvarez Gallego, Y. and de Heer, M. P., Sub-Freezing Conductivity of PFSA Membranes, *Fuel Cells*, Vol. 9, No. 4, 2009, pp. 421–431.

[116] Cappadonia, M., Erning, J. W., Saberi Niaki, S. M., and Stimming, U., Conductance of Nafion 117 membranes as a function of temperature and water content, *Solid State Ionics*, Vol. 77, 1995, pp. 65–69.

[117] Halseid, R., Vie, P., and Tunold, R., Influence of Ammonium on Conductivity and Water Content of Nafion 117 Membranes, *Journal of the Electrochemical Society*, Vol. 151, No. 3, 2004, pp. A381–A388.

[118] Kawano, Y., Wang, Y., Palmer, R. A., and Aubuchon, S. R., Stress-Strain Curves of Nafion Membranes in Acid and Salt Forms, *Polímeros*, Vol. 12, 2002, pp. 96–101.

[119] Hayden, H. W. and Moffatt, W. G., a. W. J., *Structure and Properties of Materials: Mechanical Behaviour*, Vol. 3, John Wiley & Sons Ltd., New York, USA., 1965.

[120] Satterfield, M. B. and Benziger, J. B., Viscoelastic properties of Nafion at elevated temperature and humidity, *Journal of Polymer Science Part B: Polymer Physics*, Vol. 47, No. 1, 2009, pp. 11–24.

[121] Eisenberg, A. and Kim, J.-S., *Introduction to Ionomer*, John Wiley & Sons, New York, USA., 1998.

[122] Satterfield, M. B., Majsztrik, P. W., Ota, H., Benziger, J. B., and Bocarsly, A. B., Mechanical properties of Nafion and titania/Nafion composite membranes for polymer electrolyte membrane fuel cells, *Journal of Polymer Science Part B: Polymer Physics*, Vol. 44, No. 16, 2006, pp. 2327–2345.

[123] Kusoglu, A., Tang, Y., Lugo, M., Karlsson, A. M., Santare, M. H., Cleghorn, S., and Johnson, W. B., Constitutive response and mechanical properties of PFSA membranes in liquid water, *Journal of Power Sources*, Vol. 195, No. 2, 2010, pp. 483–492.

[124] Tang, Y., Karlsson, A., Santare, M., Gilbert, M., Cleghorn, S., and Johnson, W., An experimental investigation of humidity and temperature effects on the mechanical properties of perfluorosulfonic acid membrane, *Materials Science and Engineering A*, Vol. 425, No. 1-2, 2006, pp. 297–304.

[125] Solasi, R., Zou, Y., Huang, X., Reifsnider, K., and Condit, D., On mechanical behavior and in-plane modeling of constrained PEM fuel cell membranes subjected to hydration and temperature cycles, *Journal of Power Sources*, Vol. 167, No. 2, 2007, pp. 366–377.

[126] Werner, S., Jörissen, L., and Heider, U., Conductivity and mechanical properties of recast nafion films, *Ionics*, Vol. 2, 1996, pp. 19–23.

[127] Kundu, S., Simon, L. C., Fowler, M., and Grot, S., Mechanical properties of Nafion(TM) electrolyte membranes under hydrated conditions, *Polymer*, Vol. 46, No. 25, 2005, pp. 11707–11715.

[128] Fujimoto, C. H., Hickner, M. A., Cornelius, C. J., and Loy, D. A., Ionomeric Poly(phenylene) Prepared by Diels-Alder Polymerization: Synthesis and Physical Properties of a Novel Polyelectrolyte, *Macromolecules*, Vol. 38, 2005, pp. 5010–5016.

[129] Liu, D., Kyriakides, S., Case, S. W., Lesko, J. J., Li, Y., and McGrath, J. E., Tensile behavior of Nafion and sulfonated poly(arylene ether sulfone) copolymer membranes and its morphological correlations, *Journal of Polymer Science Part B: Polymer Physics*, Vol. 44, No. 10, 2006, pp. 1453–1465.

[130] De Moor, G., Bas, C., Charvin, N., Moukheiber, E., Niepceron, F., Breilly, N., Andre, J., Rossinot, E., Claude, E., Alberola, N. D., and Flandin, L., Understanding Membrane Failure in PEMFC: Comparison of Diagnostic Tools at Different Observation Scales, *Fuel Cells*, Vol. 12, No. 3, June 2012, pp. 356–364.

[131] Lamibrac, A., Maranzana, G., Lottin, O., Dillet, J., Mainka, J., Didierjean, S., Thomas, A., and Moyne, C., Experimental characterization of internal currents during the start-up of a proton exchange membrane fuel cell, *Journal of Power Sources*, Vol. 196, No. 22, 2011, pp. 9451–9458.

[132] Borup, R., Meyers, J., Pivovar, B., Kim, Y. S., Mukundan, R., Garland, N., Myers, D., Wilson, M., Garzon, F., Wood, D., Zelenay, P., More, K., Stroh, K., Zawodzinski, T., Boncella, J., McGrath, J. E., Inaba, M., Miyatake, K., Hori, M., Ota, K., Ogumi, Z., Miyata, S., Nishikata, A., Siroma, Z., Uchimoto, Y., Yasuda, K., Kimijima, K., and Iwashita, N., Scientific Aspects of Polymer Electrolyte Fuel Cell Durability and Degradation, *Chemical Reviews*, Vol. 107, No. 10, 2007, pp. 3904–3951.

[133] Chen, C. and Fuller, T. F., The effect of humidity on the degradation of Nafion® membrane, *Polymer Degradation and Stability*, Vol. 94, No. 9, 2009, pp. 1436–1447.

[134] Yuan, X.-Z., Zhang, S., Wang, H., Wu, J., Sun, J. C., Hiesgen, R., Friedrich, K. A., Schulze, M., and Haug, A., Degradation of a polymer exchange membrane fuel cell stack with Nafion® membranes of different thicknesses: Part I. In situ diagnosis, *Journal of Power Sources*, Vol. 195, No. 22, 2010, pp. 7594–7599.

[135] Zhou, C., *Chemical durability studies of ionomers and model compounds for fuel cell applications*, Ph.D. thesis, Case Western Reserve University, Ohio, USA., 2004.

[136] Collette, F., Lorentz, C., Gebel, G., and Thominette, F., Hygrothermal aging of Nafion®, *Journal of Membrane Science*, Vol. 330, No. 1-2, 2009, pp. 21–29.

[137] Adjemian, K. T., Srinivasan, S., Benziger, J., and Bocarsly, A. B., Investigation of PEMFC operation above 100 °C employing perfluorosulfonic acid silicon oxide composite membranes, *Journal of Power Sources*, Vol. 109, No. 2, 2002, pp. 356–364.

[138] Yang, C., Srinivasan, S., Bocarsly, A., Tulyani, S., and Benziger, J., A comparison of physical properties and fuel cell performance of Nafion and zirconium phosphate/Nafion composite membranes, *Journal of Membrane Science*, Vol. 237, 2004, pp. 145–161.

[139] Thampan, T., Jalani, N., Choi, P., and Datta, R., Systematic approach to design higher temperature composite PEMs, *Journal of the Electrochemical Society*, Vol. 152, 2005, pp. A316–A325.

[140] Sacca , A., Carbone, A., Passalacqua, E., D'Epifanio, A., Licoccia, S., Traversa, E., Sala, E., Traini, F., and Ornelas, R., Nafion-TiO2 hybrid membranes for medium temperature polymer electrolyte fuel cells (PEFCs), *Journal of Power Sources*, Vol. 152, No. 1-2, 2005, pp. 16–21.

[141] Jones, D. J. and Rozière, J., Advances in the Development of Inorganic-Organic Membranes for Fuel Cell Applications, *Advances in Polymer Science*, Vol. 215, Springer Berlin Heidelberg, 2008, pp. 219–264.

[142] Pan, J., Zhang, H., Chen, W., and Pan, M., Nafion-zirconia nanocomposite membranes formed via in situ sol-gel process, *International Journal of Hydrogen Energy*, Vol. 35, No. 7, 2010, pp. 2796–2801.

[143] Alvarez, A., Guzman, C., Carbone, A., Saccà , A., Gatto, I., Passalacqua, E., Nava, R., Ornelas, R., Ledesma Garcia, J., and Arriaga, L., Influence of silica morphology in composite Nafion membranes properties, *International Journal of Hydrogen Energy*, Vol. 36, No. 22, 2011, pp. 14725–14733.

[144] Wang, Z., Tang, H., Zhang, H., Lei, M., Chen, R., Xiao, P., and Pan, M., Synthesis of Nafion/CeO2 hybrid for chemically durable proton exchange membrane of fuel cell, *Journal of Membrane Science*, Vol. 421-422, 2012, pp. 201–210.

[145] Watanabe, M., Uchida, H., Seki, Y., Emori, M., and Stonehart, P., Self-Humidifying Polymer Electrolyte Membranes for Fuel Cells, *Journal of the Electrochemical Society*, Vol. 143, No. 12, 1996, pp. 3847–3852.

[146] Choi, P., Jalani, N. H., and Datta, R., Thermodynamics and Proton Transport in Nafion III. Proton Transport in Nafion/Sulfated ZrO2 Nanocomposite Membranes, *Journal of The Electrochemical Society*, Vol. 152, No. 8, 2005, pp. A1548–A1554.

[147] Jalani, N., Dunn, K., and Datta, R., Synthesis and characterization of Nafion®-MO2 (M = Zr, Si, Ti) nanocomposite membranes for higher temperature PEM fuel cells, *Electrochimica Acta*, Vol. 51, No. 3, 2005, pp. 553–560.

[148] Damay, F. and Klein, L. C., Transport properties of NafionTM composite membranes for proton-exchange membranes fuel cells, *Solid State Ionics*, Vol. 162-163, 2003, pp. 261–267.

[149] Bauer, F. and Willert Porada, M., Zirconium phosphate Nafion® composites - a microstructure-based explanation of mechanical and conductivity properties, *Solid State Ionics*, Vol. 177, 2006, pp. 2391–2396.

[150] Uchida, H., Ueno, Y., Hagihara, H., and Watanabe, M., Self-humidifying electrolyte membranes for fuel cells. Preparation of highly dispersed TiO2 particles in Nafion 112, *Journal of the Electrochemical Society*, Vol. 150, No. 1, 2003, pp. A57–A62.

Chapter 2

Experimental protocols

1 Introduction

It is well known that the good performances of Nafion membranes in PEMFC are due to their sorption and transport properties and to their mechanical stability, which result from the particular chemical structure and morphology of the polymer. Water sorption and transport properties (*e.g.* proton conductivity and water diffusion) of Nafion have been extensively studied over the past few decades [1, 2, 3, 4, 5, 6, 7, 8, 9, 10, 11, 12, 13, 14, 15, 16, 17]. Even though these studies have provided useful information, the direct comparison between literature results is hardly possible because the Nafion properties can depend on the various pre-treatments, to which it can be subjected while the variety of experimental procedures encountered in the literature is large. In addition, the ranges of temperature and relative humidity over which the Nafion properties were studied are generally limited.

Starting from this statement, it seemed relevant to us to perform systematic sorption, water self-diffusion, proton conductivity, and stress-strain measurements using simple and reproducible experimental procedures.

In this Chapter, we provide detailed information about the experimental protocols that were followed and on the instruments that were used to perform the measurements. These experiments are done with prepared membranes using a simple pre-treatment [18].

2 Sample cleaning and conditioning

Two commercially available Nafion membranes were used for the experimental characterization: solution-cast NRE212 films with a thickness of 50.8 μm and extruded N115 films with a thickness of 127 μm, both with an equivalent weight (EW) of 1100 $g.mol^{-1}$ and with an ion-exchange capacity (IEC) of 0.91 $milliequivalent.g^{-1}$. They were provided by Dupont and Ion Power, Inc. Before the measurements, the membranes were cut into strips, cleaned and conditioned according to the procedure [18] described below.

As-received membranes (lightly brown) are pre-cleaned by boiling in 3 wt% oxygen peroxide (H_2O_2) to eliminate organic residues. At this stage, the light brown color disappeared. The clean membranes are then rinsed with demineralized water at room temperature three times to remove H_2O_2. To guarantee a complete acidification, the samples are soaked consecutively into two strong acids:

- Aqueous 10M nitric acid (HNO_3) at room temperature during 30 min in order to replace the metallic cations (Na, K, Ca, Mg, etc) with protons (H^+); the re-acidified membranes are then rinsed with demineralized water at room temperature three times to remove HNO_3.
- Aqueous 1M sulfuric acid (H_2SO_4) at 100°C during 1 h; the membranes are then immersed in boiled demineralized water during 1 h to remove H_2SO_4.

It is important to highlight that the chosen pre-treatment was performed mostly using boiling water solutions, which expands greatly the porous structure of the membranes.

The pretreated Nafion membranes are cut into 7 – 9 cm^2 pieces and dried in a heating oven at atmospheric pressure and constant temperature, T_{dry} = 60°C during 24 h. The drying procedure shrinks the expanded porous structure [3, 19] and removes most, but not all, water molecules from the membrane [20, 21, 22, 23]. This means that the samples are actually not completely dried, which is an important issue to consider for the accurate characterization of their properties. This point will be discussed in Section 4.
The effects of the drying temperature on Nafion properties and aging are discussed in Chapter 3 and Chapter 4 (T_{dry} = 60°C, 80°C, 100°C and 110°C).

3 Water uptake

3.1 Water uptake measurement protocols

Numerous authors studied water sorption in Nafion membranes using gravimetric methods [3, 9, 15, 16, 24, 25, 26, 27, 28]. These methods consist in measuring the change of the membrane weight as a function of its water content. The membrane mass change is typically measured using a dynamic vapor sorption analyzer (DVS). Several authors use quartz crystal microbalance (QCM) like Krtil *et al.* [29] for monitoring water sorption and its kinetics in Nafion thin films. Jalani *et al.* [25] uses a tapered element oscillating microbalance (TEOM), where the Nafion sample, once deposited onto an oscillating body, causes a reduction of the oscillation frequency: this frequency variation make it possible to determine the mass of the sample as a function of the relative humidity and temperature.
Some advantages of the DVS microbalance:

- Its high resolution.
- Its wide range of measuring conditions in term of vapor partial pressure (water activity) and temperature.

- Its short equilibrium time (1 h) because of the small size of samples. However, this point may be discussed considering the (sometimes) slow dynamic of water sorption/desorption in Nafion.

Despite of these advantages, DVS microbalance may present some inconveniences:

- Only one sample can be tested at a time.
- It is not well adapted to high or very high relative humidity, because of possible water condensation inside the system.
- The water sorption kinetics may depend on the carrier gas rate.
- It is not adapted to the study of long-term or slow kinetic phenomena.
- It is not adapted to water sorption in liquid phase.

Alternative techniques to DVS, like conventional gravimetric method and the use of saturated salt solutions can give access to the membrane mass change over a wide range of temperature and relative humidity. Using saturated salt solutions and an analytical balance, we can measure accurately Nafion sorption isotherms when long equilibration times as well as good temperature homogeneity are required. Moreover, this method makes it possible to treat simultaneously a high number of samples, which allows investigating phenomena that are not considered usually, like the long-term evolution of Nafion properties at constant temperature and relative humidity. (Chapter 4).

3.2 Control of the relative humidity with saturated salts

The relative humidity (RH) is defined as the ratio of vapor partial pressure to the saturation pressure at a given temperature: $RH = P_w(T)/P_{sat}(T)$. Many methods exist for controlling the relative humidity [30]. One of the most adapted to closed small volume vessels consists in using saturated salt solutions: the air surrounding a saturated salt solution will achieve the equilibrium relative humidity [30, 31, 32, 33, 34, 35] however, some precautions are taken:

- Thermodynamic equilibrium between the three phases: solid (salt crystals), liquid (solution) and gas (air and water vapor mixture).
- Long enough equilibrium time.
- Suitable and stable temperature (*e.g.* at high temperature, there would be a risk of salts crystals setting on the solution surface rather than being immersed in the solution).

For this study, the relative humidity was controlled by selecting 9 different saturated salt solutions. The saturated salt solutions were prepared from reagent grade (extra pure) salt and

distilled water. The salt was then dissolved in water until saturation (*i.e.* crystals remaining in the solution). It must be noted that to obtain a homogeneous salt solution, the salt crystals should be added to water of a much higher temperature than that required; then the solution is cooled down. The variation of RH with respect to T is an important parameter that needs to be taken into consideration when examining the effect of temperature on water sorption. As a consequence, a great care was taken over the preparation of each saline solution and the measurement of the equilibrium RH with temperature. The vapor pressure was measured using a dew point analyzer (Vaisala HUMICAP®, HMT series) after 24 hours.

The nature of each salt solution used and the corresponding values of RH at temperatures varying from 20°C to 80°C are reported in Table 2.1. Those noted [a] are taken from reference [34]. While the others noted [b] were measured. In this case, the reported errors include maximal variations of RH over several tens of days. At 20°C, the measured values and the literature values differ by 1-2 % percentage points, probably because of the following:

- slow equilibration time,
- temperature variations,
- or the presence of impurities.

In the following we use the values that were measured with our solutions (noted [b]).

Table 2.1: Saturated saline solutions and corresponding equilibrium relative humidity (RH) as a function of temperature.

Salt	LiCl	$MgCl_2$	KCO_3	NaBr
T(°C)	***RH1***	***RH2***	***RH3***	***RH4***
20	0.113±0.003 [a]	0.330±0.002 [a]	0.432±0.003 [a]	0.591±0.004 [a]
20	0.094±0.010 [b]	0.315±0.002 [b]	0.434±0.002 [b]	0.563±0.002 [b]
30	0.113±0.002 [a]	0.324±0.001 [a]	0.431±0.005 [a]	0.560±0.004 [a]
40	0.112±0.002 [a]	0.316±0.001 [a]	0.403±0.002 [b]	0.532±0.004 [a]
50	0.111±0.002 [a]	0.305±0.001 [a]	0.403±0.002 [b]	0.509±0.006 [a]
60	0.110±0.003 [a]	0.293±0.002 [a]	0.403±0.002 [b]	0.497±0.008 [a]
70	0.108±0.003 [a]	0.278±0.003 [a]	0.403±0.002 [b]	0.497±0.011 [a]
80	0.105±0.004 [a]	0.261±0.003 [a]	0.390±0.007 [b]	0.514±0.015 [a]

Salt	KI	NaCl	KCl	$Ca(H_2PO_4)_2{\cdot}H_2O$	K_2SO_4
T(°C)	***RH5***	***RH6***	***RH7***	***RH8***	***RH9***
20	0.700±0.003 [a]	0.755±0.001 [a]	0.851±0.003 [a]	0.936±0.003 [b]	0.980±0.005 [a]
20	0.673±0.011 [b]	0.740±0.001 [b]	0.833±0.004 [b]	0.921±0.002 [b]	0.968±0.004 [b]
30	0.679±0.002 [a]	0.751±0.001 [a]	0.836±0.003 [a]	0.936±0.003 [b]	0.970±0.004 [a]
40	0.661±0.002 [a]	0.747±0.001 [a]	0.823±0.003 [a]	0.936±0.003 [b]	0.964±0.004 [a]
50	0.645±0.003 [a]	0.744±0.002 [a]	0.812±0.003 [a]	-	0.958±0.005 [a]
60	0.631±0.003 [a]	0.745±0.003 [a]	0.803±0.004 [a]	-	0.953±0.008 [b]
70	0.619±0.004 [a]	0.751±0.005 [a]	0.795±0.006 [a]	-	0.953±0.008 [b]
80	0.610±0.005 [a]	0.763±0.007 [a]	0.789±0.008 [a]	-	0.915±0.003 [b]

3.3 Water sorption measurements

3.3.1 Sorption in water vapor

Each Nafion sample was placed in an open 20 cm^3 glass bottle inserted in a sealed container in which the relative humidity (RH) was controlled thanks to the saturated salt solution (Figure 2.1 (left)). The container was then put in a heating oven at temperature T for a period of 7 days (4 days proposed by Bass and Freger [36]), allowing the membrane to reach its equilibrium state before measurements (Figure 2.1 (right)), which was checked by weighing the sample daily. To carry out water uptake measurements, the glass bottle containing the sample is taken out of the sealed container, immediately closed with a screw cap, and weighed using a precision balance.

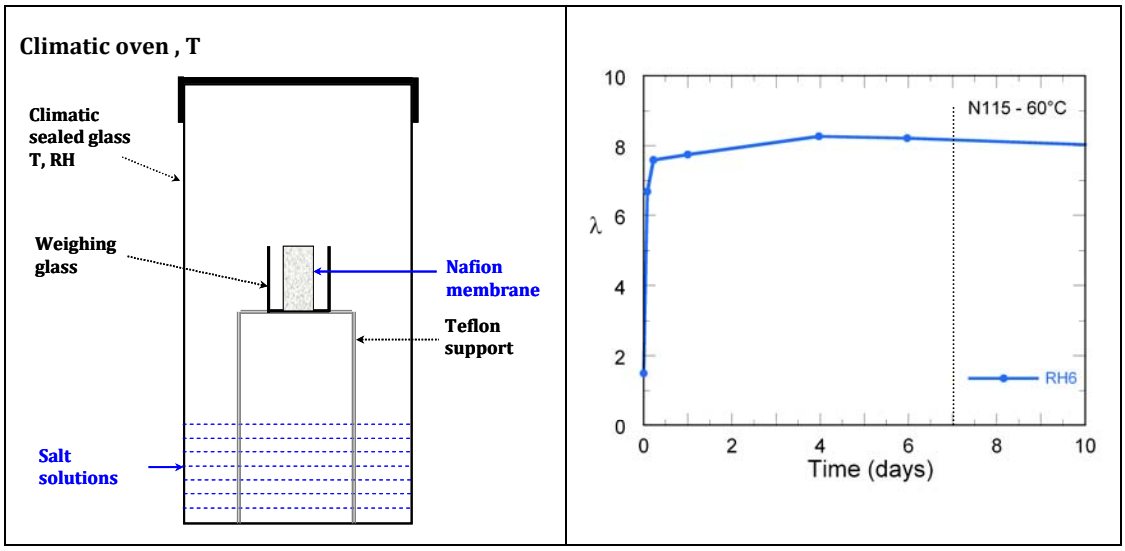

Figure 2.1: Left: schematic representation of the humidity controlled cell using a salt solution. Right: equilibrium sorption curve of N115 at 60°C and RH6 (RH = 0.74).

3.3.2 Sorption in liquid water

The membranes were immersed in distilled water at different temperatures for 1 h. This equilibrium time is necessary for the samples to reach a constant weight before the measurements [37]. The wet membranes were then surface-dried using KimWipes, and immediately weighted.

3.4 Experimental errors

The experimental errors were minimized by averaging the results over a set of three samples. The uncertainties came from errors on the relative humidity imposed by the saline solutions, the stability of the temperature of the oven, the non-homogeneity of the different samples and, mostly, systematic weighting errors resulting from the manipulation of the samples. The precision of the balance was 0.1 mg and the typical weight of a 9 cm^2 membrane sample was

about 10 mg for Nafion NRE212 and 20 mg for Nafion N115. The experimental error on λ is thus more important in NRE212 than in N115: *e.g.* about 17% and 7.6% at λ= 7, respectively.

3.5 Membrane swelling

The membrane water sorption results also in dimensional or volume changes (*i.e.* swelling). To carry out the swelling studies, several samples of approximately 2.5 cm x 2.5 cm and 3 cm x 3 cm (previously pre-treated) are measured in the three directions of space (length, y_0 ; width, x_0 ; and thickness, z_0). The samples are then put in contact with vapor and/or immersed in liquid water at 60°C. Once the equilibrium is reached, their dimensions are measured again (x_1, y_1, z_1) and the swelling is expressed as a percentage (with reference to the dry dimensions, x_0, y_0, z_0), according to equations (Eq 1), (Eq 2), and (Eq 3):

$$S_x = \frac{x_1 - x_0}{x_0} * 100 \qquad \text{Eq 1}$$

$$S_y = \frac{y_1 - y_0}{y_0} * 100 \qquad \text{Eq 2}$$

$$S_z = \frac{z_1 - z_0}{z_0} * 100 \qquad \text{Eq 3}$$

Figure 2.2 shows the swelling in percentage of volume, surface area, and the three directions of space for a Nafion 115 membrane in equilibrium with vapor at 60°C. The experimental errors were minimized by averaging the results over a set of three samples.

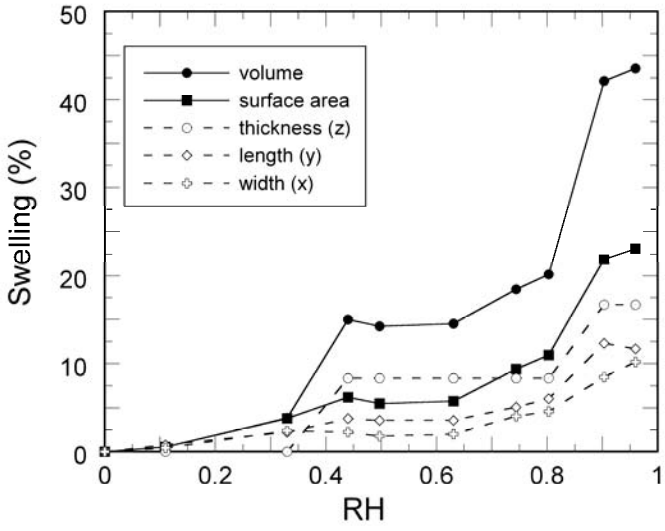

Figure 2.2: Swelling (%) of N115 membranes at 60°C.

4 Residual water

It is important to highlight that even after a drying period of 24 hours at different temperatures (60°C, 80°C, 100°C and 110°C), N115 and NRE212 membranes still contain a certain quantity of water in their structure (see Chapter 3, Section 2.1). As a consequence, the mass of water measured using a gravimetric method does not correspond to that actually adsorbed in the membrane. It is defined as:

$$m^{w}_{H_2O} = m - m^{w}_{dry} \quad \text{Eq 4}$$

where m is the mass of the wet membrane and m^{w}_{dry} is the mass measured after the drying pre-treatment. The water mass fraction with respect to the mass of the membrane measured after the drying pre-treatment (m^{w}_{dry}) should be denoted as:

$$c^{w} = \frac{m^{w}_{H_2O}}{m^{w}_{dry}} \quad \text{Eq 5}$$

The superscript (^{w}) indicates that a certain quantity of residual water remains in the structure of the membrane.

The residual mass of water ($m^{*}_{H_2O}$) as well as the real mass of dry Nafion (m_{dry}), were determined using Nuclear Magnetic Resonance (NMR).

4.1 Nuclear Magnetic Resonance (NMR) measurement protocol

NMR was used to estimate the quantity of residual water in Nafion after the drying pre-treatment. The purpose of these experiments was to determine the correction to apply to the sorption isotherms and the possible variation of this correction with temperature. Standard pulsed-field gradient (PFG) NMR was also used to measure the water self-diffusion coefficient in the membranes at the micrometric scale.

All NMR measurements were performed on a Bruker Avance spectrometer, which was operating at the proton Larmor frequency of 600 MHz. The water quantity was determined at a constant temperature of 25 ± 0.1°C by measuring directly the intensity of the hydrogen (^{1}H) nuclear magnetization following a π/2 radio frequency pulse. The accuracy of the proportionality between ^{1}H magnetization and the quantity of protons in the measurement probe was checked using a series of H_2O + D_2O mixtures with known quantities of liquids.

Measurements of the water self-diffusion coefficient (D_s) in Nafion were performed at 25 ± 0.1°C by PFGNMR, under the conventional stimulated spin-echo sequence [38]. The field gradient was applied in the z-direction, *i.e.* aligned with the main magnetic field, with a maximum strength of 20 G/cm. The diffusion time was set in the range 100-200 ms, depending on the hydration of the membrane.

Nafion samples were cut in 15 cm × 1 cm strips, rolled at the bottom of 10 mm diameter NMR tubes, and hydrated by adding a known quantity of water on the inside walls of the tubes. The time necessary for the membrane to adsorb all water was in the range of 10-15 days. The typical weight of a Nafion N115 strip was about 350 mg. Three series of Nafion samples, dried 24 h at a drying temperature T_{dry} = 60°C, 80°C, 100°C or 110°C, were measured. Each series contained 10 samples, hydrated in the range of water mass fraction of $0.02 < c^w < 0.2$.

4.2 Calibration curve

For NMR method, it is important to plot a calibration curve prior to the water self-diffusion coefficient (D_s) measurements in order to obtain a signal proportional to the mass of water measured. Figure 2.3 shows this calibration curve. The curve was determined in the range of the amount of water usually adsorbed in Nafion membranes, starting with the non-zero signal of the empty tube. The maximal systematic error in the measurement was estimated to ±5%.

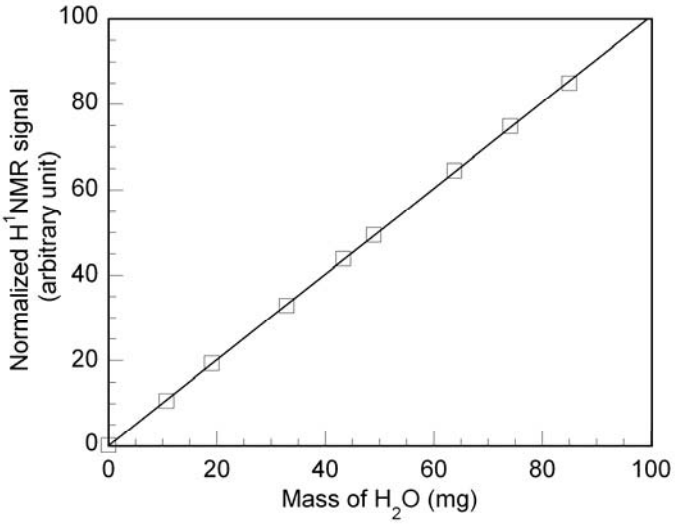

Figure 2.3: Calibration curve at 25°C.

5 Proton conductivity measurements

Several groups have previously studied the conductivity of Nafion membranes [6, 17, 26, 39, 40, 41, 42, 43]. The main difficulty in the analysis and comparison of these works is related with the utilization of different parameters, such as: cell geometry, technique employed, type of membrane, sample preparation method, and equilibration time.

As an example, there are two kind of geometry in the literature regarding the direction of the conductivity measurements: in-plane and through-plane directions. The in-plane direction conductivity method is the most used due to the simple geometry set-up. This set-up is known to be relatively insensitive to the contact impedance at the current carrying electrodes; however, the in-plane direction does not represent the real direction of ionic motion through a fuel cell membrane. In other words, the through-plane direction conductivity method must be used when anisotropic behavior exists in membranes. Anyhow, important attention has to be paid to the complexity of its cell geometry, *i.e.* the pressing effect between the membrane and the two current collectors, and the low capacity of hydration of sandwiched membranes during conductivity tests.

Based on the mentioned statements, the proton conductivity measurements of Nafion N115 and NRE212 were performed in the in-plane direction by alternating current (AC) impedance spectroscopy using a home-made 4-points conductivity cell.

5.1 4-points conductivity cell

The home-made 4-points cell is mostly used for obtaining accurate measurements of resistances. The cell is designed to give a uniform current distribution across the potential (inner) electrodes. Also, it is designed to reduce the interfacial impedances due to the potential sensing electrodes. They do not support the current flow used to perturb the system. A schematic representation of the cell is displayed on Figure 2.4. The 7.5 cm^2 membrane sample was fixed to the cell onto the four platinum electrodes and clamped. The Teflon support was opened to the environment in its upper central part to ensure a good hydration of the membrane during the measurement. Then, the cell was placed inside a temperature- and humidity-controlled steel vessel and connected to a potentiostat/galvanostat for the electrochemical impedance measurements.

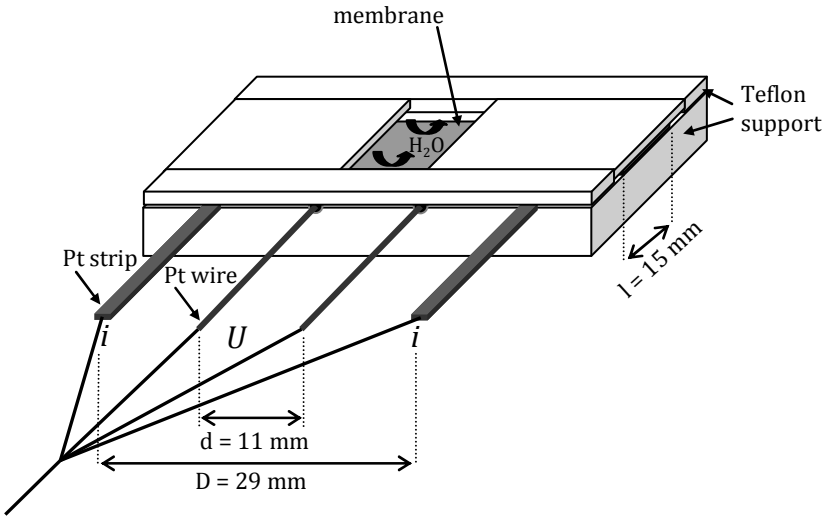

Figure 2.4: Schematic representation of the 4 probes conductivity cell designed for this study.

The impedance of the sample was calculated from the measured voltage induced by a small imposed alternating current range (i_{rms} = 1 mA). The current flowed through the outer pair of strip electrodes while the voltage difference (the potential) was measured between the inner pair of wire electrodes. The impedance was measured over frequencies ranging from 10 Hz to 100 kHz at a signal amplitude of 5 mV.

Considering the cell geometry described on Figure 2.4, the membrane proton conductivity (σ) is given by [6]:

$$\sigma = \frac{d}{ZS} \qquad \text{Eq 6}$$

where d is the distance between the potential electrodes, Z is the impedance and S is the membrane cross-section.

The impedance of the membrane is a complex number, which is defined as follow:

$$Z = Z' + iZ'' \qquad \text{Eq 7}$$

where the real part of the impedance is the resistance, and the imaginary part is the reactance, which is close to zero and neglected (Figure 2.5).

The real part of the impedance was calculated by measuring the ratio of the voltage difference amplitude to the current amplitude.

$$Z = \frac{\Delta U}{\Delta i} \approx R \qquad \text{Eq 8}$$

where U is the voltage, i is the imposed alternating current, and R is the resistance of the membrane.

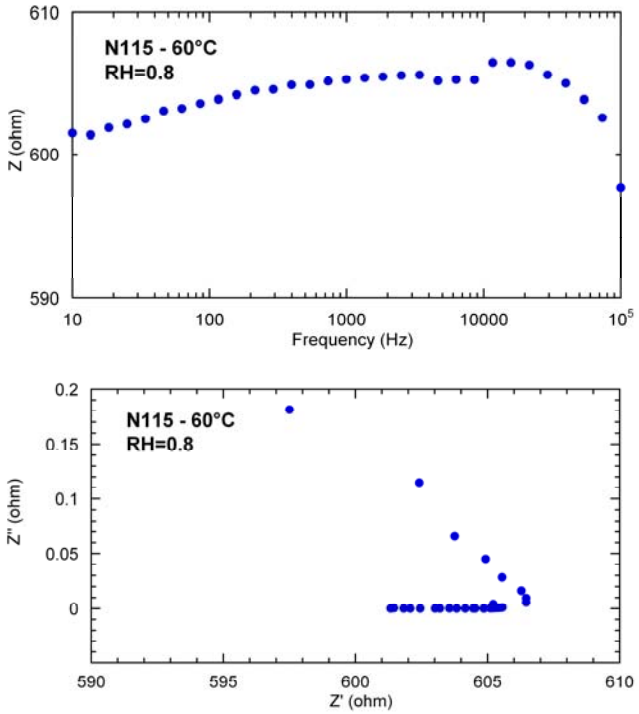

Figure 2.5: Nyquist plot of membrane impedance (N115) in the frequency range 10 Hz to 100 kHz.

Figure 2.6 shows the whole of the conductivity cell. This system is coupled to a potentiostat/galvanostat (AUTOLAB-PGSTAT 302N). As seen in the scheme, a humidifier was used in order to control the humidity into the vessel (RH = 0.1 to RH = 0.95). In addition, a heating circuit was inserted in the vessel walls (Lauda Ecoline Staredition RE 306) to homogenize the temperature. Once the cell was closed, temperature and relative humidity were measured respectively by a thermocouple and a dew point analyzer (Vaisala HUMICAP®, HMT series), and by then recorded using a LabView.

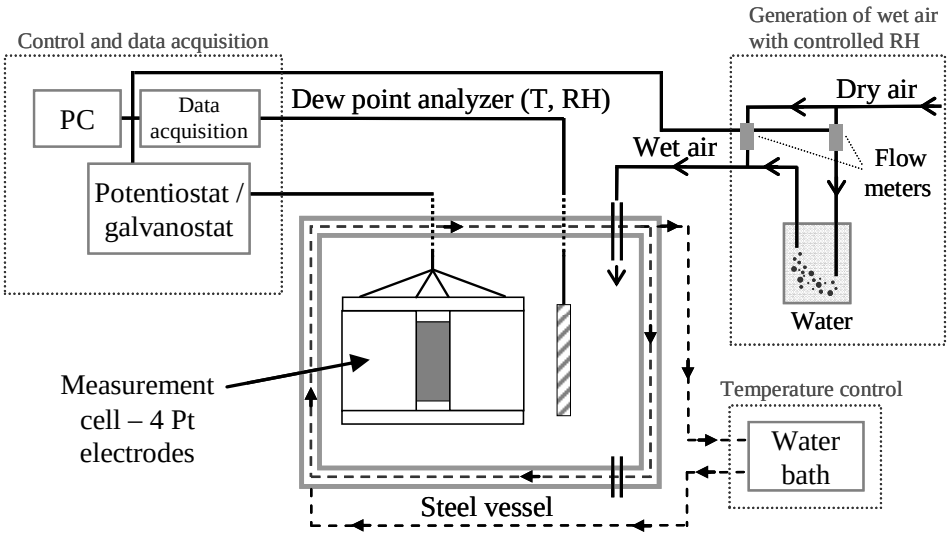

Figure 2.6: Schematic representation of the conductivity cell.

Prior to the experiment, samples were dried at T_{dry} during 24 h, removed from the oven and left at ambient conditions for 5 minutes. Then, the width and thickness of the membrane and the length between the potential electrodes were precisely determined. It was assumed a 10% increase of the thickness due to swelling in each case.

To initiate the experiment, the sample was first kept at constant temperature T (60°C) and low relative humidity (RH = 0.1) for 2 hours, to ensure that most of water remaining from the preceding experiment was gone. Then, the RH was increased slowly (from RH = 0.1 to RH = 0.95) by steps of 3 percentage points every 30 min to ensure a complete equilibrium. The conductivity was registered every 450 s, which corresponds to a total time of 8h30 (Figure 2.7 (left)). These experiments were also done by decreasing the relative humidity to check the reproducibility of the results. Moreover, the stability of the results was tested by keeping a sample at RH = 0.8 during 3h30 (Figure 2.7 (right)).

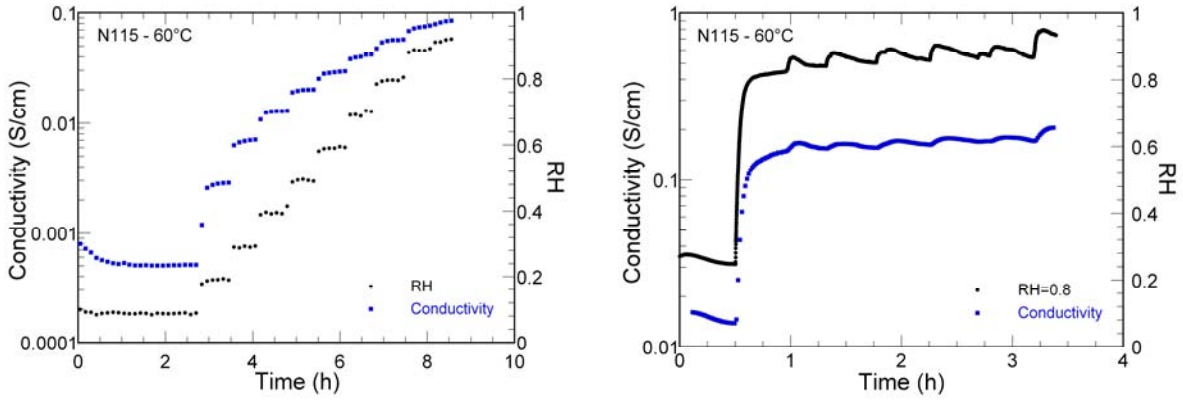

Figure 2.7: Evolution of the conductivity of N115 at 60°C and from RH = 0.1 to RH = 0.93 (left), and RH = 0.8 (right).

5.2 Experimental errors

Errors in the measurement generally arose from imperfect contacts between two electrodes or swelling of the sample inside the conductivity cell. Based on the reproducibility of the results we estimate the maximum relative error on the measurement of σ was of 3 to 5 %.

6 Stress-strain and young modulus

As for the other Nafion properties, tensile data are difficult to analyze and to compare with literature because of varying experimental parameters, such as: pre-treatment of the membrane, phase of external water (*i.e.* vapor *vs.* liquid), equilibration time, technique used, and tensile direction in the plane of membranes.

6.1 Deformation device system (DDS) machine

The samples were previously pretreated (conditioned and dried) at T_{dry}, 24 h. To follow the influence of drying pre-treatment on Nafion tensile properties, the membranes were dried at temperatures of 30°C, 80°C, 100°C, and 110°C.

The stress-strain experiments were performed in a deformation device system (DDS) machine (Kammrath and Weiss - GmbH) with a load cell of 500 N, a measuring range control from -15.000 to 15.000 µm, and an accuracy of 0.1 %. This device is displayed on Figure 2.8. In addition, the tensile system is coupled with a DDS software for the determination of the stress-strain curves.

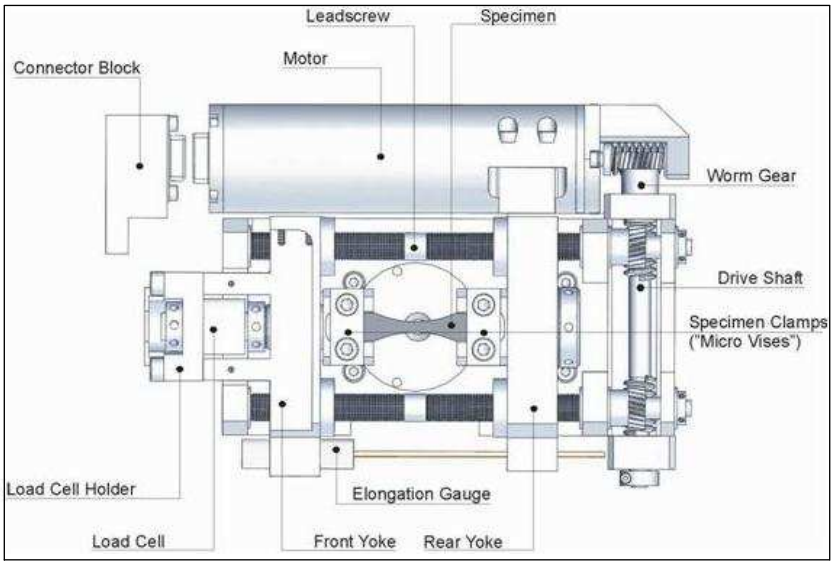

Figure 2.8: Scheme of the deformation device system - 500 N, reprinted from Kammrath & Weiss GmbH [44].

6.2 Tensile test

We conducted several tensile tests with Nafion N115 and NRE212 of around 127 µm and 50 µm of thickness, respectively. In addition to the variation on their thicknesses, these membranes were produced differently: extrusion and solution-cast. Due to that, Nafion N115 is slightly oriented, in contrast to Nafion NRE212, which has no preferred direction (before being stretched). The effect of thickness, the method of fabrication, and as consequence, the anisotropic behavior of Nafion were not considered in this work, which must be considered as a preliminary approach.

Prior to the experiments, Nafion samples were cut into small strips following a necked form (as shown in Figure 2.9) in order to observe a longer and more stable deformation until fracture. The sample cross-section area is of 5.08 x 10^{-7} m^2 for N115 and 2.03 x 10^{-7} m^2 for N212, the width and the thickness were measured using a digital caliper. Finally, the samples were stored in the ambient. T and RH were measured and controlled respectively by a thermocouple and a dew point analyzer (Vaisala HUMICAP®, HMT series).

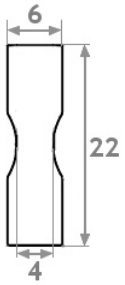

Figure 2.9: Scheme of the machined cutting die.

The sample was aligned with the machine axis and clamped with two grips (at the machine extremities). The gauge length was approximately 15 mm as determined by the grip separation. To keep the samples sandwiched between the jaws of the machine and the grips, two pieces of sandpaper were used on the sample-grips contact sides, and two pieces of rubber on the sample-machine jaw contact sides.

The dynamic experiments were performed with a strain rate of 50 µm/s and the initial static force of 0.1 N. All Nafion samples were tested at ambient atmosphere ~25°C and RH = 0.4.
The stress is defined and calculated by:

$$Stress(MPa) = \frac{F}{A} \qquad \text{Eq 9}$$

where F is the measured force and A is the original cross-sectional area (load direction).
The strain is defined as the change in the length of deformed membrane (Δl) with respect to the initial non-deformed length (l_0).

$$\varepsilon(\%) = \frac{\Delta l}{l_0} \times 100 \qquad \text{Eq 10}$$

All the curves started at $\varepsilon = 0\%$.

The Young modulus (E) was obtained from the initial slope of the stress-strain curves. The initial points of the curve were adjusted with a linear trendline. On the other hand, the plastic modulus was obtained from the final slope of the stress-strain curves, considering only the last

points of the curves. The error may occur since the coefficient of a trendline is quite dependent on the number of points considered in the initial curve.

Another important parameter to determine is the breaking point (or ultimate point) of the sample. However, it was not obtained often, since the membrane did not break down in the middle, but broke at the joints. In this case, the end of the tensile curve is not displayed on the graphs.

7 Conclusion

The experimental protocols were kept as simple as possible. Water sorption protocols were developed to allow very long equilibration times, as well as very good temperature and humidity homogeneity, this to favor the reproducibility on the measurements.

The emphasis was put on the pre-treatment of the Nafion membranes. N115 and NR212 membranes are received in the acidic $-RSO_3H$ form. Our cleaning and acidification protocol aims at making sure that each SO_3^- group is neutralized with an H^+ counter-ion. More importantly, this conditioning erases the thermal history of the membrane and prepares the membrane in a well defined reference state. This reference state is very close from the as-received state in terms of proton conductivity and water sorption. When the membrane sheet is new, but was let in the atmosphere in contact with air for a long period of time, it darkens because it adsorbs dust and its properties may be altered. In this latter case our protocol restores the membrane back to the initial state.

It is important to highlight that when the membrane samples are heat-treated at moderate temperature in the range $60°C < T_{dry} < 100°C$, some residual water stays strongly attached to the structure of the polymer and it may cause serious modifications to its properties. This is why the amount of residual water is evaluated in Chapter 3.

8 References

[1] Morris, D. R. and Sun, X., Water-sorption and transport properties of Nafion 117 H, *Journal of Applied Polymer Science*, Vol. 50, No. 8, 1993, pp. 1445–1452.

[2] Zawodzinski, Jr., T. A., Springer, T. E., Davey, J., Jestel, R., Lopez, C., Valerio, J., and Gottesfeld, S., A Comparative Study of Water Uptake By and Transport Through Ionomeric Fuel Cell Membranes, *Journal of the Electrochemical Society*, Vol. 140, No. 7, 1993, pp. 1981–1985.

[3] Hinatsu, J. T., Mizuhata, M., and Takenaka, H., Water uptake of perfluorosulfonic acid membranes from liquid water and water vapor, *Journal of the Electrochemical Society*, Vol. 141, No. 6, 1994, pp. 1493–1498.

[4] Cappadonia, M., Erning, J. W., Saberi Niaki, S. M., and Stimming, U., Conductance of Nafion 117 membranes as a function of temperature and water content, *Solid State Ionics*, Vol. 77, 1995, pp. 65–69.

[5] Werner, S., Jörissen, L., and Heider, U., Conductivity and mechanical properties of recast nafion films, *Ionics*, Vol. 2, 1996, pp. 19–23.

[6] Sone, Y., Ekdunge, P., and Simonsson, D., Proton Conductivity of Nafion 117 as Measured by a Four-Electrode AC Impedance Method, *Journal of The Electrochemical Society*, Vol. 143, No. 4, 1996, pp. 1254–1259.

[7] Broka, K. and Ekdunge, P., Oxygen and hydrogen permeation properties and water uptake of Nafion® 117 membrane and recast film for PEM fuel cell, *Journal of Applied Electrochemistry*, Vol. 27, 1997, pp. 117–123.

[8] Gates, C. M. and Newman, J., Equilibrium and diffusion of methanol and water in a nafion 117 membrane, *AIChE Journal*, Vol. 46, No. 10, 2000, pp. 2076–2085.

[9] Legras, M., Hirata, Y., Nguyen, Q. T., Langevin, D., and Métayer, M., Sorption and diffusion behaviors of water in Nation 117 membranes with different counter ions, *Desalination*, Vol. 147, No. 1-3, 2002, pp. 351–357.

[10] Kawano, Y., Wang, Y., Palmer, R. A., and Aubuchon, S. R., Stress-Strain Curves of Nafion Membranes in Acid and Salt Forms, *Polímeros*, Vol. 12, 2002, pp. 96–101.

[11] Choi, P. and Datta, R., Sorption in proton-exchange membranes. An explanation of Schroeder's paradox, *Journal of the Electrochemical Society*, Vol. 150, No. 12, 2003, pp. E601–E607.

[12] Jalani, N. and Datta, R., The effect of equivalent weight, temperature, cationic forms, sorbates, and nanoinorganic additives on the sorption behavior of Nafion®, *Journal of Membrane Science*, Vol. 264, No. 1-2, 2005, pp. 167–175.

[13] Vallieres, C., Winkelmann, D., Roizard, D., Favre, E., Scharfer, P., and Kind, M., On Schroeder's paradox, *Journal of Membrane Science*, Vol. 278, No. 1-2, 2006, pp. 357–364.

[14] Liu, D., Kyriakides, S., Case, S. W., Lesko, J. J., Li, Y., and McGrath, J. E., Tensile behavior of Nafion and sulfonated poly(arylene ether sulfone) copolymer membranes and its morphological correlations, *Journal of Polymer Science Part B: Polymer Physics*, Vol. 44, No. 10, 2006, pp. 1453–1465.

[15] Takata, H., Mizuno, N., Nishikawa, M., Fukada, S., and Yoshitake, M., Adsorption properties of water vapor on sulfonated perfluoropolymer membranes, *International Journal of Hydrogen Energy*, Vol. 32, No. 3, 2007, pp. 371–379.

[16] Majsztrik, P. W., Satterfield, M. B., Bocarsly, A. B., and Benziger, J. B., Water sorption, desorption and transport in Nafion membranes, *Journal of Membrane Science*, Vol. 301, No. 1-2, 2007, pp. 93–106.

[17] Onishi, L. M., Prausnitz, J. M., and Newman, J., Water - Nafion Equilibria. Absence of Schroeder's Paradox, *Journal of Physical Chemistry B*, Vol. 111, No. 34, 2007, pp. 10166–10173.

[18] Xu, F., *Caracterisation, Application et Modification de Membranes Echangeuses d'Ions en Milieu Hydro-Organique et Organique*, Ph.D. thesis, Université Montpellier II Sciences et Techniques du Languedoc, Montpellier, France., 2004.

[19] Zawodzinski, Jr., T. A., Derouin, C., Radzinski, S., Sherman, R. J., Smith, V. T., Springer, T. E., and Gottesfeld, S., Water Uptake by and Transport Through Nafion® 117 Membranes, *Journal of the Electrochemical Society*, Vol. 140, No. 4, 1993, pp. 1041–1047.

[20] Ostrowska, J. and Narebska, A., Infrared study of hydration and association of functional groups in a perfluorinated Nafion membrane. - Part 2, *Colloid & Polymer Science*, Vol. 262, No. 4, 1984, pp. 305–310.

[21] Laporta, M., Pegoraro, M., and Zanderighi, L., Perfluorosulfonated membrane (Nafion): FT-IR study of the state of water with increasing humidity, *Physical Chemistry Chemical Physics*, Vol. 1, No. 19, 1999, pp. 4619–4628.

[22] Korzeniewski, C., Snow, D., and Basnayake, R., Transmission infrared spectroscopy as a probe of nafion film structure: Analysis of spectral regions fundamental to understanding hydration effects, *Applied Spectroscopy*, Vol. 60, No. 6, 2006, pp. 599–604.

[23] Ludvigsson, M., Lindgren, J., and Tegenfeldt, J., FTIR study of water in cast Nafion films, *Electrochimica Acta*, Vol. 45, No. 14, 2000, pp. 2267–2271.

[24] Dreyfus, B., Gebel, G., Aldebert, P., Pineri, M., Escoubes, M., and Thomas, M., Distribution of the 'micelles' in hydrated perfluorinated ionomer membranes from SANS experiments, *Journal de physique Paris*, Vol. 51, No. 12, 1990, pp. 1341–1354.

[25] Jalani, N., Choi, P., and Datta, R., TEOM: A novel technique for investigating sorption in proton-exchange membranes, *Journal of Membrane Science*, Vol. 254, No. 1-2, 2005, pp. 31–38.

[26] Péron, J., Mani, A., Zhao, X., Edwards, D., Adachi, M., Soboleva, T., Shi, Z., Xie, Z., Navessin, T., and Holdcroft, S., Properties of Nafion® NR-211 membranes for PEMFCs, *Journal of Membrane Science*, Vol. 356, No. 1-2, 2010, pp. 44–51.

[27] Collette, F., *Vieillissement Hygrothermique du Nafion*®, Ph.D. thesis, École Nationale Supérieure d'Arts et Métiers, Paris, France., 2008.

[28] Mangiagli, P., Ewing, C.S., a. X. K., Wang, Q., and Hickner, M., Dynamic water uptake of flexible polymer networks ion-containing polymer networks, *Fuel Cells*, Vol. 9, No. 4, 2009, pp. 432–438.

[29] Krtil, P., Trojanek, A., and Samec, Z., Kinetics of Water Sorption in NafionThin Films-Quartz Crystal Microbalance Study, *Journal of Physical Chemistry B*, Vol. 105, No. 33, 2001, pp. 7979–7983.

[30] Wexler, A. and Brombacher, W. G., Methods of Measuring Humidity and Testing Hygrometers, Tech. Rep. Circular 512, National Bureau of Standards, 1951.

[31] Wexler, A. and Hasegawa, S., Relative Humidity - Temperature Relationships of Some Saturated Salt Solutions in the Temperature Range 0°C to 50°C, *Journal of Research of the National Bureau of Standards*, Vol. 53, 1954, pp. 19–26.

[32] Young, J. F., Humidity control in the laboratory using salt solutions-a review, *Journal of Applied Chemistry*, Vol. 17, No. 9, 1967, pp. 241–245.

[33] Arai, C., Hosaka, S., Murase, K., and Sano, Y., Measurements of the relative humidity of saturated aqueous salt solutions, *Journal of Chemical Engineering of Japan*, Vol. 9, No. 4, 1976, pp. 328–330.

[34] Greenspan, L., Humidity Fixed Points of Binary Saturated Aqueous Solutions, *Journal of Research of the National Bureau of Standards-A, Physic and Chemestry*, Vol. 81A, 1977, pp. 89–96.

[35] The scale of relative humidity of air certified against saturated salt solutions, Tech. rep., Organisation Internationale de Métrologie Légale (OIML), 1996.

[36] Bass, M. and Freger, V., Hydration of Nafion and Dowex in liquid and vapor environment: Schroeder's paradox and microstructure, *Polymer*, Vol. 49, No. 2, 2008, pp. 497–506.

[37] Alberti, G., Narducci, R., and Sganappa, M., Effects of hydrothermal/thermal treatments on the water-uptake of Nafion membranes and relations with changes of conformation, counter-elastic force and tensile modulus of the matrix, *Journal of Power Sources*, Vol. 178, No. 2, 2008, pp. 575–583.

[38] Stejskal, E. and Tanner, J., Spin diffusion measurements: Spin echoes in the presence of a time-dependent field gradient, *Journal of Chemical Physics*, Vol. 42, No. 1, 1965, pp. 288–292.

[39] Slade, S., Campbell, S., Ralph, T., and Walsh, F., Ionic conductivity of an extruded Nafion 1100 EW series of membranes, *Journal of the Electrochemical Society*, Vol. 149, No. 12, 2002, pp. A1556–A1564.

[40] Silva, R. F., De Francesco, M., and Pozio, A., Tangential and normal conductivities of Nafion® membranes used in polymer electrolyte fuel cells, *Journal of Power Sources*, Vol. 134, No. 1, 2004, pp. 18–26.

[41] Casciola, M., Alberti, G., Sganappa, M., and Narducci, R., On the decay of Nafion proton conductivity at high temperature and relative humidity, *Journal of Power Sources*, Vol. 162, No. 1, 2006, pp. 141–145.

[42] Xie, Z., Song, C., Andreaus, B., Navessin, T., Shi, Z., Zhang, J., and Holdcroft, S., Discrepancies in the measurement of ionic conductivity of PEMs using two- and four-probe AC impedance spectroscopy, *Journal of the Electrochemical Society*, Vol. 153, No. 10, 2006, pp. E173–E178.

[43] Kidena, K., Ohkubo, T., Takimoto, N., and Ohira, A., PFG-NMR approach to determining the water transport mechanism in polymer electrolyte membranes conditioned at different temperatures, *European Polymer Journal*, Vol. 46, No. 3, 2010, pp. 450–455.

[44] Kammrath-Weiss, http://www.kammrath-weiss.com.

Chapter 3

Characterization of Nafion® N115 and NRE212 membranes: influence of temperature, heat treatment and drying protocol on sorption, transport and mechanical properties

1 Introduction

The properties of Nafion membranes used in polymer electrolyte fuel cells are important to the performance and durability. For instance, ionic conductivity is, in term of performance, its most important property and mechanical response is, in term of durability, its most important property, both are strongly coupled to the water quantity in the membrane. In general, water sorption, ionic conductivity, water self-diffusion, and mechanical response represent fundamental properties that are needed in every study involving water transport, water management and durability in Nafion-based PEMFCs.

A large variety of research articles have been devoted to the characterization of Nafion membrane properties (see for example the review in reference [1]). In particular, the evolutions of water sorption, ionic conductivity and mechanical properties have all been characterized as a function of relative humidity (RH) and/or temperature (T) [2, 3, 4, 5, 6, 7, 8, 9, 10, 11, 12, 13, 14, 15, 16, 17, 18, 19, 20]. However the direct comparison between literature results is hardly possible because the membrane properties greatly depend on the membrane structure and pre-treatment. Pre-treatment includes heat treatment during the drying of the membrane and chemical treatments (exchange of the membrane in the neutralized form $-RSO_3M$ where M is the exchangeable cation, or in the acidic form $-RSO_3H$) and/or cleaning in boiling distilled water. The reason for this strong dependence of properties to physical and chemical treatments comes from the uncrosslinked hydrophilic/hydrophobic nature of the polymeric membrane. As a result, these membranes can exhibit a wide range in water uptake, ionic conductivity, water self-diffusion coefficient and mechanical response.

The membrane pre-treatment in terms of heating temperature influences greatly the Nafion properties. Moreover, most of the results reported in the literature correspond to a small range of experimental conditions in terms of RH and temperature. Consequently, and despite the large quantity of available data, it remains difficult to gather a complete set of properties, measured with similar Nafion samples, pre-treatment, and over wide RH and temperature ranges. Based on this observation, it seemed important to us to perform systematic sorption, water self-diffusion, proton conductivity, and stress-strain measurements using a simple, reproducible, experimental protocol. Our primary objective is to make available experimental data that can be used either for simulation or modeling or with a more fundamental purpose, in view of getting a deeper understanding on the thermodynamics of sorption, transport and mechanical phenomena in Nafion.

2 Influence of heat treatment and drying protocol on Nafion® properties

The water sorption capacity of Nafion at different relative humidity and its evolution with temperature can vary largely depending on the thermal treatment of the membrane [4, 5, 11, 21]. It is commonly accepted that water sorption (the number of water molecules per ionic site λ = n[H2O] / n[SO_3-H^+]) is higher for a membrane that was not dried before the measurement. It was also shown that water sorption decreases when increasing the drying temperature. Furthermore, what is usually called a "Schroeder's paradox" was reported in several studies when comparing water uptake at 100% RH and in liquid water [15, 16, 17, 18, 22]: most of the authors measured a higher sorption capacity in liquid phase than in vapor phase, but a more recent study demonstrated that Schroeder's paradox may originate in Nafion from the effect of pre-drying on the morphology of the polymer, a too short equilibration time and/or a humidification air that may not have been at 100% RH [19].

2.1 Quantity of residual water

The quantity of "residual water" corresponds to the quantity of water that remains in the structure of the membrane after a drying period in the range of temperature [60°C – 100°C]. In order to know the number of water molecules per ionic site SO_3^-, it is important to determine first the number of residual water molecules and its possible dependence with the drying temperature.

The quantity of protons (nH) was determined by Nuclear Magnetic Resonance (NMR) in each sample and plotted as a function of c^w (as shown in Figure 3.1), where c^w is defined as the water mass fraction with respect to the mass of the membrane after drying at T_{dry} during 24 h. The superscript (^{w}) indicates that a certain quantity of residual water remains in the structure of the membrane.

Let c be the water mass fraction with respect to the dry membrane, c is given by:

$$c = \frac{m_{H_2O}}{m_{dry}} \qquad \text{Eq 1}$$

where m_{H_2O} is the total mass of water in the membrane and m_{dry} is the mass of the dry membrane.

If we note $m^*_{H_2O}$ the mass of residual water after drying at T_{dry} during 24 h, we have:

$m_{H_2O} = m^w_{H_2O} + m^*_{H_2O}$ and $m_{dry} = m^w_{dry} - m^*_{H_2O}$ Eq 2

Introducing Eq 2 into Eq 1 leads to:

$$c = \frac{c^w + c^*}{1 - c^*}$$ Eq 3

with c^* the residual water mass fraction, with respect to the mass of the membrane after drying:

$$c^* = \frac{m^*_{H_2O}}{m^w_{dry}}$$ Eq 4

Using these definitions, the absolute number of water molecules per ionic site SO_3^- , λ, is given by:

$$\lambda = \frac{[H_2O]}{[SO_3^-]} = \frac{EW}{M(H_2O)} c$$ Eq 5

where EW is the equivalent weight of the membrane considered. In this study we used the value $EW = 1100$ g/eq for both Nafion N115 and NRE212. $M(H_2O) = 18$ g/mol is the molar mass of water.

λ^* , the number of residual water molecules per ionic site SO_3^- , is then:

$$\lambda^* = \frac{EW}{M(H_2O)} \frac{c^*}{1 - c^*}$$ Eq 6

The total number of protons in a Nafion sample, nH , can be decomposed into two contributions. The left part of Eq 7 represents the number of protons from water and the right part represents the number of counter-ions.

$$nH = \frac{2}{M(H_2O)} m_{H_2O} + \frac{1}{EW} m_{dry}$$ Eq 7

In Eq 7 both quantities are expressed in mol. Introducing Eq 2 into Eq 7 and dividing by m^w_{dry} gives:

$$\frac{nH}{m^w_{dry}} = \frac{2}{M(H_2O)} c^w + \frac{1}{EW} + \frac{2EW - M(H_2O)}{EW.M(H_2O)} c^*$$ Eq 8

A plot of $\frac{nH}{m^w_{dry}}$ as a function of c^w gives access to c^* through the Y-intercept, and thus to the number of residual water molecules λ^* . The theoretical slope is given by $\frac{2}{M(H_2O)} = 1/9$ mol.g^{-1}.

The results of the measurements performed on three series of Nafion N115 membranes dried at 60°C, 80°C, and 100°C are plotted on Figure 3.1. The difference between the three series is

hardly perceptible. The slope of the best linear fit to the group of data is 0.095 mol.g^{-1}, slightly different from the theoretical $1/9 = 0.110$ mol.g^{-1} value. The values of c^* and λ^* extracted from Figure 3.1 are reported in Table 3.1. When we consider the three series separately, the values of the residual water from the best linear fit are higher than those from the theoretical fit. Moreover, they follow the order $c^*(60°C) > c^*(80°C) > c^*(100°C)$, which would indicate a decrease of the amount of residual water with the drying temperature. However, considering the uncertainties in the preparation of the membranes and the errors introduced during the hydration of the membranes, we shall retain for Nafion N115 dried in the range 60°C < T_{dry} < 100°C the following averaged values:

$\overline{c^*} = 0.024 \pm 0.008$ and $\overline{\lambda^*} = 1.50 \pm 0.50$

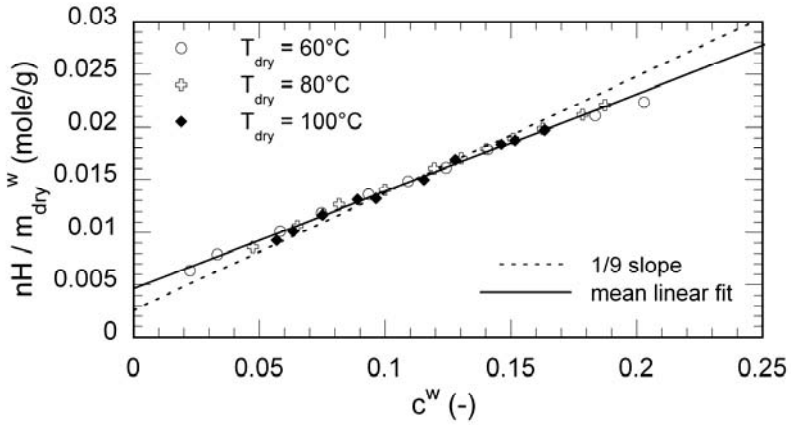

Figure 3.1: Quantity of protons nH measured by NMR in Nafion N115 as a function of the water mass fraction determined by weighing c^w. Membranes dried at T_{dry} = 60°C, 80°C and 100°C during 24 hours.

Table 3.1: Measured values of c and λ* for Nafion N115 dried at T_{dry} = 60°C, 80°C and 100°C during 24 hours.*

T_{dry} (°C)	best linear fit		1/9 slope fit	
	c^*	λ^*	c^*	λ^*
60	0.037	2.36	0.016	0.97
80	0.033	2.09	0.014	0.89
100	0.028	1.79	0.015	0.92

In the following sections, the number of water molecules per ionic site SO_3^-, determined by weighing:

$$\lambda^w = \frac{EW}{M(H_2O)} \frac{m^w_{H_2O}}{m^w_{dry}} \quad \text{Eq 9}$$

will thus be corrected using:

$$\lambda = \overline{\lambda^*} + \frac{\lambda^w}{1 - \overline{c^*}} \quad \text{Eq 10}$$

Note that in this study, the value of $\overline{\lambda^*}$ was not measured in Nafion NRE212. The correction applied to the sorption curves in Nafion NRE212 is $\overline{\lambda^*} = 1.20$ at 60°C, value measured in the literature by thermo-gravimetric analysis [23]. We further assume that this value is constant in the range 60°C < T_{dry} < 100°C.

2.2 Water uptake

The dependence of sorption properties on drying conditions can be of importance regarding the use of Nafion in polymer electrolyte membrane fuel cells (PEMFCs). Since hot-pressing takes place at high temperature, water can be removed from the membrane during this process and an incomplete rehydration of the membrane can occur. It is thus important to have access to experimental data measured on different Nafion membranes, over a wide range of temperature, and on materials prepared in standard and easily reproducible conditions. In this section, we present results on the effect of the drying temperature on sorption in liquid water and water vapor.

2.2.1 In liquid water

Figure 3.2 displays hydration values measured at 30°C, 60°C, 80°C and 100°C in Nafion N115 and NRE212 samples heat-treated at different temperatures. The λ values are listed in Table 3.2. For a given drying temperature T_{dry}, the hydration number increases dramatically with temperature. As an example, λ (30°C) = 14.3 and λ (100°C) = 26.7 for NRE212 dried at T_{dry} = 80°C. This effect, observed here both in N115 and NRE212 membranes, and associated to the softening of the polymeric structure with temperature, is well-known and detailed in the literature [4, 5, 19, 24, 25]. As an example, Zawodzinski *et al*. [4] reported an increase of lambda values in N117 dried at T_{dry} = 105°C from λ (27°C) = 12 to λ (80°C) = 16. Without heat treatment (T_{dry} = 30°C), it is interesting to note that the membrane sorption capacity stays the same in both membranes when the immersion temperature increases. This λ value corresponds to the maximum amount of water that the membrane can adsorb. This behavior was also observed by Kreuer *et al*. in Nafion N117 and in sulfonated polyaromatic membranes [26].

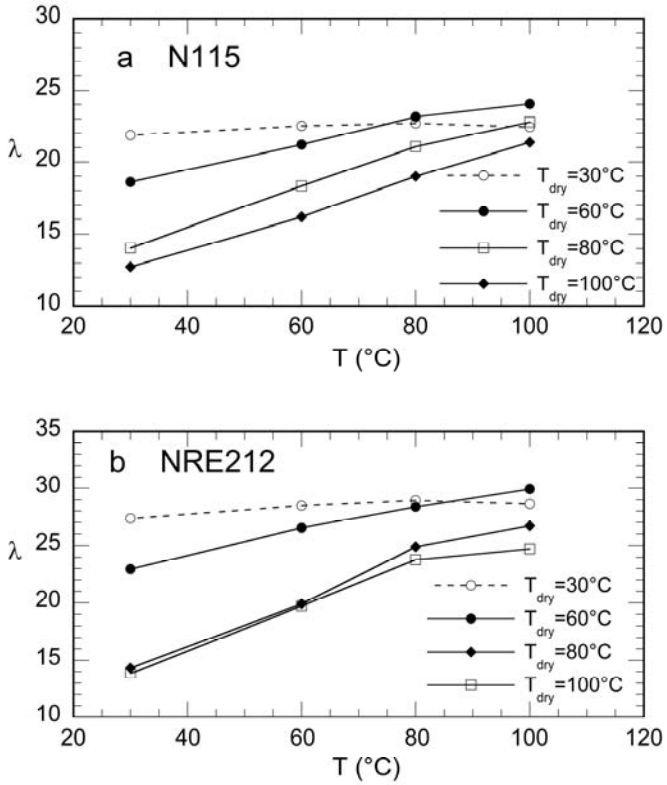

Figure 3.2: Influence of drying temperature T_{dry} on sorption in liquid water measured at different temperatures. (a) Nafion N115. (b) Nafion NRE212.

Table 3.2: Water sorption (λ) as a function of temperature T and drying conditions T_{dry}.

		T = 30°C	T = 60°C	T = 80°C	T = 100°C
N115	$T_{dry} = 30°C$	21.87±0.60	22.52±0.60	22.70±0.61	22.44±0.60
	$T_{dry} = 60°C$	18.59±0.53	21.20±0.54	23.15±0.55	24.04±0.55
	$T_{dry} = 80°C$	14.04±0.57	18.32±0.60	21.06±0.61	22.79±0.62
	$T_{dry} = 100°C$	12.74±0.60	16.17±0.61	18.98±0.63	21.36±0.64
		T = 30°C	T = 60°C	T = 80°C	T = 100°C
NRE212	$T_{dry} = 30°C$	27.35±1.30	28.47±1.32	28.94±1.32	28.62±1.32
	$T_{dry} = 60°C$	22.96±1.23	26.52±1.26	28.37±1.28	29.92±1.30
	$T_{dry} = 80°C$	14.34±1.21	19.91±1.27	24.90±1.33	26.71±1.35
	$T_{dry} = 100°C$	13.86±1.14	19.73±1.20	23.78±1.29	24.71±1.31

Moreover, we can see that the water content is reduced when the drying temperature increases. Again, this result was already discussed in extruded Nafion N112, N115 and N117. It is worth noting that Peron *et al*. [25] did not observe this effect in Nafion NR-211. The authors attributed their findings to the solution casting process used to obtain the membrane NR-211, that played the role of a heat treatment (thermal annealing) and was insufficient to modify the membrane

properties. In our study, the influence of heat treatment on liquid sorption properties is clearly visible in the dispersion cast NRE212 film. In both types of membranes, this effect is more pronounced at low temperature: in N115, the ratio $\lambda(T_{dry} = 30°C) / \lambda(T_{dry} = 100°C)$ decreases from 1.75 at T = 30°C to 1.05 at T = 100°C. As stated by Hinatsu *et al*. [5], this result reveals that the structural differences caused by pre-drying are reduced upon immersion in water at temperatures close to and above the glass-transition temperature (about 110°C). When the membrane is not dried, the polymeric structure stays expended because of the pre-treatment, and the sorption capacity stays at its maximum value, with no variation with temperature.

2.2.2 In water vapor

Figure 3.3 and Figure 3.4 present the influence of drying temperature on sorption isotherms of Nafion N115 and NRE212 measured in the range 30°C < T < 80°C. The experimental values are given in Table 3.3. As in liquid phase, the water sorption in vapor decreases when the drying temperature increases. Onishi *et al*.[19] presented similar behaviors in N117 equilibrated with saturated water vapor: the water content measured at 30°C decreased from λ= 23 to λ = 13.7 for a as-received membrane and a membrane dried at 105°C, respectively. In addition, Hinatsu *et al*. [5] reported values of $\lambda \sim 13.5$ and $\lambda \sim 11.4$ for Nafion N117 dried at T_{dry} = 80 and 105°C, respectively. In this study, this effect is clearly visible in N115 at 30°C and 60°C but less noticeable at 80°C, where all measurements are superimposed, considering the experimental error. It is interesting to note that the shape of the sorption curve changes with heat treatment as sorption is less impacted at low RH. This can be explained considering the changes in the structural properties of the membrane due to heat treatment. After the drying period, the structure of the membrane is more rigid; this limits the swelling of the polymer and reduces its sorption capacity at high RH. At low RH, the sorption properties are mainly controlled by the hydrophilicity and the porous structure of Nafion.

On Figure 3.3 and Figure 3.4 lambda values in liquid water are displayed at the right of each plot for comparison. Since our measurements in vapor phase were not performed at RH values close enough to 100 %, and because the sorption isotherms are very steep in the high relative humidity domain, we are not able to discuss any differences between sorption in liquid and in vapor at 100 % RH (what is called the “Schroeder’s paradox” in the literature). We can notice, however, that the ratio λ(liquid phase) / $\lambda(RH \sim 0.95)$ is more important in Nafion NRE212 than in N115 (1.60 and 1.35 respectively at T=60°C and T_{dry}=60°C).

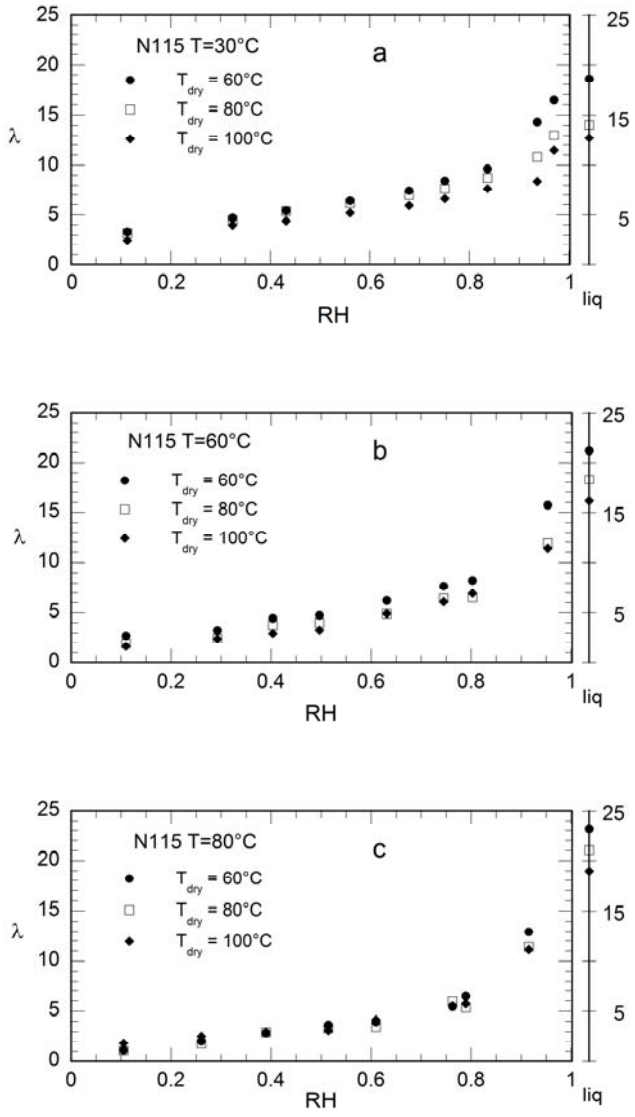

Figure 3.3: Influence of drying temperature T_{dry} on water vapor sorption in Nafion N115 measured at (a) 30°C, (b) 60°C and (c) 80°C. The liquid water sorption is plotted as a guide for the eye at the right of each figure.

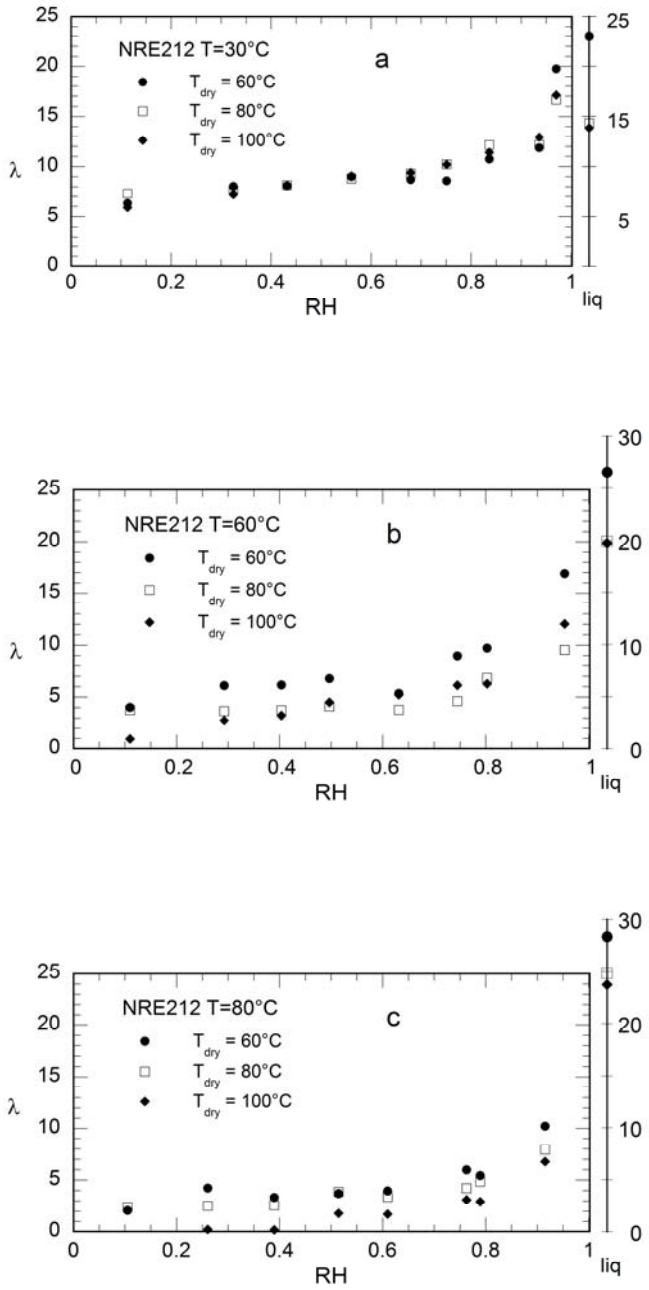

Figure 3.4: Influence of drying temperature T_{dry} on water vapor sorption in Nafion NRE212 measured at (a) 30°C, (b) 60°C and (c) 80°C. The liquid water sorption is plotted as a guide at the right of each figure at an arbitrary RH position.

Table 3.3: Water sorption (λ) as a function of relative humidity RH, temperature T and drying conditions T_{dry} (The values of RHi are given in chapter 2 as a function of temperature T).

	N115 T = 30°C		
	T_{dry} = 60°C	T_{dry} = 80°C	T_{dry} = 100°C
RH1	3.32±0.45	3.20±0.49	2.47±0.48
RH2	4.69 ±0.43	4.47±0.47	3.99±0.46
RH3	5.41±0.42	5.36±0.47	4.41±0.43
RH4	6.40±0.44	6.13±0.47	5.20±0.43
RH5	7.43±0.44	6.98±0.47	5.92±0.45
RH6	8.43±0.43	7.63±0.46	6.62±0.45
RH7	9.64±0.41	8.73±0.44	7.63±0.44
RH8	14.33±0.62	10.81±0.46	8.38±0.44
RH9	16.44±0.42	13.00±0.43	11.48±0.45

	NRE212 T = 30°C		
	T_{dry} = 60°C	T_{dry} = 80°C	T_{dry} = 100°C
RH1	6.32±1.73	7.31±1.38	5.91±1.37
RH2	8.04±1.40	7.66±1.17	7.19±1.21
RH3	8.10±1.39	8.17±1.21	8.14±1.27
RH4	9.02±1.43	8.82±1.21	9.06±1.17
RH5	8.71±1.09	9.30±1.26	9.40±1.22
RH6	8.58±1.13	10.23±1.19	10.22±1.20
RH7	10.74±1.24	12.15±1.18	11.41±1.17
RH8	11.87±1.24	12.16±1.06	12.93±1.29
RH9	19.76±1.45	16.65±1.09	17.13±1.19

	N115 T = 60°C		
	T_{dry} = 60°C	T_{dry} = 80°C	T_{dry} = 100°C
RH1	2.72±0.66	1.92±0.48	1.65±0.47
RH2	3.25±0.63	2.42±0.48	2.41±0.45
RH3	4.44±0.65	3.78±0.46	2.97±0.43
RH4	4.74±0.71	3.98±0.47	3.29±0.43
RH5	6.21±0.60	4.90±0.47	4.93±0.45
RH6	7.67±0.43	6.45±0.46	6.10±0.45
RH7	8.25±0.41	6.51±0.43	6.94±0.44
RH9	15.71±0.43	11.91±0.43	11.37±0.45

	NRE212 T = 60°C		
	T_{dry} = 60°C	T_{dry} = 80°C	T_{dry} = 100°C
RH1	4.02±1.69	3.76±1.32	0.95±1.38
RH2	6.12±1.40	3.66±1.17	2.75±1.21
RH3	6.16±1.39	3.75±1.21	3.24±1.25
RH4	6.77±1.42	4.11±1.21	4.52±1.17
RH5	5.36±1.05	3.78±1.25	5.24±1.22
RH6	8.97±1.06	4.60±1.20	6.14±1.20
RH7	9.71±1.24	6.84±1.19	6.30±1.17
RH9	16.91±1.45	9.54±1.08	12.03±1.19

	N115 T = 80°C		
	T_{dry} = 60°C	T_{dry} = 80°C	T_{dry} = 100°C
RH1	1.10±0.43	1.06±0.48	1.85±0.53
RH2	2.03±0.42	1.80±0.48	2.55±0.45
RH3	2.88±0.42	2.94±0.46	2.96±0.43
RH4	3.66±0.44	3.33±0.47	3.14±0.43
RH5	3.96±0.44	3.47±0.46	4.17±0.45
RH6	5.46±0.43	5.97±0.46	5.48±0.45
RH7	6.46±0.41	5.36±0.43	5.73±0.44
RH9	12.94±0.43	11.42±0.43	11.13±0.45

	NRE212 T = 80°C		
	T_{dry} = 60°C	T_{dry} = 80°C	T_{dry} = 100°C
RH1	2.08±1.67	2.39±1.32	-0.47±1.24
RH2	4.24±1.40	2.51±1.17	0.21±1.21
RH3	3.33±1.39	2.58±1.21	0.19±1.24
RH4	3.71±1.43	3.86±1.21	1.81±1.18
RH5	3.95±1.07	3.36±1.26	1.73±1.21
RH6	5.98±1.07	4.22±1.19	3.10±1.21
RH7	5.43±1.24	4.85±1.18	2.94±1.16
RH9	10.22±1.45	7.92±1.09	6.77±1.18

	N115		
	T_{dry} = 60°C		
	T = 40°C	T = 50°C	T = 70°C
RH1	2.81±0.44	2.58±0.44	1.12±0.43
RH2	4.10±0.43	3.89±0.42	2.26±0.43
RH3	4.86±0.42	4.64±0.42	3.10±0.42
RH4	5.55±0.44	5.11±0.44	3.68±0.44
RH5	6.79±0.44	6.11±0.44	5.07±0.44
RH6	7.79±0.43	7.52±0.43	6.58±0.43
RH7	8.99±0.42	8.45±0.42	7.30±0.42
RH8	14.22±0.62		
RH9	16.00±0.42	15.78±0.42	13.11±0.43

2.3 Proton conductivity and water self-diffusion

The transport of water and protons in Nafion membranes plays a fundamental role in the performances of the polymer electrolyte. Transports mechanisms through the membrane are of different nature. They include water self-diffusion, water transport by electro-osmosis and proton transport. These mechanisms are coupled to each other and described by parameters that depend all on water content λ. Since water plays the role of the transport medium for protons [27], water dynamics, and its relationship with the structure of the membrane, represents a relevant parameter [28]. We have seen that sorption in Nafion is influenced by thermal history. In this section, we present the effect of drying on proton conductivity and water self-diffusion.

2.3.1 Proton conductivity

Figure 3.5 and Figure 3.6 present measurements of proton conductivity respectively in Nafion N115 and NRE212 as a function of RH. The membranes were dried at T_{dry} during 24 h before the measurements. The experimental values are in Table 3.4 and Table 3.5. At low temperature (T = 30°C), the effect of drying temperature on conductivity is visible in both types of membranes (Figure 3.5a and Figure 3.6a) and σ is slightly reduced when the drying temperature increases. This variation is effective over the entire RH range. At 60°C and 80°C the effect seems to disappear, in accordance with our observations on the variations of water content (Figure 3.3 and Figure 3.4). The absolute values, as well as their variations with respect to RH are in line with literature results [6, 13]. For example, Sone *et al*. [6] measured conductivity values in Nafion N117 at 30°C and RH =0.8 of σ ~ 0.06, 0.05, and 0.04 S/cm for a as-received membrane, a membrane dried at 80°C, and a membrane dried at 105°C, respectively. Peron *et al*. [25] measured a drying temperature-independent conductivity in Nafion NR-211 of σ ~ 0.07 S/cm at 25°C and σ ~ 0.18 S/cm at 100°C, once the membranes are immersed in water for 1 h.

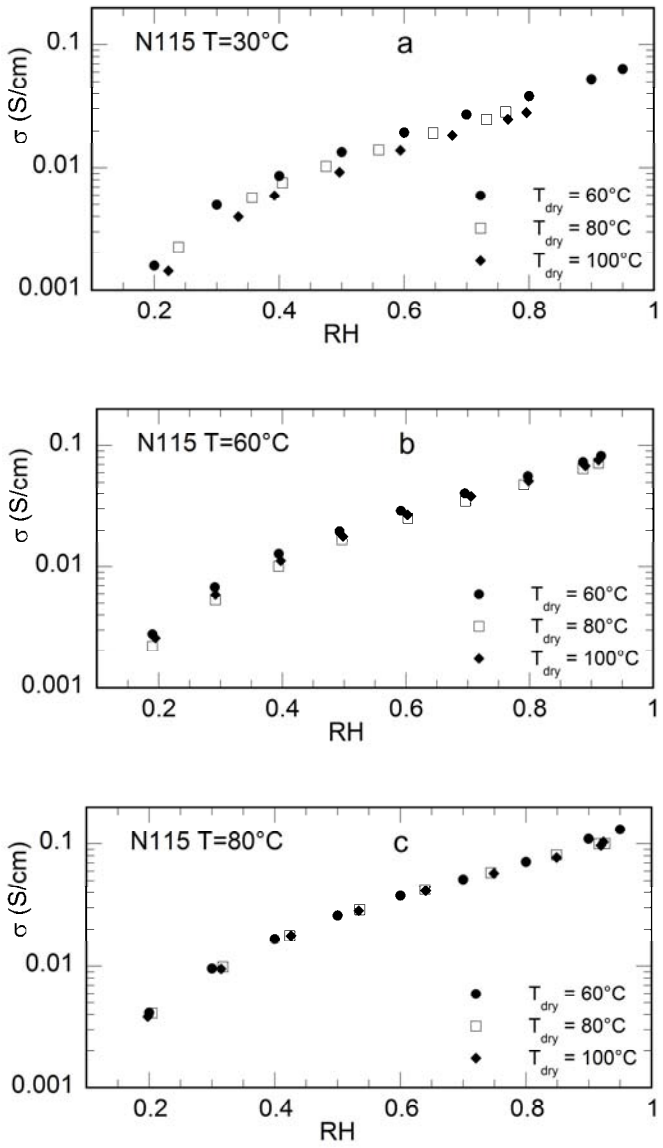

Figure 3.5: Influence of drying temperature T_{dry} on proton conductivity in Nafion N115 measured at (a) 30°C, (b) 60°C and (c) 80°C.

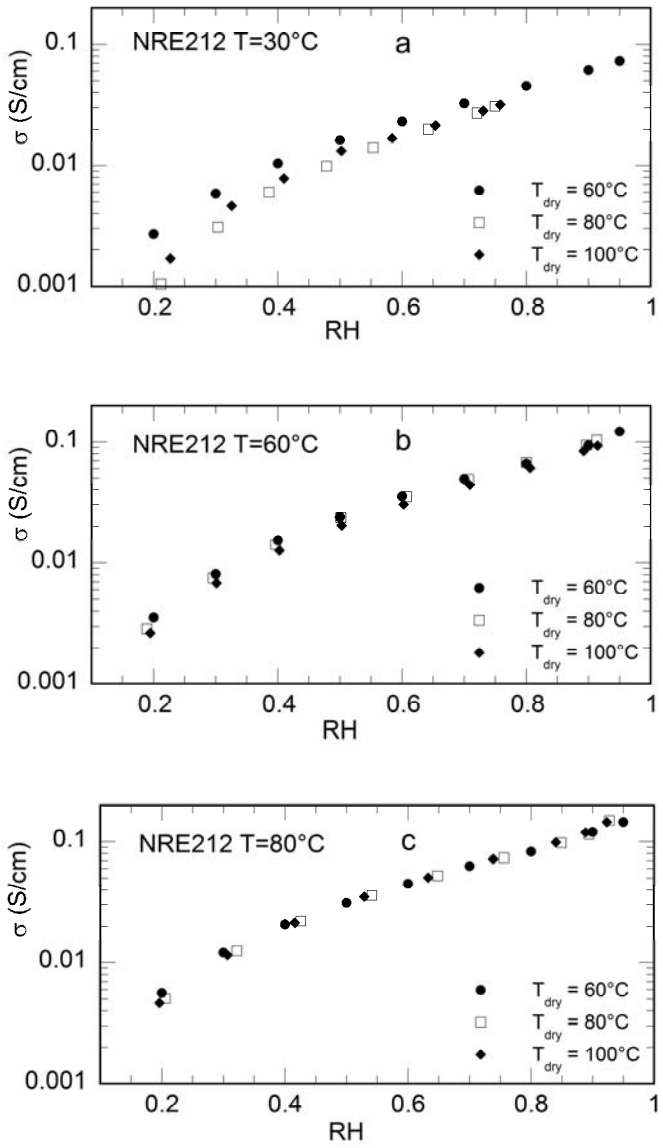

Figure 3.6: Influence of drying temperature T_{dry} on proton conductivity in Nafion NRE212 measured at (a) 30°C, (b) 60°C and (c) 80°C.

Table 3.4: Proton conductivity σ (S/cm) as a function of relative humidity RH, temperature T and drying conditions T_{dry}.

N115 T = 30°C					
T_{dry} = 60°C		T_{dry} = 80°C		T_{dry} = 100°C	
RH	σ	RH	σ	RH	σ
0.20	0.002	0.24	0.002	0.22	0.001
0.30	0.005	0.36	0.006	0.34	0.004
0.40	0.009	0.41	0.008	0.39	0.006
0.50	0.013	0.48	0.010	0.50	0.009
0.60	0.019	0.56	0.014	0.59	0.014
0.70	0.027	0.65	0.019	0.68	0.019
0.80	0.038	0.73	0.025	0.77	0.025
0.90	0.053	0.76	0.028	0.80	0.028
0.950	0.063				

NRE212 T = 30°C					
T_{dry} = 60°C		T_{dry} = 80°C		T_{dry} = 100°C	
RH	σ	RH	σ	RH	σ
0.20	0.003	0.21	0.001	0.23	0.002
0.30	0.006	0.30	0.003	0.33	0.005
0.40	0.010	0.39	0.006	0.41	0.008
0.50	0.016	0.48	0.010	0.50	0.013
0.60	0.023	0.55	0.014	0.58	0.017
0.70	0.032	0.64	0.020	0.65	0.022
0.80	0.045	0.72	0.027	0.73	0.028
0.90	0.062	0.75	0.031	0.76	0.032
0.95	0.073				

N115 T = 60°C					
T_{dry} = 60°C		T_{dry} = 80°C		T_{dry} = 100°C	
RH	σ	RH	σ	RH	σ
0.19	0.003	0.19	0.002	0.20	0.003
0.29	0.007	0.29	0.005	0.29	0.006
0.39	0.013	0.39	0.010	0.40	0.011
0.49	0.020	0.50	0.016	0.50	0.018
0.59	0.029	0.60	0.025	0.60	0.027
0.70	0.040	0.70	0.035	0.71	0.038
0.80	0.056	0.79	0.048	0.80	0.051
0.89	0.073	0.89	0.065	0.89	0.068
0.92	0.082	0.91	0.072	0.91	0.076

NRE212 T = 60°C					
T_{dry} = 60°C		T_{dry} = 80°C		T_{dry} = 100°C	
RH	σ	RH	σ	RH	σ
0.20	0.004	0.19	0.003	0.20	0.003
0.30	0.008	0.30	0.007	0.30	0.007
0.40	0.015	0.40	0.014	0.40	0.013
0.50	0.024	0.50	0.024	0.50	0.020
0.60	0.035	0.61	0.035	0.60	0.030
0.70	0.049	0.71	0.049	0.71	0.044
0.80	0.066	0.80	0.068	0.81	0.061
0.90	0.094	0.90	0.094	0.89	0.084
0.95	0.123	0.91	0.104	0.91	0.093

N115 T = 80°C					
T_{dry} = 60°C		T_{dry} = 80°C		T_{dry} = 100°C	
RH	σ	RH	σ	RH	σ
0.20	0.004	0.20	0.004	0.20	0.004
0.30	0.010	0.32	0.010	0.32	0.010
0.40	0.017	0.42	0.018	0.43	0.018
0.50	0.026	0.54	0.029	0.53	0.028
0.60	0.038	0.64	0.042	0.64	0.041
0.70	0.051	0.74	0.058	0.75	0.057
0.80	0.071	0.85	0.081	0.85	0.077
0.90	0.109	0.92	0.100	0.92	0.097
0.95	0.131	0.93	0.100	0.92	0.103

NRE212 T = 80°C					
T_{dry} = 60°C		T_{dry} = 80°C		T_{dry} = 100°C	
RH	σ	RH	σ	RH	σ
0.20	0.006	0.21	0.005	0.20	0.005
0.30	0.012	0.32	0.013	0.31	0.012
0.40	0.021	0.43	0.022	0.42	0.021
0.50	0.031	0.54	0.036	0.53	0.035
0.60	0.045	0.65	0.052	0.63	0.051
0.70	0.063	0.76	0.074	0.74	0.072
0.80	0.083	0.85	0.098	0.84	0.099
0.90	0.121	0.89	0.116	0.89	0.120
0.95	0.146	0.93	0.150	0.92	0.146

Table 3.5: Proton conductivity σ (S/cm) as a function of RH and T of N115 (top) and NRE212 (bottom) dried at 60°C.

N115						
$T_{dry} = 60°C$						
RH	40°C	50°C	70°C	100°C	RH	110°C
0.20	0.002	0.003	0.004	0.005	0.30	0.013
0.30	0.006	0.007	0.009	0.011	0.39	0.022
0.40	0.010	0.012	0.016	0.018	0.49	0.035
0.50	0.016	0.019	0.024	0.028	0.53	0.039
0.60	0.024	0.028	0.035	0.041	0.58	0.046
0.70	0.033	0.039	0.047	0.056	0.60	0.049
0.80	0.046	0.054	0.063	0.074	0.63	0.053
0.90	0.063	0.075	0.095	0.103	0.68	0.061
0.95	0.076	0.084	0.111	0.126	0.74	0.068

NRE212							
$T_{dry} = 60°C$							
RH	40°C	50°C	70°C	RH	100°C	RH	110°C
0.20	0.003	0.003	0.004	0.20	0.006	0.20	0.007
0.30	0.007	0.007	0.010	0.25	0.008	0.25	0.010
0.40	0.012	0.013	0.018	0.30	0.012	0.30	0.014
0.50	0.019	0.020	0.027	0.35	0.016	0.35	0.018
0.60	0.028	0.029	0.040	0.40	0.023	0.40	0.023
0.70	0.039	0.041	0.054	0.45	0.028	0.45	0.029
0.80	0.053	0.057	0.076	0.50	0.034	0.50	0.036
0.90	0.074	0.085	0.118	0.55	0.041	0.54	0.040
0.95	0.088	0.107	0.144	0.60	0.048		
				0.70	0.063		

2.3.2 Water self-diffusion

Figure 3.7 shows the evolution of the water self-diffusion coefficient D_s measured by PFGNMR at 25°C as a function of water content λ in Nafion N115 dried at different temperatures. As reported in the literature, D_s increases significantly with λ [27] and approximately follows the phenomenological equation [28]:

$$D_s = \alpha\lambda\left(1 - \exp\left[-\beta(\lambda - \lambda_0)\right]\right) \qquad \text{Eq 11}$$

In Figure 3.7 the solid lines represent the best fits to the curves using Eq 11. The parameters α, β and λ_0, as well as the experimental values, are listed in Table 3.6. When the drying temperature is increased, the diffusion is slowed down, especially in the low water content range where the observed differences can be important. As an example, $D_s(T_{dry} = 60°C) / D_s(T_{dry} = 100°C) \sim 1.55$ at λ=5. The difference is less pronounced at higher λ values. In these experiments, it is important to note that the hydration of the membranes was evaluated directly during the experiment by measuring the proton NMR signal. We were thus able, following the procedure described in Chapter 2 (Section 4), to determine precisely the value of λ. This is of great importance considering the steepness of the curve $D_s = f(\lambda)$ at low hydration. Indeed, small

errors on the evaluation of λ in this region would lead to important changes in the shape of the curve and prevent us from comparing the different curves.

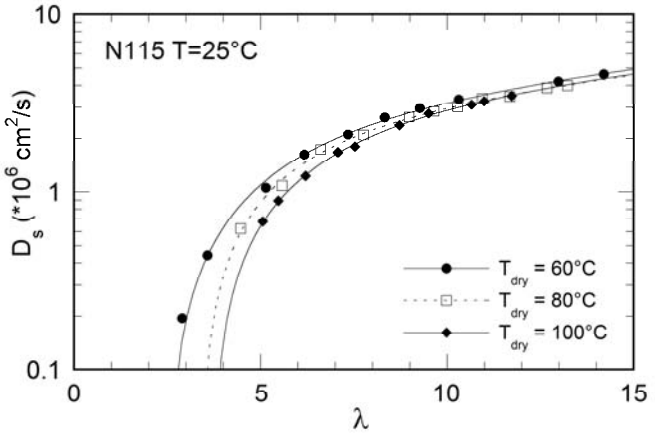

Figure 3.7: Influence of drying temperature T_{dry} on water self-diffusion coefficient in Nafion N115. Measurements performed at room temperature (T=25°C). The solid lines are fitted curves using equation Eq 11 with parameters α, β and λ_0, listed in Table 3.6.

Table 3.6: Water self-diffusion coefficient in Nafion N115 at 25°C (10^{-6} cm^2/s).

$T_{dry} = 60°C$			$T_{dry} = 80°C$			$T_{dry} = 100°C$		
λ	D_s		λ	D_s		λ	D_s	
14.20	4.614		13.23	3.992		11.73	3.500	
12.99	4.201		12.68	3.868		11.00	3.253	
10.31	3.333		11.68	3.457		10.66	3.120	
9.27	2.972		10.95	3.375		9.51	2.768	
8.33	2.629		10.28	3.017		8.72	2.377	
7.35	2.103		9.65	2.847		7.53	1.803	
6.18	1.618		8.98	2.643		7.07	1.669	
5.14	1.053		7.76	2.090		6.21	1.227	
3.58	0.442		6.61	1.731		5.47	0.893	
2.90	0.195		5.58	1.084		5.06	0.682	
			4.46	0.623				
Fitting parameters (Eq 11)								
α	β	λ_0	α	β	λ_0	α	β	λ_0
0.330	0.440	2.515	0.305	0.530	3.386	0.312	0.411	3.700

*The maximal systematic error in the measurement of D_s is estimated to ±5%.

If we consider that, at the scale of the measurement, the diffusion of water is isotropic, then the PFGNMR method probes the water dynamics at a length scale of about $l = \sqrt{2D_s\Delta}$, where $100 < \Delta < 200$ ms is an acquisition parameter that was varied as a function of the hydration of the membrane. In our experiments, considering the two extreme values of D_s, l falls within the range $3 < l < 10$ µm. Thus, the results of the measurements indicate that the changes induced by the heat-treatment on the structural organization of Nafion are effective on the transport properties at a length scale shorter than 1 µm. These changes then impact on proton

conductivity at a much larger scale, proton conductivity being a measure of the mobility of protons over the entire thickness of the membrane (~ 125 µm in Nafion N115). A more detailed study would be necessary to determine precisely where the structural modifications occur and at which time / length scale(s) water dynamics is impacted. Such measurements could be performed at the molecular scale (picosecond-nanosecond timescale) using quasi-elastic neutron scattering [29, 30].

2.4 Mechanical properties

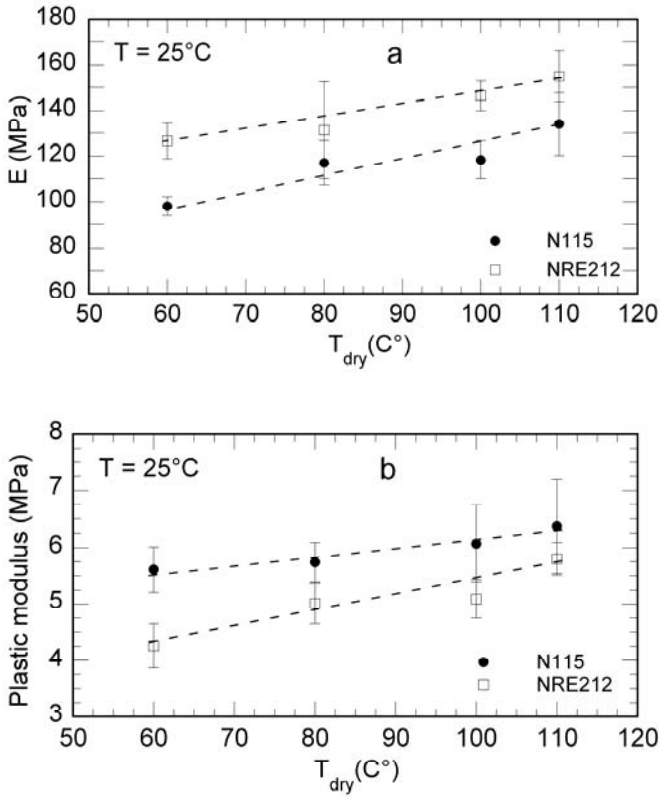

Figure 3.8: Evolution of (a) Young modulus and (b) Plastic modulus of Nafion N115 and NRE212 at 25°C , as a function of drying temperature.

Studies on the mechanical behavior of Nafion membranes are little-known in the literature. Moreover, the data found are often incomplete and insufficient either because the applied method, or the external condition, or the pre-treatment. The objective of this section is to study and thus to put in evidence the effect of drying pre-treatment on the mechanical properties of Nafion, in particular the Young modulus and the Plastic modulus (see Chapter 2 "Experimental Protocols").

For this experience, we dried samples of N115 and NRE212 at 30°C, 60°C, 80°C, 100°C and 110°C. To obtain a representative average, four samples were generally used for each

temperature. Figure 3.8 and Table 3.7 show the Young modulus and the Plastic modulus *vs.* the drying temperature.

Table 3.7: Mechanical parameters of N115 and NRE212 at 25°C, as a function of drying temperature.

	N115		NRE212	
	Young modulus E (MPa)	Plastic modulus (MPa)	Young modulus E (MPa)	Plastic modulus (MPa)
$T_{dry} = 60°C$	98±4	5.6±0.4	127±8	4.3±0.4
$T_{dry} = 80°C$	117±10	5.7±0.4	131±21	5±0.4
$T_{dry} = 100°C$	118±8	6.1±0.7	146±6	5.1±0.3
$T_{dry} = 110°C$	134±14	6.4±0.8	155±11	5.8±0.3

We observe that Young modulus, which is obtained from the initial slope of each stress-strain curve as shown in Figure 3.9, increases with the drying temperature in both cases: it seems that increasing the drying temperature stiffens the membranes. Furthermore, the Plastic modulus (Figure 3.8b) seems to have the same behavior but this effect is less marked, especially with Nafion N115. The experimental errors are ± 4 to 13 % for the Young modulus, and 0.29 to 0.83% for the Plastic modulus.

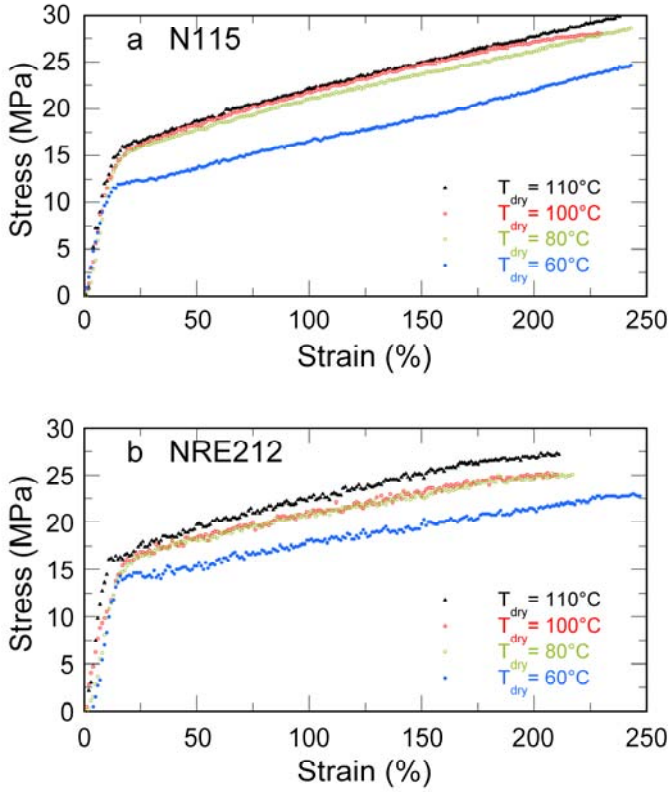

Figure 3.9: Evolution of the stress-strain curves of (a) Nafion N115 and (b) Nafion NRE212 at 25°C as a function of drying temperature.

3 Characterization of Nafion® membranes as a function of temperature and relative humidity conditions

In this section we present water vapor uptake and proton conductivity measurements in Nafion N115 and NRE212 membranes dried at 60°C for 24 h and we discuss the effects of temperature on sorption and transport properties. When possible, our experimental results are confronted to literature values. The experimental curves are fitted using empirical expressions. These continuous functions are close enough to the data to be used in numerical models. The parameters of the fits and the experimental data are listed in Table 3.8, Table 3.9 and Table 3.10.

3.1 Water uptake

Figure 3.10 shows sorption isotherms of N115 and NRE212 at different temperatures between 30°C and 80°C. The solid lines are best fits curves using Eq 12. This "linear-exponential" relation matches our data better (in the range 0.2 < RH < 0.9) than more conventional polynomial expressions used in the literature [5, 31, 32]. However the polynomial relations can be used advantageously if one wants to evaluate conductivity values in the range 0 < RH < 0.2.

$$\lambda = a + bRH + c\exp(dRH) \qquad \text{Eq 12}$$

At a relative humidity close to 0.95, the variation of water uptake with temperature is very limited. For relative humidities comprised between 0.1 and 0.9 the sorption capacity decreases with temperature. This second observation, valid in this study for both Nafion N115 and NRE212, has been already made by several authors, either in Nafion [2, 7, 33], in Flemion® [10], or in other sulfonated proton conducting polymers [33]. Certain authors attributed this effect to a decrease of the number of clustered water at high temperature (80°C) [10] while others did not give any explanation. Here, the decrease in water content is approximately 45% in N115 between 30°C and 80°C at RH = 0.4. This loss of sorption capacity is moderate for 30°C < T < 60°C but more important for 60°C < T < 80°C. The same behavior is observed in NRE212, with a drop in lambda as high as 60% at RH = 0.4. (Note that the error bars are larger in NRE212 because the mass of NRE212 samples is lower than that of N115 samples).

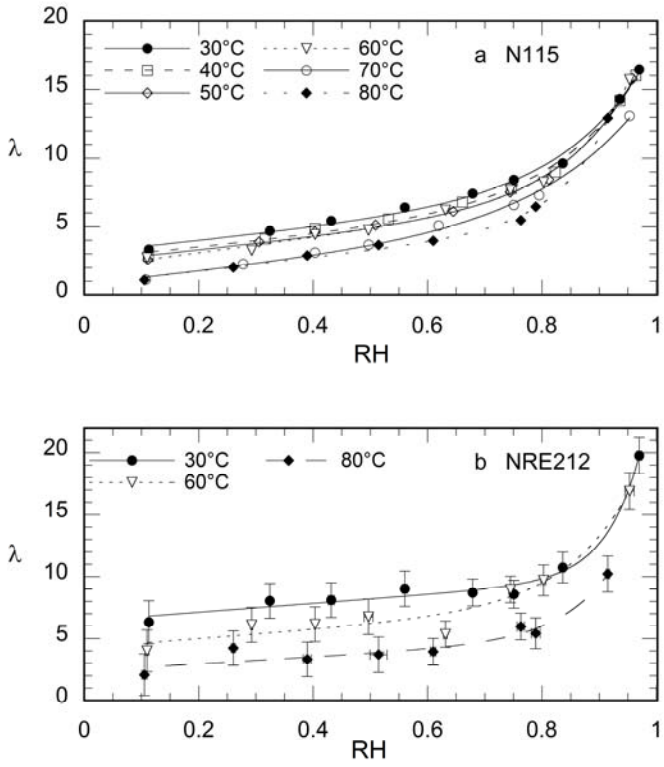

Figure 3.10: Sorption isotherms of (a) Nafion N115 and (b) Nafion NRE212 as a function of temperature. The membranes were dried prior to experiment at T_{dry} = 60°C during 24 hours. The solid lines are fitted curves using equation Eq 12. Parameters a, b, c and d are listed in Table 3.8.

At first, this behavior and the amplitude of these variations can be surprising considering the mechanical properties of the polymer with respect to temperature. The elastic modulus (Young modulus) of Nafion has been measured in the literature as a function of temperature and water content. It was demonstrated that, as in Polytetrafluoroethylene (PTFE), the modulus decreases in Nafion immersed in water when the temperature increases [20, 11]. The softening of the polymer following the increase of temperature would then lead to an increase of sorption capacity because water can invade the polymer more easily. This is observed in Nafion, but only in heat-treated samples (Figure 3.1 and ref [26]). When the membrane is not dried its structure stays in the "expended" form and consequently, its sorption capacity in liquid water is not a function of temperature. This argumentation, although valid at high water content, may be questioned when the membranes are equilibrated with water vapor at low RH. Less data are available in the literature about the mechanical properties of Nafion in these conditions because it is critical to maintain a constant hydration during a strain-stress experiment. However, several studies have shown that, at all temperatures, increasing hydration seems to decrease the elastic modulus of Nafion NRE212 [34] and N115 [35]. Other studies have demonstrated that water acts as a plasticizer in the membrane, reducing the modulus, yield stress and glass transition

temperature of the polymer [20, 11]. As a consequence, the mechanical behavior of the membrane cannot be responsible by itself for the changes that we observe in the sorption properties. The hydrophilicity of the polymeric matrix in the vicinity of the polymer chains and the accessibility of the porous structure to water vapor must also be considered. In the framework of the Flory-Huggins model which describes the activity of water within the membrane, the χ parameter accounts for intermolecular interactions between the polymer and the solvent. Our results play in favor of an increase of the interaction parameter χ with temperature when the membrane is exposed to water vapor. These findings are in agreement with the results of the work by Futerko *et al*. [36] who found a linear dependence of the Flory parameter χ on the reciprocal of temperature in the form $\chi = a - b/T$, where a and b are constants. However, a more detailed study of the relative variation of the hydrophilicity of Nafion and of the rigidity of the structure with respect to temperature would be required for a better understanding of the sorption phenomena as a function of temperature.

Table 3.8: Water sorption in Nafion. Fitting parameters for 0.2<RH<0.95 (Eq 12).

N115				
$T_{dry} = 60°C$				
T(°C)	*a*	*b*	*c*	*d*
30	3.074	4.402	0.0124	6.7795
40	2.627	4.196	0.0130	6.7970
50	2.366	4.550	0.0052	7.7760
60	1.966	5.528	0.0019	8.8045
70	0.769	4.376	0.0453	5.4310
80	0.759	4.944	0.00016	11.7430
$T_{dry} = 80°C$				
30	2.723	5.483	0.0020	7.9452
60	1.1076	5.887	0.00015	10.9637
80	0.653	4.872	0.00012	11.8375
$T_{dry} = 100°C$				
30	2.053	5.429	0.00011	10.6731
60	1.300	5.121	0.0003	10.3002
80	1.616	3.180	0.0006	10.1036

NRE212				
$T_{dry} = 60°C$				
T(°C)	*a*	*b*	*c*	*d*
30	7.122	1.440	0.00015	11.3832
60	4.291	3.533	0.002007	8.8565
80	2.416	2.753	0.000135	11.5490
$T_{dry} = 80°C$				
30	6.831	2.884	0.004	7.7150
60	3.355	0.750	0.0073	6.9680
80	2.451	0.850	0.0030	8.0448
$T_{dry} = 100°C$				
30	5.852	3.999	0.008	6.8519
60	1.897	3.594	0.0075	7.1050
80	0.015	1.524	0.0074	7.1830

3.2 Proton conductivity

Figure 3.11 presents proton conductivity measurements on Nafion N115 and NRE212 in equilibrium with water vapor at different temperatures in the range 30°C < T < 110°C. At high temperature, it becomes difficult to maintain high RH in the measurement chamber while avoiding the condensation of water at the surface of the membrane: thus, the measurements

were performed only up to RH = 0.75 at 110°C for N115 and RH = 0.60 and 0.55 for NRE212 at 100°C and 110°C, respectively. The solid lines correspond to best fits to the experimental data using Eq 13 (Table 3.9). This expression, used by several authors in the literature [6], provides useful relations that can be used for modeling purposes. The equation perfectly fits the data for RH values higher than 0.3 at every temperature. In most cases, the fit stays satisfactory for 0.2 < RH < 0.3.

$$\sigma = e + fRH + gRH^2 + hRH^3 \qquad \text{Eq 13}$$

We observe on the figure that the proton conductivity increases significantly with temperature. The temperature variation of σ is represented in the right column of the figure on an Arrhenius plot at different RH. The activation energies decrease between ~15 kJ/mol and ~11kJ/mol in both N115 and NRE212 for 0.2 < RH < 0.9, which traduces a slight change in the shape of the curve as temperature increases. The values of σ conform to literature values in Nafion 1100 membranes [6, 37, 38], are in every case a little higher in NRE212 than in N115. The activation energies also match literature data, in the same range of temperature, and in similar membranes [12, 14, 19].

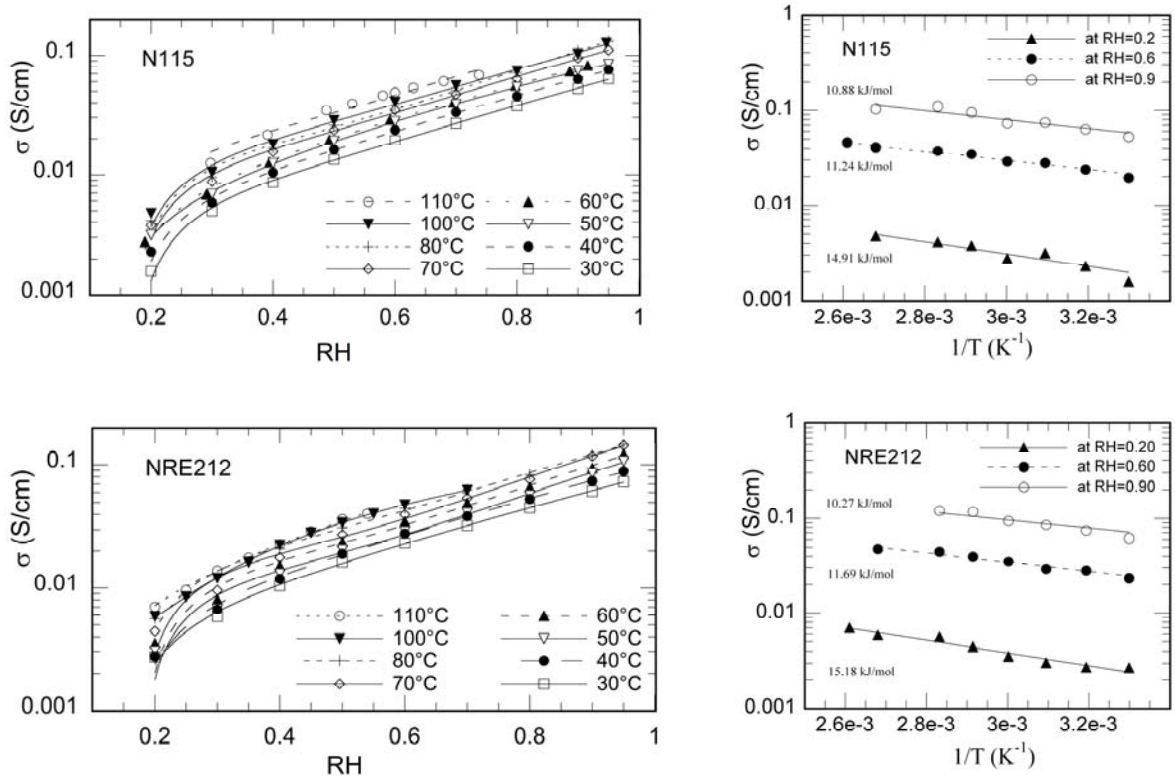

Figure 3.11: Left column: Proton conductivity of Nafion N115 and Nafion NRE212 as a function of temperature. The membranes were dried prior to experiment at T_{dry} = 60°C during 24 hours. The solid lines are fitted curves using equation Eq 13. Parameters e, f, g and h are listed in Table 3.9. Right column: Arrhenius plot of the proton conductivity in Nafion N115 and Nafion NRE212 collected at RH=0.2, 0.6 and 0.9, and values of the corresponding activation energies.

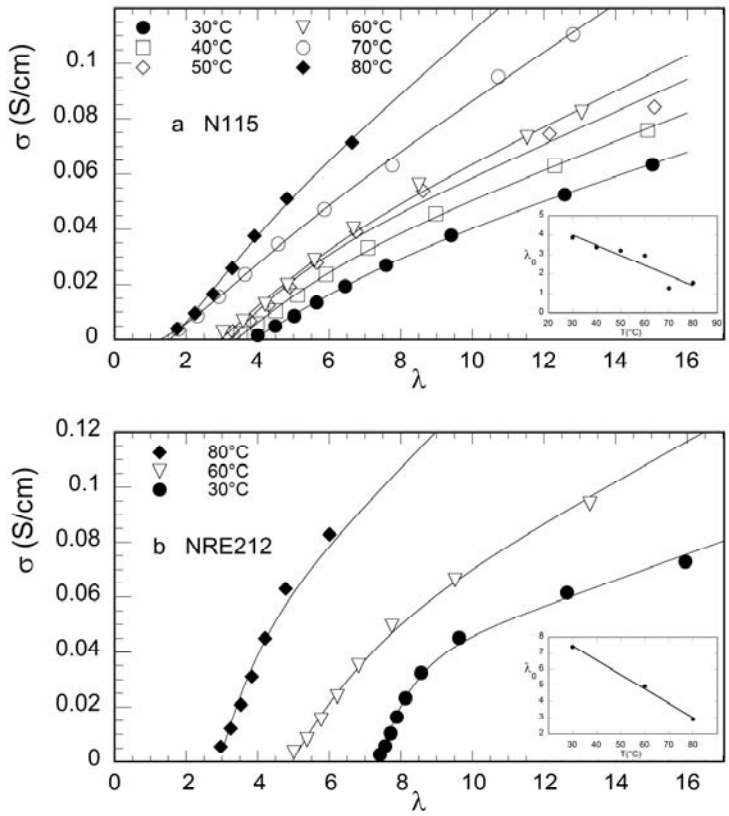

Figure 3.12: Proton conductivity in (a) Nafion N115 and (b) Nafion NRE212 as a function of water content λ. The values of λ were calculated from the experimental sorption isotherms using Eq 12 and the fitting parameters from Table 3.8. The solid lines are fitted curves using equation Eq 11. Parameters α, β and λ_0 are listed in Table 3.10. The evolution of parameter λ_0 is plotted in the insets.

The variation of proton conductivity in Nafion membranes as a function of RH and T raises fewer questions than that of water content. Even if proton transport depends a lot more on RH than does water content (two orders of magnitude separate conductivity values at low and high RH), the temperature represents essentially the key parameter that controls conductivity. In other words, the acceleration of the ionic transport under the influence of temperature is more important than its decline due to a loss of water content. As a consequence, the proton conductivity stays an increasing function of temperature when the curves are plotted against water content. This is illustrated on Figure 3.12, where σ is plotted as a function of λ for different temperatures. The λ values have been calculated using the experimental sorption isotherms and their respective fits (Eq 12). The equation used to fit the conductivity data in Figure 3.12 has the same form as the one used to fit the water self-diffusion coefficient in Figure 3.7 (Eq 11). Water is indeed the transport media for protons, and vehicular transport is recognized as an efficient mechanism, especially at low water content [27]. It is thus not surprising that D_s and σ behave in the same way with respect to λ, even if other mechanisms, such as structure diffusion, play a

fundamental role in the global process. In Eq 11, λ_0 depicts a threshold above which proton transport is effective and proton conductivity takes measurable values. The evolution of λ_0 (insets in Figure 3.12) indicates that at low water content a higher temperature is needed for the protons to be transported efficiently through the membrane. This is particularly true in Nafion NRE212 where, given the sorption properties of the membrane, a low hydration state is rarely reached during the operation of a PEMFC (Figure 3.10).

Table 3.9: Proton conductivity of Nafion as a function of RH. Fitting parameters for 0.2<RH<0.95 (Eq 13).

N115					NRE212				
$T_{dry} = 60°C$					$T_{dry} = 60°C$				
T (°C)	*e*	*f*	*g*	*h*	T (°C)	*e*	*f*	*g*	*h*
30	-0.0111	0.0860	-0.1477	0.1464	30	-0.0080	0.0670	-0.1018	0.1266
40	-0.0107	0.0850	-0.1390	0.1519	40	-0.0119	0.0948	-0.1535	0.1725
50	-0.0052	0.0474	-0.0512	0.1065	50	-0.0258	0.2043	-0.4026	0.3498
60	-0.0088	0.0730	-0.1007	0.1407	60	-0.0285	0.2223	-0.4217	0.3690
70	-0.0204	0.1645	-0.2947	0.2808	70	-0.0347	0.2800	-0.5586	0.4846
80	-0.0291	0.2361	-0.4609	0.4098	80	-0.0271	0.2232	-0.4031	0.3766
100	-0.0230	0.1841	-0.3150	0.3000	100	0.0061	-0.0552	0.2958	-0.1455
110	-0.0223	0.2100	-0.3982	0.3985	110	-0.0033	0.0549	-0.0492	0.1875
$T_{dry} = 80°C$					$T_{dry} = 80°C$				
30	-0.0067	0.0482	-0.0647	0.0800	30	-0.0042	0.0286	-0.0368	0.0803
60	-0.0067	0.0568	-0.0840	0.1262	60	-0.0154	0.1272	-0.2294	0.2524
80	-0.0061	0.0523	-0.0394	0.1166	80	-0.0462	0.3589	-0.6981	0.5699
$T_{dry} = 100°C$					$T_{dry} = 100°C$				
30	-0.0048	0.0346	-0.0464	0.0681	30	-0.0074	0.0494	-0.0629	0.0857
60	-0.0085	0.0701	-0.1078	0.1429	60	-0.0150	0.1234	-0.2309	0.2445
80	-0.0132	0.1079	-0.1623	0.1932	80	-0.0330	0.2657	-0.5073	0.4579

Table 3.10: Proton conductivity of Nafion as a function of λ. Fitting parameters (Eq 11).

N115				NRE212			
$T_{dry} = 60°C$				$T_{dry} = 60°C$			
T (°C)	*α*	*β*	λ_0	T(°C)	*α*	*β*	λ_0
30	0.00426	0.476	3.856	30	0.0047	1.273	7.396
40	0.00514	0.595	3.385	60	0.0073	0.632	4.950
50	0.00590	0.736	3.204	80	0.0134	1.200	2.923
60	0.00644	0.606	2.947				
70	0.0083	0.724	1.430				
80	0.0112	0.748	1.546				

4 Conclusion

We performed systematic sorption, transport, and mechanical measurements in two types of Nafion membranes, Nafion N115 and Nafion NRE212. The experimental protocols used are simple and were developed to favor reproducibility. The emphasis was put on the measurement of the effects of the drying temperature (thermal history) on the water content of the membrane, its proton conductivity, the value of the water self-diffusion coefficient, and its correlation with the Young modulus.

When the membrane samples are heat-treated at moderate temperature in the range 60°C < T_{dry} < 100°C some residual water stays strongly attached to the structure of the polymer. The amount of residual water, expressed as a number of water molecules per ionic site, was measured by NMR and evaluated to $\lambda = 1.5 \pm 0.5$ in Nafion N115. In heat-treated membranes, the sorption capacity is reduced due to shrinkage of the polymeric structure during the drying. This effect is visible in both liquid and vapor phase, increases with the drying temperature, and decreases with the measuring temperature. Consequently, proton conductivity, water self-diffusion coefficient and mechanical properties are also reduced in heat-treated samples due to this drop in sorption capacity. However, for transport properties these differences vanish when increasing the measuring temperature because the effects of temperature are predominant over the effects of hydration. When the samples are not heat-treated, the sorption capacity is not a function of temperature.
It is important to highlight that certain effects such as internal compression and/or constraints in Nafion may also alter its properties through morphological changes. These two effects may also be a key tool for understanding the heat pre-treatment effect on Nafion properties.
Few researchers have associated the internal compression and constraints effects with the nature of manufactured Nafion (*e.g.* extruded and casted) and with the swelling process, in particular with the swelling pressure (defined as the pressure applied by the polymer matrix to the water swollen domains). As an example, Kusoglu *et al*. [39] developed a mechanics-based model in order to study the evolution of water sorption in ionomers as a function of the swelling pressure, at a micrometer scale. In general, more studies (theoretical and experimental) on these types of effects have to be made in order to understand clearly their influences on the alteration of the Nafion properties (through morphological changes), and to correlate them with the drying temperature effect.

Rather than elucidating in details the nature of the observed behaviors, the objectives of this study are to provide an important set of experimental data, measured over a wide range of

experimental conditions. The measurement of sorption isotherms between 30°C and 80°C show a decrease in sorption capacity in the vapor phase with increasing temperature. The decrease of the elastic modulus of the polymer with temperature cannot explain this behavior. Other properties of the membrane, such as changes of its hydrophilicity with temperature, have then to be considered to gain a deeper understanding of sorption in this system. The proton conductivity, measured over a wide range of temperatures, follows a polynomial law when plotted as a function of relative humidity. When expressed as a function of water content, a threshold above which proton transport becomes efficient can be emphasized. Our measurements show that the water content corresponding to this threshold decreases with temperature.

The present study points out that the hygro-thermo-mechanical properties of Nafion must always be taken into account when evaluating the properties of this polymer. Thus the effects of pre-treatment and temperature should be carefully considered when comparing sorption, transport and mechanical values, since there exists controversy in the literature about these effects. As a reflection of this, several researchers found that for a certain relative humidity, water sorption decreases when temperature increases [2, 7, 10, 40] while others reported the opposite trend in which water sorption goes up as temperature rises [3, 9, 41].

5 References

[1] Mauritz, K. A. and Moore, R. B., State of Understanding of Nafion, *Chemical Reviews*, Vol. 104, No. 10, 2004, pp. 4535–4586.

[2] Rieke, P. and Vanderborgh, N., Temperature dependence of water content and proton conductivity in polyperfluorosulfonic acid membranes, *Journal of Membrane Science*, Vol. 32, No. 2-3, 1987, pp. 313–328.

[3] Morris, D. R. and Sun, X., Water-sorption and transport properties of Nafion 117 H, *Journal of Applied Polymer Science*, Vol. 50, No. 8, 1993, pp. 1445–1452.

[4] Zawodzinski, Jr., T. A., Springer, T. E., Davey, J., Jestel, R., Lopez, C., Valerio, J., and Gottesfeld, S., A Comparative Study of Water Uptake By and Transport Through Ionomeric Fuel Cell Membranes, *Journal of the Electrochemical Society*, Vol. 140, No. 7, 1993, pp. 1981–1985.

[5] Hinatsu, J. T., Mizuhata, M., and Takenaka, H., Water uptake of perfluorosulfonic acid membranes from liquid water and water vapor, *Journal of the Electrochemical Society*, Vol. 141, No. 6, 1994, pp. 1493–1498.

[6] Sone, Y., Ekdunge, P., and Simonsson, D., Proton Conductivity of Nafion 117 as Measured by a Four-Electrode AC Impedance Method, *Journal of The Electrochemical Society*, Vol. 143, No. 4, 1996, pp. 1254–1259.

[7] Broka, K. and Ekdunge, P., Oxygen and hydrogen permeation properties and water uptake of Nafion® 117 membrane and recast film for PEM fuel cell, *Journal of Applied Electrochemistry*, Vol. 27, 1997, pp. 117–123.

[8] Legras, M., Hirata, Y., Nguyen, Q. T., Langevin, D., and Métayer, M., Sorption and diffusion behaviors of water in Nation 117 membranes with different counter ions, *Desalination*, Vol. 147, No. 1-3, 2002, pp. 351–357.

[9] Jalani, N. and Datta, R., The effect of equivalent weight, temperature, cationic forms, sorbates, and nanoinorganic additives on the sorption behavior of Nafion®, *Journal of Membrane Science*, Vol. 264, No. 1-2, 2005, pp. 167–175.

[10] Takata, H., Mizuno, N., Nishikawa, M., Fukada, S., and Yoshitake, M., Adsorption properties of water vapor on sulfonated perfluoropolymer membranes, *International Journal of Hydrogen Energy*, Vol. 32, No. 3, 2007, pp. 371–379.

[11] Alberti, G., Narducci, R., and Sganappa, M., Effects of hydrothermal/thermal treatments on the water-uptake of Nafion membranes and relations with changes of conformation, counter-elastic force and tensile modulus of the matrix, *Journal of Power Sources*, Vol. 178, No. 2, 2008, pp. 575–583.

[12] Cappadonia, M., Erning, J. W., Saberi Niaki, S. M., and Stimming, U., Conductance of Nafion 117 membranes as a function of temperature and water content, *Solid State Ionics*, Vol. 77, 1995, pp. 65–69.

[13] Silva, R. F., De Francesco, M., and Pozio, A., Tangential and normal conductivities of Nafion® membranes used in polymer electrolyte fuel cells, *Journal of Power Sources*, Vol. 134, No. 1, 2004, pp. 18–26.

[14] Halseid, R., Vie, P., and Tunold, R., Influence of Ammonium on Conductivity and Water Content of Nafion 117 Membranes, *Journal of the Electrochemical Society*, Vol. 151, No. 3, 2004, pp. A381–A388.

[15] Gates, C. M. and Newman, J., Equilibrium and diffusion of methanol and water in a nafion 117 membrane, *AIChE Journal*, Vol. 46, No. 10, 2000, pp. 2076–2085.

[16] Choi, P. and Datta, R., Sorption in proton-exchange membranes. An explanation of Schroeder's paradox, *Journal of the Electrochemical Society*, Vol. 150, No. 12, 2003, pp. E601–E607.

[17] Vallieres, C., Winkelmann, D., Roizard, D., Favre, E., Scharfer, P., and Kind, M., On Schroeder's paradox, *Journal of Membrane Science*, Vol. 278, No. 1-2, 2006, pp. 357–364.

[18] Majsztrik, P. W., Satterfield, M. B., Bocarsly, A. B., and Benziger, J. B., Water sorption, desorption and transport in Nafion membranes, *Journal of Membrane Science*, Vol. 301, No. 1-2, 2007, pp. 93–106.

[19] Onishi, L. M., Prausnitz, J. M., and Newman, J., Water - Nafion Equilibria. Absence of Schroeder's Paradox, *Journal of Physical Chemistry B*, Vol. 111, No. 34, 2007, pp. 10166–10173.

[20] Kawano, Y., Wang, Y., Palmer, R. A., and Aubuchon, S. R., Stress-Strain Curves of Nafion Membranes in Acid and Salt Forms, *Polímeros*, Vol. 12, 2002, pp. 96–101.

[21] Evans, C. E., Noble, R. D., Nazeri Thompson, S., Nazeri, B., and Koval, C. A., Role of conditioning on water uptake and hydraulic permeability of Nafion® membranes, *Journal of Membrane Science*, Vol. 279, No. 1-2, 2006, pp. 521–528.

[22] Bass, M. and Freger, V., Hydration of Nafion and Dowex in liquid and vapor environment: Schroeder's paradox and microstructure, *Polymer*, Vol. 49, No. 2, 2008, pp. 497–506.

[23] Xu, F., Leclerc, S., Lottin, O., and Canet, D., Impact of chemical treatments on the behavior of water in Nafion® NRE-212 by 1H NMR: Self-diffusion measurements and proton quantization, *Journal of Membrane Science*, Vol. 371, No. 1-2, 2011, pp. 148–154.

[24] Alberti, G., Casciola, M., Massinelli, L., and Bauer, B., Polymeric proton conducting membranes for medium temperature fuel cells (110-160°C), *Journal of Membrane Science*, Vol. 185, No. 1, 2001, pp. 73–81.

[25] Péron, J., Mani, A., Zhao, X., Edwards, D., Adachi, M., Soboleva, T., Shi, Z., Xie, Z., Navessin, T., and Holdcroft, S., Properties of Nafion® NR-211 membranes for PEMFCs, *Journal of Membrane Science*, Vol. 356, No. 1-2, 2010, pp. 44–51.

[26] Kreuer, K. D., On the development of proton conducting materials for technological applications, *Solid State Ionics*, Vol. 97, No. 1-4, 1997, pp. 1–15.

[27] Kreuer, K.-D., Paddison, S., Spohr, E., and Schuster, M., Transport in proton conductors for fuel-cell applications: Simulations, elementary reactions, and phenomenology, *Chemical Reviews*, Vol. 104, No. 10, 2004, pp. 4637–4678.

[28] Perrin, J.-C., *Etude Expérimentale multi-échelles de la dynamique de l'eau dans les membranes ionomères utilisées en pile à combustible.*, Ph.D. thesis, Université Joseph Fourier, Grenoble I, Grenoble, France., 2006.

[29] Pivovar, A. M. and Pivovar, B. S., Dynamic Behavior of Water within a Polymer Electrolyte Fuel Cell Membrane at Low Hydration Levels, *Journal of Physical Chemistry B*, Vol. 109, No. 2, 2005, pp. 785–793.

[30] Perrin, J.-C., Lyonnard, S., and Volino, F., Quasielastic Neutron Scattering Study of Water Dynamics in Hydrated Nafion Membranes, *Journal of Physical Chemistry C*, Vol. 111, No. 8, 2007, pp. 3393–3404.

[31] Meier, F. and Eigenberger, G., Transport parameters for the modelling of water transport in ionomer membranes for PEM-fuel cells, *Electrochimica Acta*, Vol. 49, No. 11, 2004, pp. 1731–1742.

[32] Springer, T., Zawodzinski, T., and Gottesfeld, S., Polymer electrolyte fuel cell model, *Journal of the Electrochemical Society*, Vol. 138, No. 8, 1991, pp. 2334–2342.

[33] Kidena, K., Ohkubo, T., Takimoto, N., and Ohira, A., PFG-NMR approach to determining the water transport mechanism in polymer electrolyte membranes conditioned at different temperatures, *European Polymer Journal*, Vol. 46, No. 3, 2010, pp. 450–455.

[34] Silberstein, M. N. and Boyce, M. C., Constitutive modeling of the rate, temperature, and hydration dependent deformation response of Nafion to monotonic and cyclic loading, *Journal of Power Sources*, Vol. 195, No. 17, 2010, pp. 5692–5706.

[35] Satterfield, M. B. and Benziger, J. B., Viscoelastic properties of Nafion at elevated temperature and humidity, *Journal of Polymer Science Part B: Polymer Physics*, Vol. 47, No. 1, 2009, pp. 11–24.

[36] Futerko, P. and Hsing, I.-M., Thermodynamics of Water Vapor Uptake in Perfluorosulfonic Acid Membranes, *Journal of The Electrochemical Society*, Vol. 146, No. 6, 1999, pp. 2049–2053.

[37] Alberti, G. and Casciola, M., Solid state protonic conductors, present main applications and future prospects, *Solid State Ionics*, Vol. 145, No. 1-4, 2001, pp. 3–16.

[38] Dupuis, A.-C., Proton exchange membranes for fuel cells operated at medium temperatures: Materials and experimental techniques, *Progress in Materials Science*, Vol. 56, No. 3, 2011, pp. 289–327.

[39] Kusoglu, A., Tang, Y., Lugo, M., Karlsson, A. M., Santare, M. H., Cleghorn, S., and Johnson, W. B., Constitutive response and mechanical properties of PFSA membranes in liquid water, *Journal of Power Sources*, Vol. 195, No. 2, 2010, pp. 483–492.

[40] Maldonado, L., Perrin, J.-C., Dillet, J., and Lottin, O., Characterization of polymer electrolyte Nafion membranes: Influence of temperature, heat treatment and drying protocol on sorption and transport properties, *Journal of Membrane Science*, Vol. 389, No. 0, 2012, pp. 43–56.

[41] Jalani, N., Choi, P., and Datta, R., TEOM: A novel technique for investigating sorption in proton-exchange membranes, *Journal of Membrane Science*, Vol. 254, No. 1-2, 2005, pp. 31–38.

Chapter 4

Long-term evolution of the properties of Nafion® N115 exposed to constant temperature and humidity conditions

1 Introduction

In the characterization work of Nafion membranes properties presented in the previous chapter, it was observed that the equilibrium water content decreased with time, as shown in Figure 4.1: λ drops from 8.1 to 7.2 after 7 days at constant temperature and relative humidity (60°C and RH = 0.74). Of course, this opens questions about the validity of the results discussed previously. In addition, it appears necessary to identify the whole of the parameters involved in this phenomenon and its possible consequences on the other properties of Nafion.

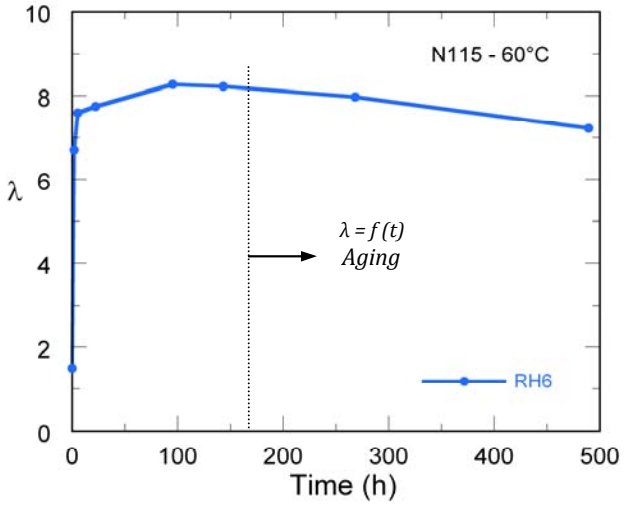

Figure 4.1: Water sorption of N115 at 60°C and RH6 (RH = 0.74) as function of time.

Similar observations were recently reported by Collette *et al*. [1], who measured a decrease of water sorption, associated with a drop in the proton conductivity of NR212 and N112. They also observed some changes in the mechanical properties of Nafion. This long-term exposure effect has been named "hygrothermal aging" and a mechanism based on the formation of sulfonic anhydrides (RSO_2-O-SO_2R) was proposed to explain the experimental results. The explored experimental conditions were, however, limited (aging at 80°C and at constant RH = 0.8 and RH = 0). The same authors have also shown in an another study that the hygrothermal aging was, at least to some extent, reversible: Collette *et al*. [2] demonstrated that the aged Nafion recovers its initial properties when immersed in an acid solution, or put in the presence of acid vapor. In these conditions, the Nafion chemical structure would return to its initial state. A possible explanation of these results could be the hydrolysis of the sulfonic anhydrides into sulfonic acid groups (RSO_3H), allowing their re-hydration.

In order to complete these observations, we exposed Nafion N115 to high temperatures (60°C and 80°C) over a wide range of relative humidities (RH = 0.2 to RH = 0.95) for a long period of time, up to 800 days. Water sorption, water self-diffusion, proton conductivity and mechanical properties of the Nafion samples were frequently measured using the experimental protocol described in the Chapter 2.

As mentioned in the previous chapter, the properties of Nafion depend also on thermal pre-treatments: this is the case for instance for water sorption, which is lower when Nafion is dried at high temperatures because of the shrinkage of the polymer structure. In this chapter, we choose to dry the membranes at two different temperatures: T_{dry} = 60°C and T_{dry} = 80°C.

It must be noted that the main objective of this study is to provide a set of experimental data about the long-term evolution of the Nafion properties. This will be one of the first steps toward the full understanding of the hygrothermal aging. To be more specific, our priority is to confirm the reality of the long-term evolution of Nafion properties, to establish which properties are actually affected, and to precise in which range of temperature and relative humidity this phenomenon occurs. Then, it could be considered to analyze in more details the changes induced in the chemical structure of the polymer. More generally, such studies can bring relevant information for the development of alternative membranes with more stable properties, and able to endure harsh operating conditions such as hydration/dehydration or voltage cycling.
Finally, the last part of the chapter is about the effects of Nafion long-term storage on the fuel cell operation: aged N115 membranes are tested in a cell and their performances are compared to those of pristine membranes.

2 Aging protocol

The Nafion N115 membranes are conditioned and heat treated as indicated in Chapter 2. Their water sorption capacity is then measured (after 7 days of equilibrium) as indicated in Chapter 3. After this initial characterization, the membranes are exposed to constant temperature and relative humidity conditions for a long period of time. Table 4.1 shows the main parameters involved in this work: drying temperature, aging temperature, relative humidity, and exposure time.

Table 4.1: Aging conditions applied on N115. The relative humidity corresponding to each salt solution (RH2-RH9) slightly depends on temperature.

Pre-treatment	Aging parameters										
Drying	T	Relative humidity								In	Maximal
T (°C)	(°C)	RH2	RH3	RH4	RH5	RH6	RH7	RH8	RH9	water	exposure (days)
60	60	0.29	0.40	0.50	0.63	0.74	0.80	0.93	0.95	√	800
60	80	0.28					0.79		0.91	√	400
80	80	0.28		0.51			0.79		0.91		400

After a period of seven days, the membranes reach the equilibrium state, which we considered as the reference state. After this 7-days period, we assumed that the aging started and the membrane is then referred as "aged N115". In practice, a set of three to seven samples is considered and their water content, water-self diffusion, proton conductivity and mechanical properties are evaluated at different aging times.

3 Water sorption

The water sorption of aged N115 is defined as the water mass fraction with respect to the dry mass of N115, expressed in percentage according to the procedure defined in Chapter 3 (Eq 6). Figure 4.2 presents the evolution of the sorption isotherm of N115, measured at 60°C, as a function of the aging time. The corresponding experimental values are gathered in Table 4.2 and Table 4.3.

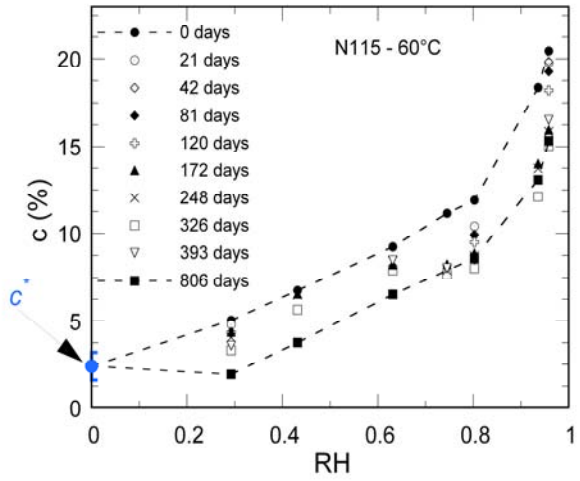

Figure 4.2: Sorption isotherm of N115 at 60°C, measured at different aging times. c^* is the residual water mass fraction (2.4±0.8%).

Table 4.2: Water content of N115 at 60°C and different RH at different times.

	$c(\%)$ of N115 at T = 60°C									
Day	0	21	42	81	120	172	248	326	393	806
RH2	5.1±0.6	4.8±0.4	4.4±0.4	4.3±0.4	4.3±0.4	4.4±0.4	4.1±0.4	3.3±0.4	3.6±0.4	1.9±0.4
RH3	6.8±0.7	-	-	-	-	6.6±0.7	6.5±0.7	5.7±0.7	5.2±0.7	3.8±0.6
RH5	9.2±0.6	-	-	-	-	8.2±0.6	8.4±0.6	7.9±0.6	8.5±0.6	6.5±0.6
RH6	11.2±0.5	-	-	-	-	8.3±0.5	7.9±0.5	7.7±0.5	8.0±0.5	-
RH7	11.9±0.4	10.4±0.4	10±0.4	9.9±0.4	9.5±0.4	8.9±0.4	8.7±0.4	8.0±0.4	8.5±0.4	8.6±0.4
RH8	18.4±0.7	-	-	-	-	14±0.7	13.7±0.7	12.1±0.7	14.9±0.7	13.1±0.7
RH9	20.5±0.5	19.8±0.5	19.8±0.5	19.3±0.5	18.2±0.5	16±0.5	15.9±0.5	15.0±0.5	16.5±0.5	15.3±0.5

Table 4.3: Normalized loss of water content in N115.

	% loss of c at T = 60°C									
day	0	21	42	81	120	172	248	326	393	806
RH2	0	5	14	14	14	14	20	34	29	62
RH3	0	-	-	-	-	3	4	16	23	44
RH5	0	-	-	-	-	11	9	14	8	29
RH6	0	-	-	-	-	26	29	31	28	-
RH7	0	13	16	17	20	25	27	33	28	28
RH8	0	-	-	-	-	24	25	34	19	29
RH9	0	3	3	6	11	22	22	26	19	25

We can observe that the water content of the membrane is globally decreasing as a function of time. This observation is valid whatever the relative humidity. Moreover, the general shape of the sorption isotherm is evolving with the aging time. The Langmuir contribution, which corresponds to the initial increase of water uptake at low RH (0<RH<0.3) is vanishing and disappears completely after 800 days. Since the Langmuir contribution is associated to a strong interaction between the first water molecules and the ionic acid groups, $SO_3^-H^+$ (see Chapter 1), this evolution could mean that the number of sulfonic acid sites is decreasing with time, as suggested by Collette *et al*. [1].

To better appreciate the variations of the water sorption, Figure 4.3a presents the evolution of the water mass fraction measured at each RH as a function of time. The corresponding relative variations are also given on Figure 4.3b, using the normalized values $c(t)/c_0 = c(t)/c(t=0)$.

The results in Figure 4.3a can be viewed as the kinetics of water desorption with aging time: this kinetics is fast until ~180 days and then it is slower. Moreover, the desorption does not seem to be finished after 800 days. In addition, the loss of water content is on the order of 20-40% after ~ 800 days (Figure 4.3b).

The water content seems to decrease more at low relative humidity (RH2 and RH3). However, the correlation between the RH and the water loss is not systematic.

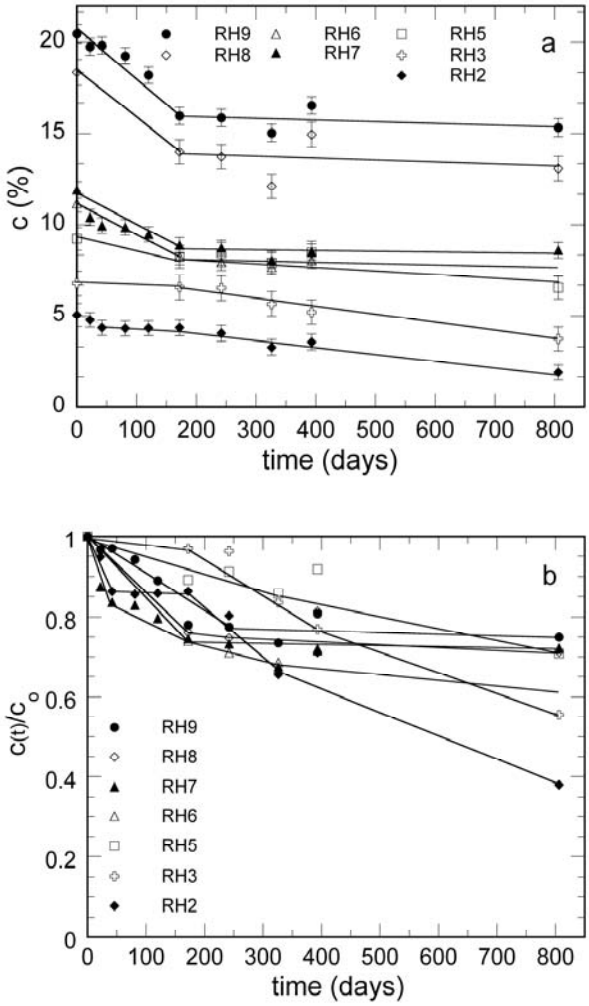

Figure 4.3: (a) Evolution of the water mass fraction in N115 as a function of the aging time. (b) Normalized values.

3.1 Effect of temperature

As the rate of desorption may depend on the aging temperature, we also exposed the N115 membranes to a temperature of 80°C and relative humidity of RH2, RH7, and RH9. The maximum aging time was 402 days. Figure 4.4, Table 4.4, and Table 4.5 present these results.

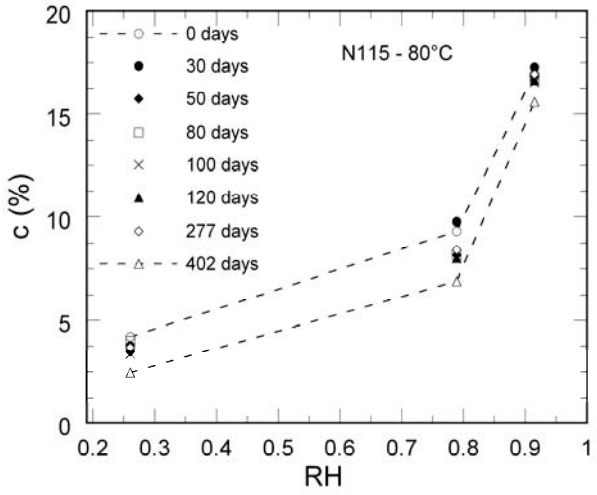

Figure 4.4: Sorption isotherm of N115 at 80°C and different aging times.

Again, we observe a decrease of the water content over time. The first period, characterized by a steep decrease, seems finished after ~ 100-120 days (Figure 4.5), which means that the desorption kinetics is faster at higher temperature.

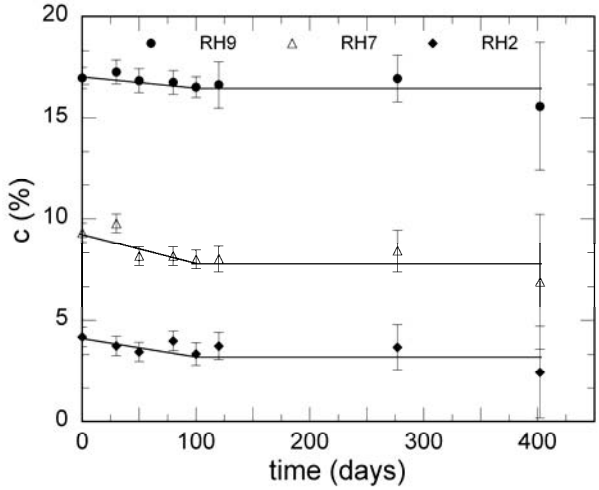

Figure 4.5: Water mass fraction in N115 at 80°C as a function of time.

Table 4.4 and Table 4.5 present the water content and the % loss of water in N115 at 80°C. The experimental errors were minimized by averaging the measurements over a set of seven samples. Uncertainties also resulted from water mass fluctuations observed for samples equilibrated at high RH (these fluctuations being probably caused by the formation of liquid droplets at the surface of the samples).

Table 4.4: Water content of N115 at 80°C and different RH at different times.

	$c(\%)$ of N115 at T = 80°C							
day	0	30	50	80	100	120	277	402
RH2	4.2±0.5	3.8±0.5	3.5±0.5	4±0.5	3.4±0.6	3.8±0.7	3.7±1.1	2.4±2.3
RH7	9.3±0.5	9.8±0.5	8.2±0.5	8.2±0.5	8±0.5	8±0.6	8.4±1.0	6.9±3.3
RH9	17±0.5	17.3±0.6	16.8±0.6	16.8±0.6	16.5±0.5	16.6±1.1	17±1.1	15.6±3.2

Table 4.5: Normalized loss of water content in N115.

	% loss of c at T = 80°C							
day	0	30	50	80	100	120	277	402
RH2	0	10	17	5	20	10	12	42
RH7	0	-5	12	12	14	14	10	26
RH9	0	-2	1	1	3	2	0	8

In order to compare the losses of water content of N115 aged at 60°C and at 80°C, we gathered some of the results in Table 4.6. We observe that, even if the kinetics is faster at 80°C compared to 60°C, the total loss of water is on the same order in both cases.

Table 4.6: Comparison of the values of $c(t)/c_0$ of N115 aged at 60°C and 80°C.

Aging time (days)	$c(t)/c_0$ at 60°C		$c(t)/c_0$ at 80°C	
	RH2	RH7	RH2	RH7
80	0.86	0.83	0.95	0.88
120	0.86	0.80	0.90	0.86
393-400	0.71	0.72	0.58	0.74

3.2 Effect of drying pre-treatment

In the previous chapter, we showed that a thermal pre-treatment can alter the membrane structure due to the shrinkage of the polymer matrix. As a consequence, it alters the Nafion properties too. In this section, we present the results obtained with N115 membranes pre-dried at 80°C before the long-term exposition at a temperature of 80°C and different RH for a maximum period of 371 days. These results are summarized in Figure 4.6, Table 4.7, and Table 4.8.

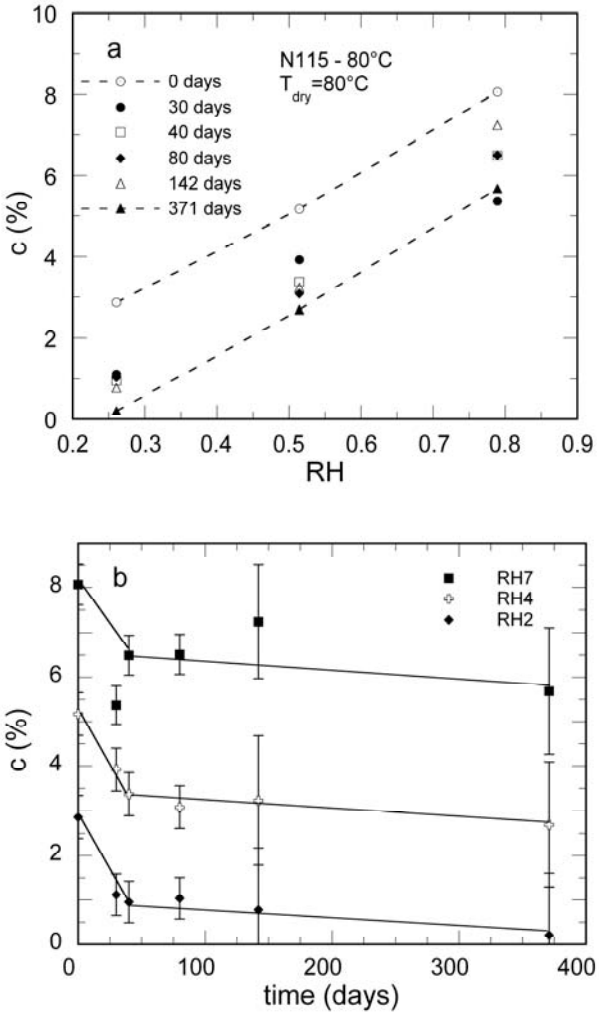

Figure 4.6: (a) Sorption isotherm of N115 at 80°C, measured at different aging times. (b) Evolution of the water mass fraction in N115 as a function of time.

Table 4.7: Water content of N115 at 80°C and different RH at different times.

	c(%) of N115-T_{dry}80°C at T = 80°C					
day	0	30	40	80	142	371
RH2	2.9±0.5	1.1±0.5	1±0.5	1±0.5	0.8±1.4	0.2±1.4
RH4	5.2±0.5	3.9±0.5	3.4±0.5	3.1±0.5	3.2±1.5	2.7±1.4
RH7	8.1±0.5	5.4±0.4	6.5±0.5	6.5±0.5	7.2±1.3	5.7±1.4

Table 4.8: Normalized loss of water content in N115.

	% loss of c at T = 80°C (T_{dry}80°C)					
day	0	30	40	80	142	371
RH2	0	61	67	64	73	93
RH4	0	24	35	40	37	48
RH7	0	33	19	19	10	29

The water content of N115 aged at 80°C and at different RH decreases as a function of time. Furthermore, the kinetics of desorption seem to be faster for the samples dried at 80°C than for those dried at 60°C. As an example, samples dried at 80°C and RH2 or RH7 (Figure 4.6b) lost 64% and 19% of their water content in the first 80 days while those dried at 60°C lost only 5% and 12% (Figure 4.5).

It must be noted however that the experimental errors are important because three samples only were tested. It is thus difficult to draw a definitive conclusion based on these observations. Despite of these difficulties it is still possible to state that the effect of the heat treatment on the evolution of the sorption capacity is on the second order, compared to the main aging phenomenon.

3.3 In liquid water

In the previous section we discussed the long-term decrease of the water sorption capacity of N115 in the presence of humid air. In this section, the sorption experiments are carried out in liquid water to see if the same phenomenon occurs. Figure 4.7, Table 4.9, and Table 4.10 present the evolution of the water content of N115 immersed in water at 60°C and 80°C as a function of time.

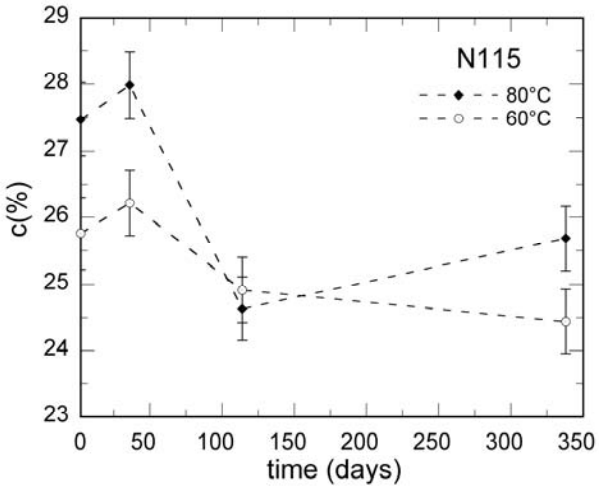

Figure 4.7: Evolution of the water sorption of N115 immersed in liquid water at 60°C and 80°C.

Table 4.9: Water content of N115 in liquid water at 60°C and 80°C for different aging times.

	$c(\%)$ of N115 at T = 60°C			
day	0	36	114	338
	25.8±0.5	26.2±0.5	24.9±0.5	24.4±0.5
	$c(\%)$ of N115 at T = 80°C			
day	0	36	114	338
	27.5±0.6	28±0.5	24.6±0.5	25.7±0.5

Table 4.10: Normalized loss of water content in N115.

	% loss of c at T = 60°C			
day	0	36	114	338
	~0	0	3	5
	% loss of c at T = 80°C			
day	0	36	114	338
	~0	0	10	7

We observe a moderate decrease of the water sorption in liquid water over time. The loss of water is on the order of 5 to 7 % after 338 days. By comparison, the loss of water sorption in vapor at 60°C and RH = 0.9 is of 26 %, after 326 days, which is much higher.

4 Mechanical properties

As seen in Chapter 3, the mechanical properties of Nafion are linked to its water content (λ) and depend on the drying temperature (T_{dry}): an increase of the drying temperature up to 110°C caused a moderate shrinkage of the structure of the membrane and resulted in a lower water uptake. This behavior was reflected by an increase of the initial slope of the stress-strain curves and thus a higher Young modulus.
The loss of water sorption in N115 exposed to constant (T, RH) conditions for a long time might be caused by changes in the Nafion microstructure, which can be confirmed (or not) by studying the stability of the mechanical properties of the aged membranes. To do so we performed uniaxial tensile tests following the experimental protocol described in Chapter 2.

Mechanical model

Without calling upon a detailed analysis of the experimental data, the general description of the shape of the stress-strain curves is generally very useful as it gives information concerning the elastic modulus (slope at the origin), the yield point (beginning of the plastic deformation), the failure point, the toughness, and others. In the case of aged membranes, however, the shape of the stress-strain response is different from that of pristine Nafion. As it will be seen in the next paragraph, this is especially true at small strains: the response to the applied stress is not linear and the curve is rounded near the origin.

Based on this observation, we have considered that aged N115 could behave as a viscoelastic material, since Nafion, in general, can exhibit elastic and viscous behaviors when undergoing deformation [3, 4, 5]. We have selected a mechanical model that describes the viscoelastic

behavior by considering a combination of the elastic spring and the viscous dash-pot [6, 7]. This model, named standard linear solid model (SLS), is represented on Figure 4.8b.

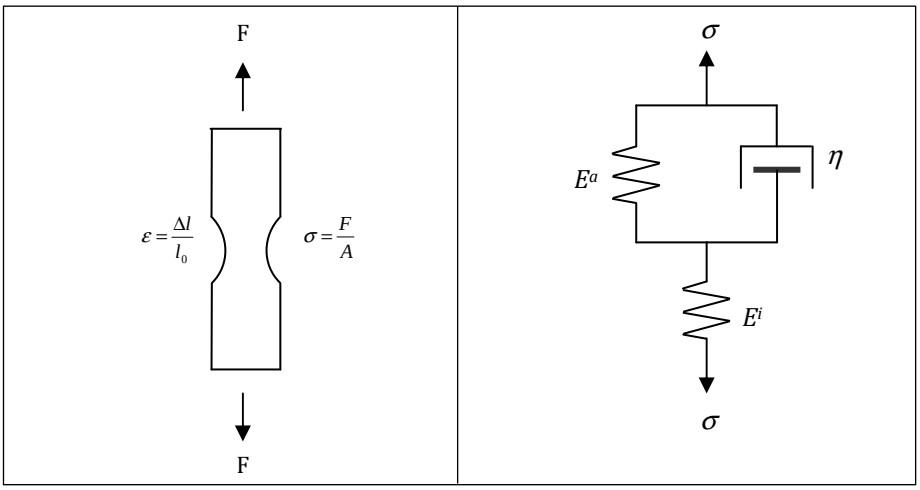

Figure 4.8: Left column: scheme of the tensile force applied on Nafion. Right column: standard linear solid (SLS) model.

The SLS model is referred to as "solid", since materials could react instantaneously as elastic materials and recover completely upon unloading; the equation is represented in Eq 1. The SLS model is also referred to as "fluid", since materials could respond as viscous fluids and do not recover upon unloading (Eq 2). The resulted viscoelastic equation is obtained by a combination of these two equations with the help of Laplace transforms (Eq 3) [8]. It is then possible to estimate the apparent elastic modulus (E^a) by taking the limit of Eq 3 when ε approaches zero (Eq 4).

Solid spring	$\sigma = E.\varepsilon$	Eq 1
Viscous dash-pot	$\xi = \frac{1}{\eta}.\sigma$	Eq 2
Viscoelastic	$\sigma(\varepsilon) = \tau\left(E^i - E_r\right)\xi + E_r\xi\varepsilon + \xi\tau\left(E_r - E^i\right)e^{-\varepsilon/\tau}$	Eq 3
Apparent elastic modulus	$E^a = \frac{1}{\varepsilon}\lim_{\varepsilon\to 0}\sigma(\varepsilon) = \xi(E^i - E_r)$	Eq 4

The known parameters are:

σ the imposed stress (Pa)

ε the measured strain (% of µm/µm)

ξ the strain rate (s^{-1}), equal to $\Delta\varepsilon/\Delta t = 0.0056$ (s^{-1}) in our experiments

The parameters introduced into the model (Eq 3) are:

τ the ratio of viscosity of sample to elastic modulus (s)

E^i the instantaneous elastic modulus response of the sample (Pa)

E_r is equal to $\frac{E^a.E^i}{E^a+E^i}$ (Pa)

The indirect parameters from (Eq 1) and (Eq 2) are:

E the elastic modulus (Pa)

η the viscosity of the material (N s/m^2)

Stress-strain curves of aged N115

The tensile tests were performed at 23°C and ambient humidity conditions (RH = 0.38). The aged N115 membranes were classified in accordance with their aging conditions as described in the following table:

aged N115	aging conditions
N115 (1)	60°C, RH7(RH = 0.8), 256 days
N115 (2)	60°C, RH7, 714 days
N115 (3)	80°C, RH7, 277 days
N115 (4)	80°C, RH7, 324 days
N115 (5)	60°C, in water, 338 days
N115 (6)	80°C, in water, 338 days

Three to five tensile tests were performed in order to minimize the experimental errors. The average of the stress-strain curves is represented in the graphics as the "mean" and was fitted against the SLS model (Eq 3). The corresponding curve is represented on the plots as the "model".

The stress-strain curves of N115 exposed to 60°C and RH7 over 256 and 714 days are showed in Figure 4.9.

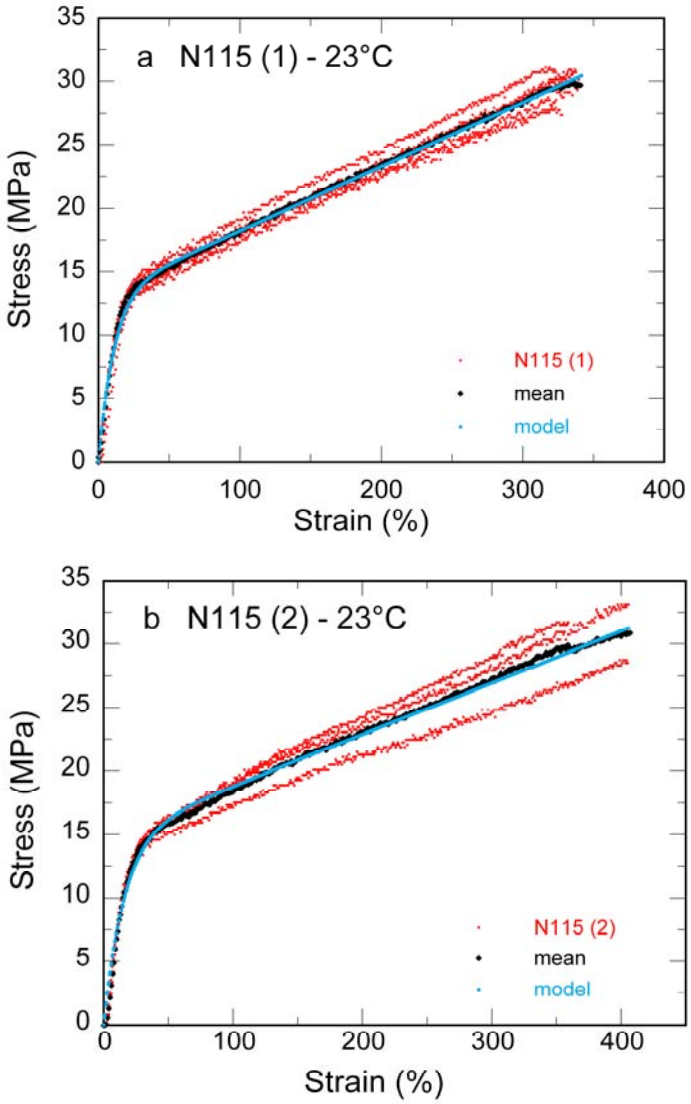

Figure 4.9: Stress-strain curves at 23°C and RH = 0.38 of (a) aged N115 (1), and (b) aged N115 (2).

The model fits well the stress-strain data of aged N115, it also provides homogeneous information about the elastic region (0-50%) up to the plastic region (>50%) of the curves.

The stress-strain curves of N115 exposed to the temperature of 80°C and RH7 over 277 and 324 days are shown in Figure 4.10. Note that, for clarity, we only show here the averaged values of the experimental data.

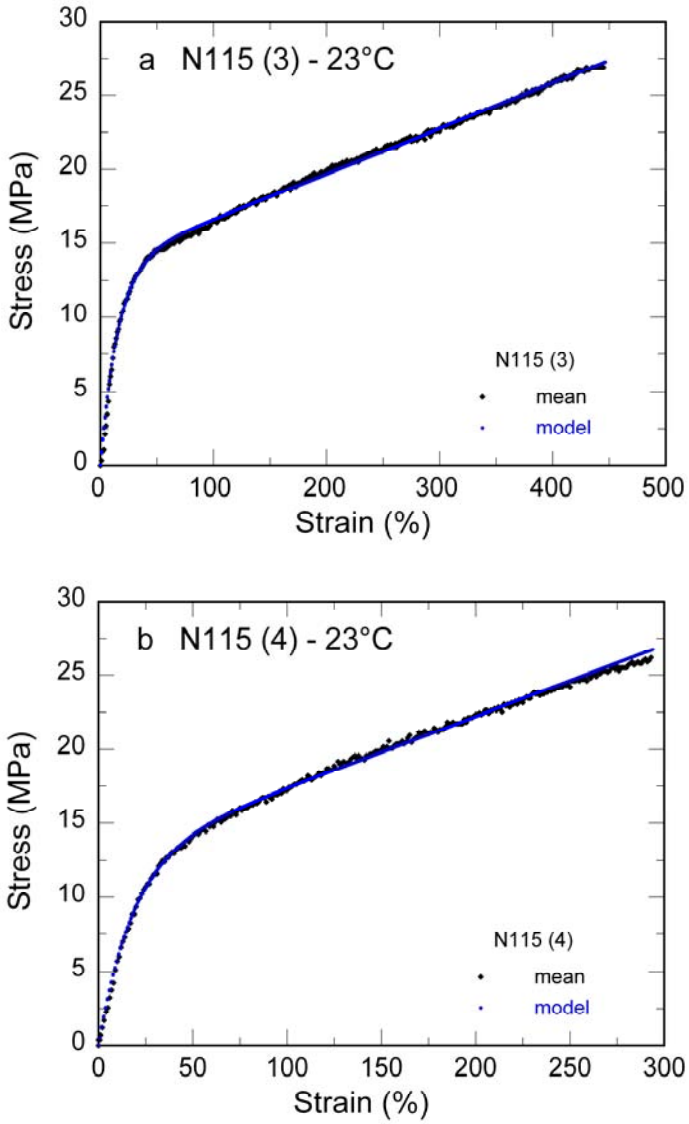

Figure 4.10: Stress-strain curves at 23°C and RH = 0.38 of (a) aged N115 (3), and (b) aged N115 (4).

The compilation of the stress-strain curves of aged N115 (60°C and 80°C) and of the N115 reference is shown in Figure 4.11. The reference curve corresponds to the average of five tests.

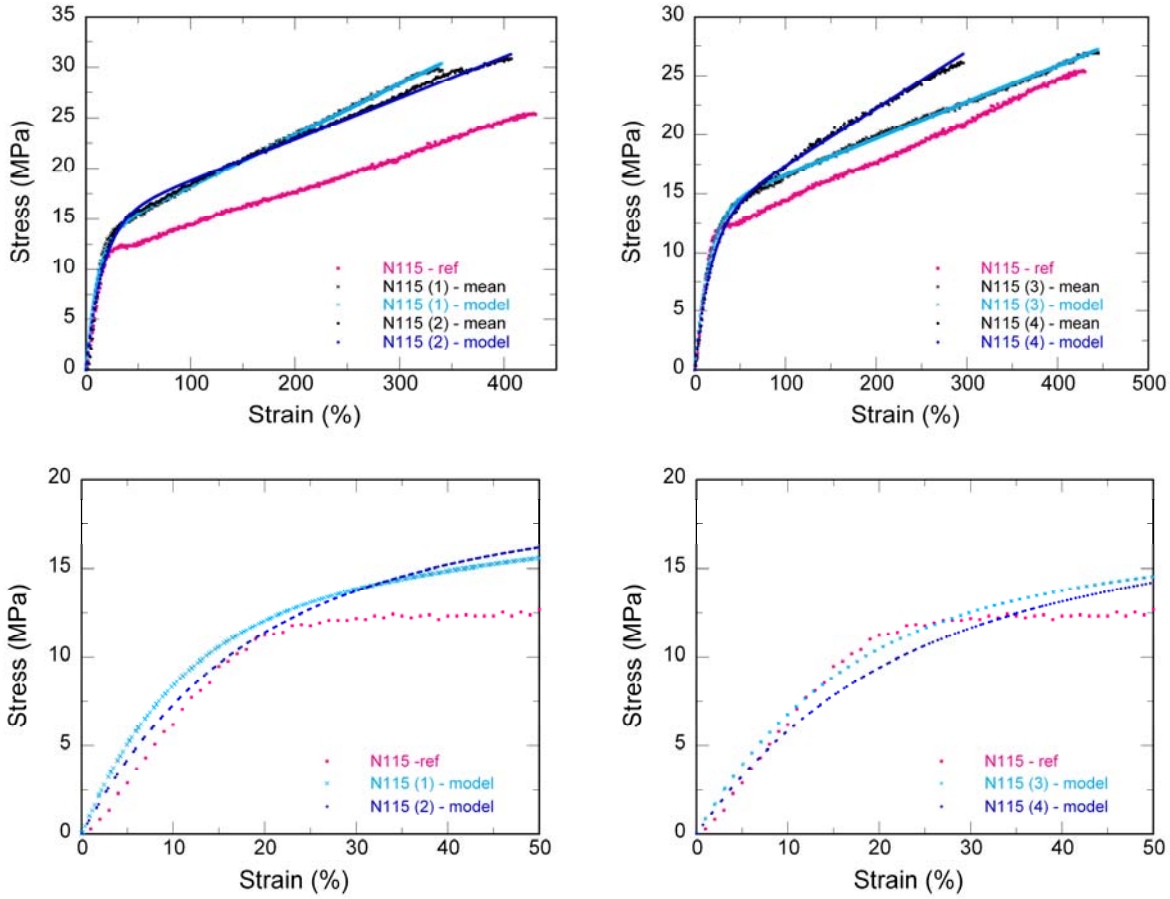

Figure 4.11: Stress-strain curves of the aged N115 and the reference at 23°C and RH = 0.38. Left column: aging at 60°C. Right column: aging at 80°C.

Table 4.11 shows the mechanical parameters of aged N115 and of the reference. The data were obtained from the experimental stress-strain curves with the exception of the apparent elastic modulus (E^a) of the aged N115, which were obtained from the model (Eq 4).

Table 4.11: Mechanical parameters of N115 exposed at 60°C and 80°C and RH7 for a long period of time.

Mechanical parameters of N115 at T = 23°C, RH = 0.38						
Aging conditions			Strain to failure (%)	Stress to failure (MPa)	E (MPa) curve	E^a (MPa) Eq 3
N115	T°C, RH	Time (days)				
N115 - ref	-	0	433±27	26±2	67±3	-
N115 (1)	60, 0.8	256	342±20	30±1	-	121±20
N115 (2)	60, 0.8	714	407±43	31±2	-	93±8
Aging conditions			Strain to failure (%)	Stress to failure (MPa)	E (MPa) curve	E^a (MPa) Eq 3
N115	T°C, RH	Time (days)				
N115 – ref	-	0	433±27	26±2	67±3	-
N115 (3)	80, 0.8	277	445±25	27±1	-	88±7
N115 (4)	80, 0.8	324	349±73	28±5	-	70±6

As noted previously, we observe that aged N115 do not behave similarly as the reference. Aged N115 requires higher stresses to be elongated at the imposed strain rate of 0.0056 s^{-1}. These high stresses may be interpreted as higher resistances of the membrane to unidirectional deformation, resulting in a more rigid aged N115. This is reflected in the previous Table by an increase of the (apparent) Young modulus.

The failure point of aged N115 is reached at a slightly higher stress than the reference. This shows that the aged membrane does not become brittle upon aging. We can also note that the yield point, which corresponds to the beginning of the plastic deformation (strain < 50%) is visible on the reference curve, but seems to disappear on the aged N115 curves (Figure 4.11). The transition between elastic and plastic deformation in (pristine) Nafion is generally considered difficult to observe [3]. In our case, this transition is also observed in composite membranes (Chapter 5). However, we did not vary the strain rate (0.0056 s^{-1}) nor the temperature or the relative humidity during the tests to check if these results were reproducible in other conditions.

The stress-strain response of N115 immersed in liquid water at 60°C and 80°C over 338 days is shown on Figure 4.12 and compared to the fully-hydrated (24 h in water) reference sample.

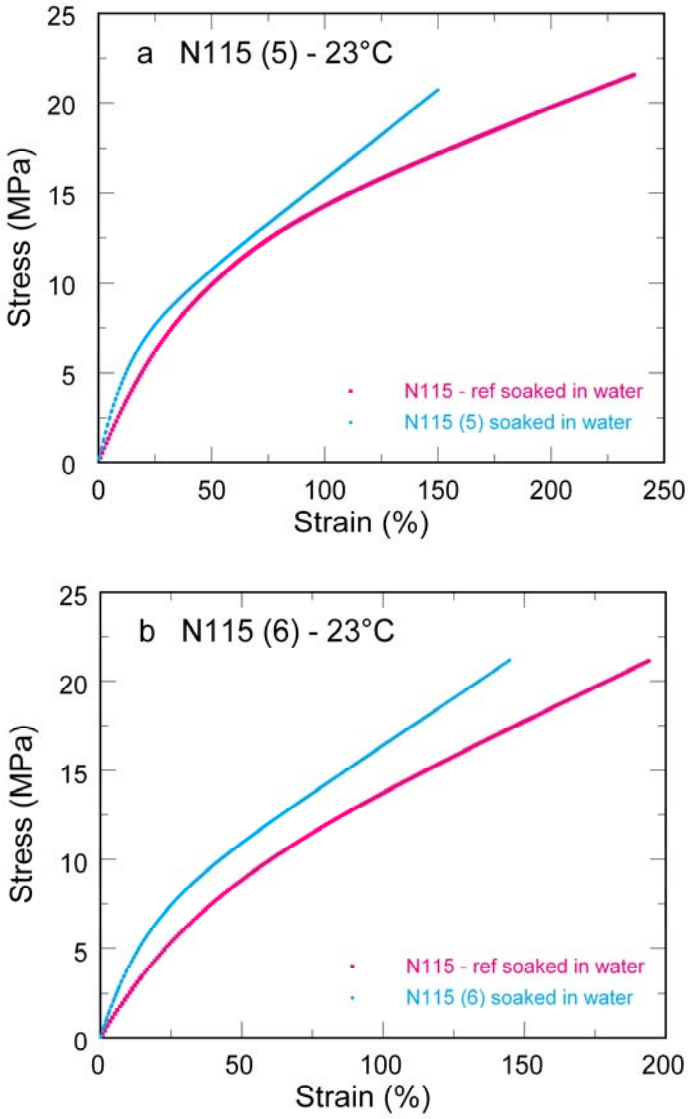

Figure 4.12: Stress-strain curves at 23°C and RH = 0.6 of (a) aged N115 at 60°C, and (b) aged N115 at 80°C, in liquid water during 338 days.

Table 4.12 presents the corresponding mechanical parameters.

Table 4.12: Mechanical values of N115 exposed at 60°C and 80°C in liquid water for a long period of time.

Mechanical parameters of saturated N115 at T = 23°C, RH = 0.38					
Aging conditions			Strain to failure (%)	Stress to failure (MPa)	E^a (MPa) Eq 3
N115	T°C	Time (days)			
N115 - ref	60, in water	0	213±33	21±1	25±5
N115 (5)	60, in water	338	147±57	19±6	51±16
Aging conditions			Strain to failure (%)	Stress to failure (MPa)	E^a (MPa) Eq 3
N115	T°C	Time (days)			
N115 - ref	80, in water	0	173±29	19±5	20±2
N115 (6)	80, in water	338	126±58	19±6	43±25

As described in the literature, fully hydrated samples display a much lower Young modulus (~20 MPa for the reference N115 soaked in water compared to 67 MPa for N115 equilibrated at RH = 0.38 at the same temperature) which traduces the fact that water acts in the hydrated membranes as a plasticizer [3, 5].
In the water-aged membranes, the apparent Young modulus increases by comparison with the reference sample, showing an increase of the rigidity of the polymer. Moreover, the failure point of aged N115 was reached at higher stress than that of the reference.

Interpretation of the stress-strain curves of aged N115

As seen in the previous section of this chapter, the water sorption capacity of aged Nafion N115 is reduced compared to that of pristine membranes. The stress-strain curves being measured at constant RH conditions, the quantity of adsorbed water in aged membranes was therefore lower in aged membranes than in new membranes. Two effects have thus to be taken into account when analyzing the mechanical tests: the water content effect and the effect of aging at constant (T, RH) conditions. The water content effect is significant as the Young modulus can be reduced by a 5 factor when the membrane is equilibrated between RH=0.4 and RH=1 [3]. The analysis and the interpretation of the stress-strain curves are thus challenging since the results depend on several, coupled, parameters.

In this study, the effect of aging seems to correspond to an increase of the Young modulus and thus an increase of the stiffness of the membrane. Without any aging effect, a decrease of the quantity of adsorbed water would also correspond to an increase of the Young modulus. It is thus not possible at this stage to discriminate the effect of water content and a potential effect of aging on the microstructure of the membrane. The full knowledge of the effect of time on the

mechanical properties of N115 stored at constant (T, RH) conditions would be possible only by performing the stress-strain tests at constant hydration (λ), which would considerably complicate the experimental protocol.

Nevertheless our study clearly shows that the aging effect is not predominant over the water content effect since the observed increase of the Young modulus is moderate: the membrane does not become brittle during the aging process.

5 Water and protons transport

The ionic conductivity of the Nafion membrane represents its most important property for the fuel cell application. We have already seen in the first chapter of this manuscript that the proton transport is strongly coupled to the quantity of water adsorbed in the structure of the polymer. In the last sections of the present chapter, we have measured a substantial decrease of the water sorption capacity of N115 exposed to constant (T, RH) conditions for a long time. The mechanical properties are also impacted by the aging, but the observed differences between aged samples and the references are not much significant. In this section, we study the impact of aging on the transport properties of N115 membranes. For this purpose, we performed multiple measurements of the water self-diffusion coefficient and the ionic conductivity following the experimental protocols described in Chapter 2.

5.1 Water-self diffusion

Pulsed Field Gradient Nuclear Magnetic Resonance (PFGNMR) is a technique able to probe the mobility of water molecules in the membrane at a scale of a few microns. Because the water self-diffusion coefficient is reduced in the membrane (compared to bulk water) due to the tortuosity of the diffusion path, any change of the microstructure of the polymer due to aging could then be detected by a variation of this parameter. Figure 4.13 shows the water self-diffusion coefficient measured by PFGNMR at 25°C as a function of the imposed water concentration in pristine N115 and in aged N115 (80°C, RH4 and RH7), for different aging times.

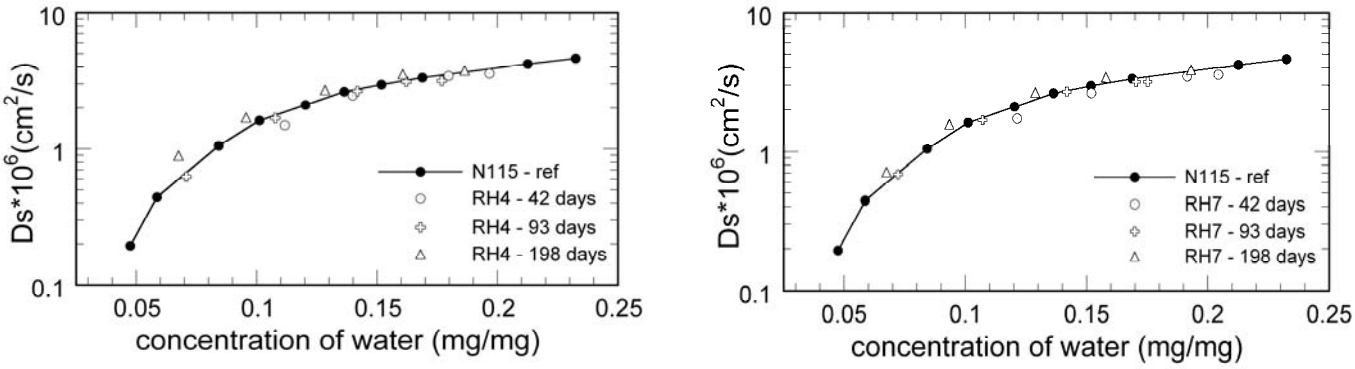

Figure 4.13: Water self-diffusion curves of aged N115 at 25°C. Aging at 80 °C, RH4 (left column) and RH7 (right column).

We can observe that the water self-diffusion coefficient does not vary at all in aged Nafion, compared to pristine Nafion equilibrated at the same water content. Similar results were presented by Collette [9] in Nafion 212. We can conclude from these results, that the structure of water channels (at the micrometer scale) is probably not affected by aging.

5.2 Proton conductivity

Figure 4.14 shows the proton conductivity curves of N115 exposed to a constant temperature of 60°C (left column) and 80°C (right column) and different relative humidity conditions (RH2, RH7, and RH9) for different durations. All measurements were performed at 60°C. The reference curve (thick black line "N115-ref") corresponds to the average of data collected over five tests carried out before aging. This curve thus incorporates the experimental errors. On the other hand, the curve of each aged sample corresponds to the data of one test. The plots at the bottom of the Figure represent the evolution of the ionic conductivity as a function of the aging time.

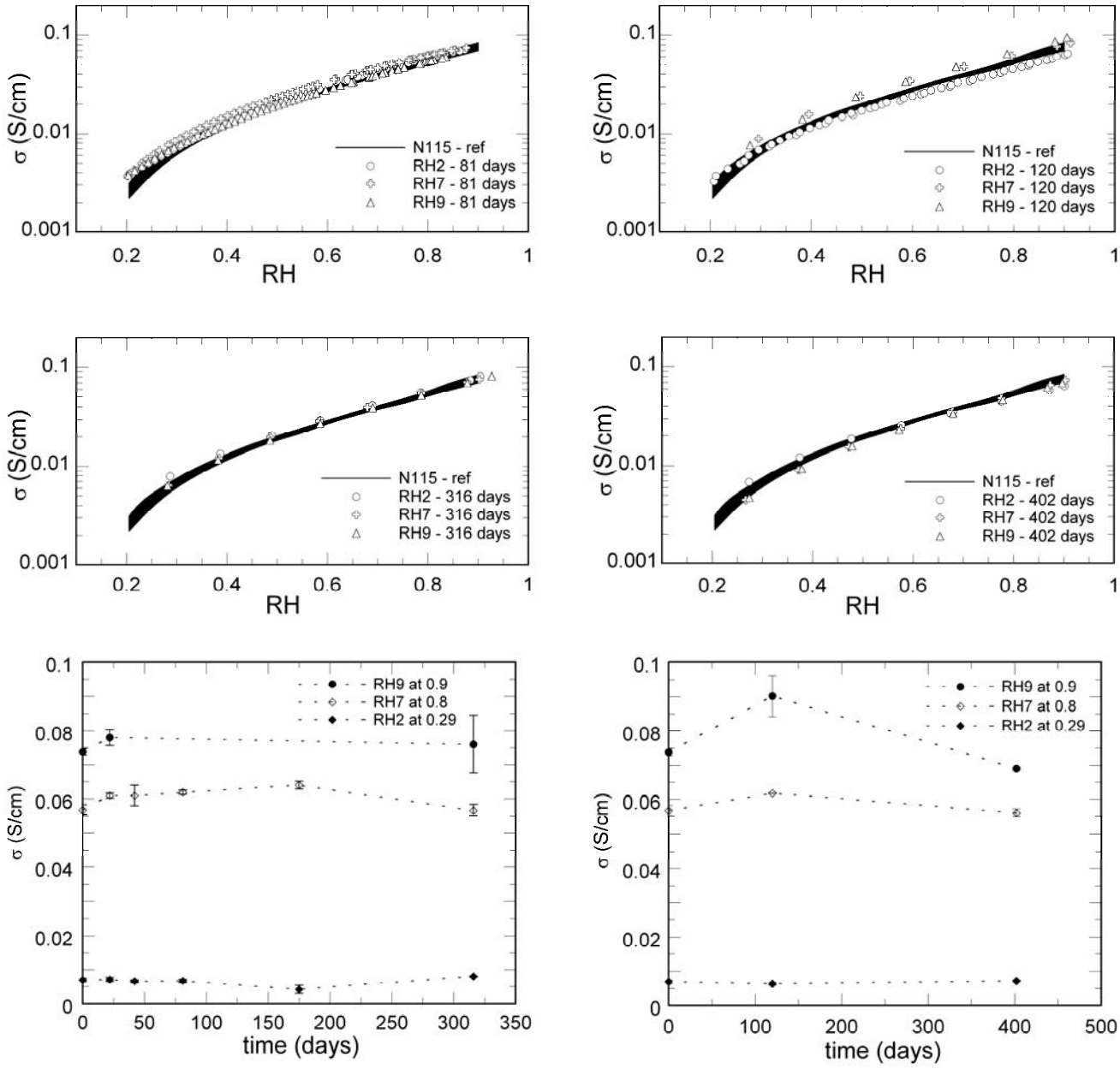

Figure 4.14: Proton conductivity of aged N115 at 60°C as a function of relative humidity and aging time. Left column: aging at 60°C. Right column: aging at 80°C.

We can see on Figure 4.14 that the ionic conductivity is not varying with time. This observation is valid for the different RH conditions and for the two temperatures considered. These results seem to lead to the conclusion that the ionic conductivity is not impacted by the aging at 60°C or 80°C.

We also measured the proton conductivity of N115 aged at 80°C and RH2, RH4, RH7 and RH9 over 370 days and previously heat-dried at 80°C. Figure 4.15 shows the results obtained at 60°C.

The reference curve (black line "N115-T_{dry} = 80°C") and the data on the aged samples correspond to one test.

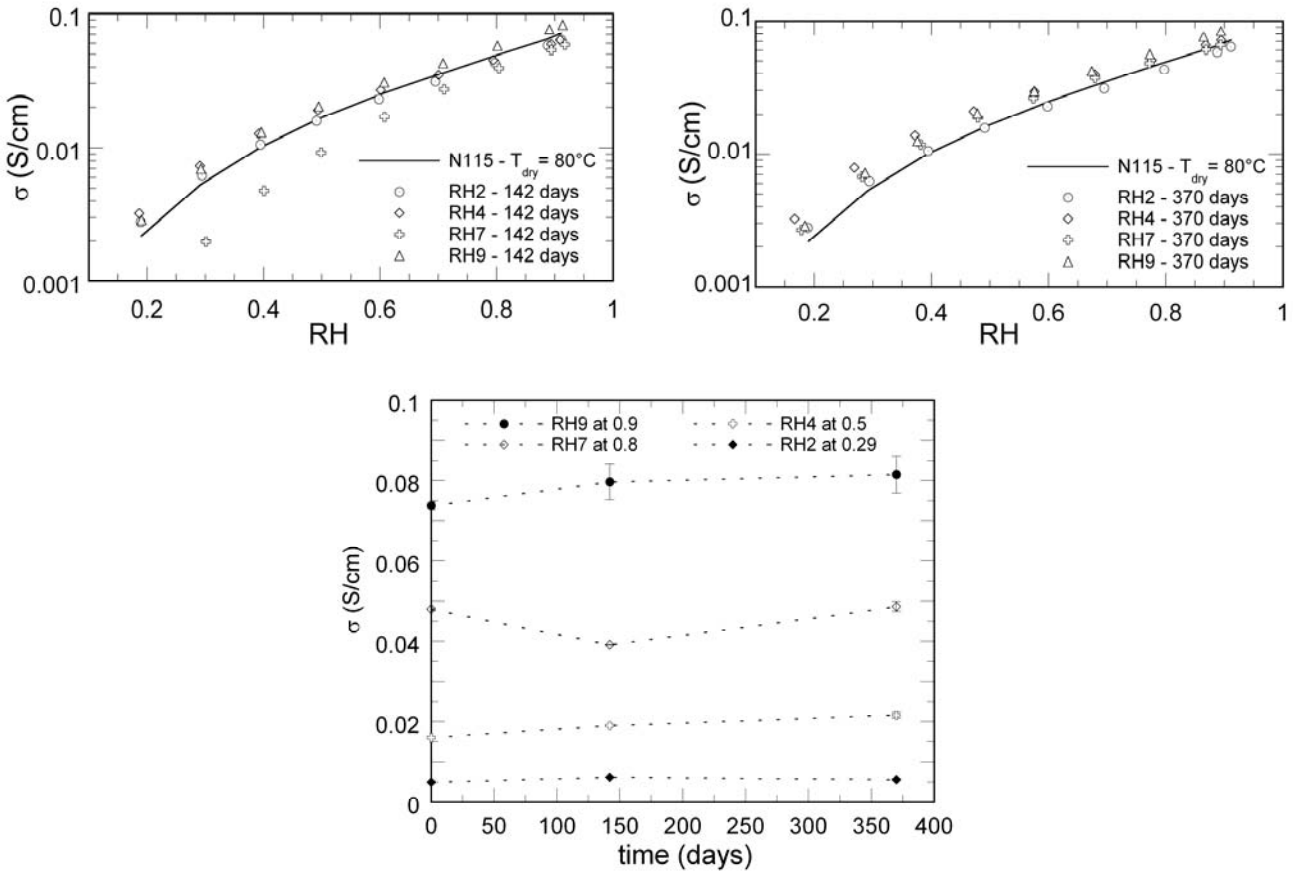

Figure 4.15: Proton conductivity of aged N115 at 60°C as a function of relative humidity (top) and aging time (bottom).

Again, we do not observe any significant variation of the conductivity with the aging time, except for the sample aged at RH7 (RH = 0.8) over 142 days of exposure. Its decrease in proton conductivity may result from a defect in the sample.

All these measurements tend to show that the decrease of the sorption capacity of N115 is not causing any effect on the ionic conductivity. This result is very surprising considering the fact that the ionic conductivity is strongly dependent on the water content. In Chapter 3 for example, we measured a loss of 26% in λ in a N115 membrane dried at 80°C and 100°C, compared to a reference dried at 60°C (the measurement was performed at 60°C, RH = 0.29, see Table 4.13). The corresponding drop in proton conductivity was 21%. At RH = 0.8, λ was decreased by 19% and σ by 12%. Here, the aging in the same conditions leads to a decrease of 29% and 28% in λ, respectively, after 393 days but no corresponding drop in σ is detected.

Table 4.13: Losses (%) of water sorption and proton conductivity of Nafion N115 at 60°C, caused by drying pre-treatment and by hygrothermal aging effects.

Measurements parameters	% of losses due to drying effect (T_{dry} = 80°C and 100°C)		% of losses due to aging effect (60°C, RH = 0.29, RH = 0.8, 393 aging days)		
	$\overline{\Delta\lambda}/\lambda$	$\overline{\Delta\sigma}/\sigma$	$\Delta\lambda/\lambda$	$\Delta\sigma/\sigma$ measured	$\Delta\sigma/\sigma$ expected
60°C, RH = 0.29	26	21	29	no variation	~23
60°C, RH = 0.8	19	12	28	no variation	~18

In order to understand these results, we considered reviewing certain specifications of our experimental protocol. As described in Chapter 2, the proton conductivity is measured in the in-plane direction of the membrane by impedance spectroscopy using a home-made 4-points conductivity cell. When designing this cell, we assumed that the mobility of the charges in the in-plane direction of the membrane was representative of the mobility of the charges through the membrane without taking any anisotropic behavior into consideration.

Our experimental results could then be interpreted by considering that the aging phenomenon at the origin of the decrease in sorption capacity is non-homogeneous. For example, it may impact only the volume properties of the membrane, leaving the surface properties unchanged. Since it is mostly the surface properties that are probed by the in-plane measurement of the conductivity, the conductivity remains unchanged.

To test this hypothesis, we decided to perform a test of the measurement of the proton conductivity of aged N115 in the through-plane direction using the equipment owned by the SPrAM laboratory (UMR 5819), at CEA Grenoble. The measurements were performed in saturated conditions (23°C) on two samples aged at 60°C, RH4 (RH = 0.5) during 484 days. The samples were equilibrated in deionized water for three days and placed in a home made conductivity cell. This cell consists of two electrodes placed on both side of the sample and containing gold wires regularly spaced (5 mm). The measurements were performed between 5 MHz and 100 Hz with an amplitude of 0.005V. The results are shown below.

	σ (S/cm) at 23°C	% loss
N115 reference	0.050±0.001	_
Aged at 60°C, RH4 for 484 days	0.034±0.004	32
N115 reference at 23°C, RH=0.9 (this study)	0.053*	_

*This value is obtained from the Arrhenius plot of the in-plane proton conductivity measurements (Chapter 3).

We observe that the conductivity of the aged samples decreases from 0.050 S/cm to 0.034 S/cm, which represents a drop of 32%. This is not surprising since there is a considerable decrease of their water content (~20-30%) in the same aging conditions. Therefore, there are two possible reasons which can explain the divergence with our results:

- The aging phenomenon impacts only the volume properties of the membrane leaving the surface properties unchanged. Since our conductivity cell measures the proton conductivity in the plane direction, we are not able to detect the differences induced by aging.

- A certain reversibility of the aging phenomenon occurs before or during the measurement of the proton conductivity. In this hypothesis, aging is not observed because the hydration state of the membrane during the conductivity measurements does not correspond to that measured in the sorption experiments. Indeed, our protocol implies a complete desorption phase before starting the conductivity measurements. Then, the membrane is gradually rehydrated up to a state identical or very close to what it was before aging.

6 Fuel cell test

After a long-term exposure at high T and constant RH, the lower water sorption capacity of N115 may limit the fuel cell performance. In this section, we present results obtained with Membrane Electrodes Assemblies (MEAs) built from aged N115. The N115 was previously maintained at 80°C and RH7 (RH = 0.76) during 160 days. At this aging time, the membrane loses 13 % of its initial water content.

6.1 Conditioning step

The aged and the reference membrane are hot-pressed between two 25 cm^2 Gas Diffusion Electrodes (GDEs). These electrodes are based on graphitized carbon paper (Sigracet® GDL 10BC) with a thickness of 420 µm and a load of platinum (Pt) of 1 mg/cm^2. They were provided by BalticFuelCells GmbH. Then, the membrane electrodes assemblies went through a conditioning stage in order to reach their best performance. For this, the fuel cell was operated at a constant current density of 7A (0.28 A/cm^2) during 24 hours. It was supplied with air and hydrogen (H_2), both humidified at RH = 1 and its temperature was set to 65°C. The Figure 4.16 shows the evolution of the voltage of both MEAs.

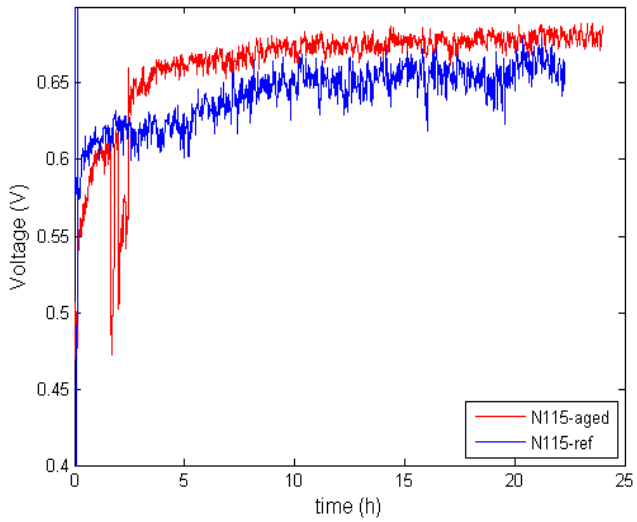

Figure 4.16: Fuel cell voltage as a function of time, measured at 65°C and 7A.

At the beginning of the conditioning stage, from 0 h to 3 h, the performance of the aged MEA seems less stable than that of the reference MEA; however it improves over time and even exceeds the reference after 24 h. The final voltage reached by the aged N115 was ~ 0.67 V, and 0.65 V for the reference membrane. However, this small variation in voltage was not observed again when we compared the polarization curves showed in Figure 4.17a. It must be noted that the polarization curves correspond to the average of three measurements, contrary to the conditioning stage which was performed only once.

6.2 Polarization curves

The polarization curves where measured using 100% humidified air and H_2 with a stoichiometry of 3 and 1.4, respectively. These curves are displayed on Figure 4.17.

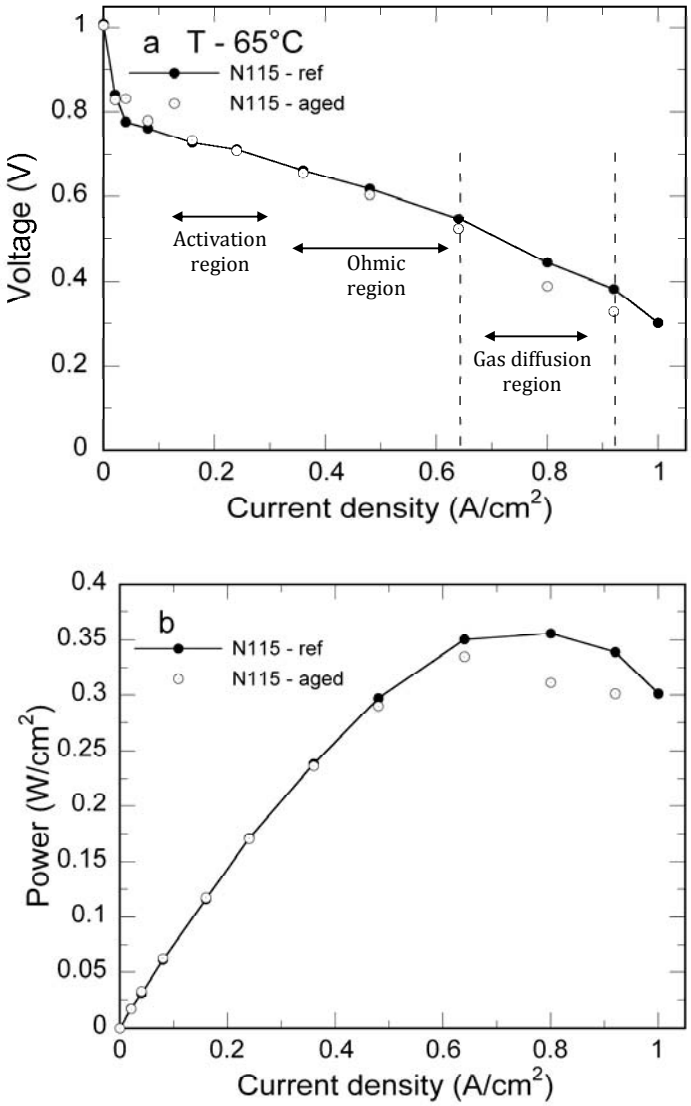

Figure 4.17: (a) Polarization curves obtained with aged N115 and as received N115, at 65°C with 100% humidified air and H_2 stoichiometry of 3 and 1.4, respectively. (b) Power density vs. current density.

We see on Figure 4.17a, that at low current density the polarization curve of the aged N115, does not seem to be altered, when compared with the reference membrane. This result is consistent with the absence of modification of the membrane conductivity during aging, despite of the drop of water sorption. However, at high current density the polarization curve of the aged N115 falls below that of the reference membrane. This decrease occurs in the high current density region where losses due to the limited oxygen diffusion become significant, possible because of electrode flooding and/or gas channel clogging. The difference observed between both membranes could be linked to the decrease of water sorption observed with the aged N115, which would lead to an excess of liquid water in the rest of the MEA.

7 Regeneration

7.1 In acid

In this section, we consider the possible regeneration of aged N115 by *ex-situ* re-acidification step. For this, we selected eight N115 aged at 60°C with different relative humidities and durations: RH6 (RH = 0.74) over 393 days, RH5 (RH = 0.63) and RH8 (RH = 0.93) over 806 days, and RH9 (RH = 0.95) over 861 days. The aged membranes were soaked in chloride acid HCl-1M at 25°C for 1 h, then rinsed three times in DI water at 25°C. They were then soaked in nitric acid HNO_3-10M at 25°C for 3 h and rinsed three more times in DI water. The membranes were boiled in DI water for 1 h and dried in the oven at 60°C for 24 h. Finally, the re-acidified membranes were equilibrated in water vapor (RH5, RH6, RH8 and RH9) at 60°C during 7 days. Table 4.14 shows the water contents of unaltered, aged, and re-acidified N115.

Table 4.14: Evolution of water content at 60°C of regenerated N115 in acid solution.

RH	c(%) – unaltered	c(%) – 393 aging days	c(%) re-acidified
RH6-1	9.4 ±0.5	7.7±0.5	8.5±0.5
RH6-2	9.8±0.4	8±0.4	8.8±0.4
RH	c(%) – unaltered	c(%) – 806 aging days	c(%) re-acidified
RH5-1	9.4±0.7	6.5±0.6	9.6±0.5
RH5-2	9.3±0.6	6.6±0.6	9.8±0.5
RH8-1	18.4±0.7	12.9±0.7	14.9±0.7
RH8-2	18.6±0.7	14.1±0.7	15.9±0.7
RH	c(%) – unaltered	c(%) – 861 aging days	c(%) re-acidified
RH9-1	19.9±0.4	14.8±0.4	20.4±0.4
RH9-2	19.8±0.5	14.8±0.5	20.9±0.5

It was observed that the water concentrations of re-acidified samples approached their initial values: some of them are a little lower such as RH6-1 (c(%) = 8.5) and RH8-1 (c(%) = 14.9), and some others are a little higher such as RH5-1 (c(%) = 9.6) and RH9-1 (c(%) = 20.4). In general, the water sorption properties returned close enough to their initial states so that we can consider the regeneration as complete.

7.2 In water

We selected seven N115 samples aged at 60°C with different relative humidities and aging times: RH2 (RH = 0.29) over 120 days, RH7 (RH = 0.8) over 806 days, and RH9 (RH = 0.95) over 1072 days. The aged membranes were soaked in DI water at 60°C for 1 h, and then dried at 60°C for 24 h. Then, the membranes were equilibrated in water vapor (RH2, RH7, and RH9) at 60°C during 7 days. Table 4.15 shows their water contents.

Table 4.15: Evolution of water content of regenerated N115 in water.

RH	c(%) – unaltered	c(%) – 120 aging days	c(%) re-hydrated
RH2 -1	5.1±0.4	3.7±0.4	6±0.4
RH2 -2	5.2±0.4	3.9±0.4	5.4±0.4
RH	c(%) – unaltered	c(%) – 806 aging days	c(%) re-hydrated
RH7-1	11.9±0.5	8.6±0.5	11.8±0.5
RH7-2	11.4±0.5	9.2±0.5	11.6±0.5
RH	c(%) – unaltered	c(%) – 1072 aging days	c(%) re-hydrated
RH9-1	20.3±0.5	10.9±0.5	19.7±0.5
RH9-2	21.4±0.5	11.8±0.5	19.9±0.5
RH9-3	19.6±0.5	11.8±0.5	20.3±0.5

It can be seen that, the water concentration of re-hydrated N115 membranes at 60°C also reaches similar level than their initial values: some of them are a little lower such as RH9-1 (c(%) = 19.7), however, some others are a little higher such as RH2-1 (c(%) = 6). In summary, the water sorption properties return to their initial states once the membrane is immersed in water at 60°C, 1 h.

Infrared Spectroscopy (IR)

IR spectroscopy was used by Collette *et al*. [1] to characterize the hygrothermal aging effect in Nafion. The authors were able to identify the changes of the Nafion N112 chemical structure during hygrothermal aging such as sulfonic anhydride formations (RSO_2-O-SO_2R). In addition, this technique permitted to analyse the state of water in the structure of aged N112. Figure 4.18 shows the IR spectra measured by Collette *et al*.

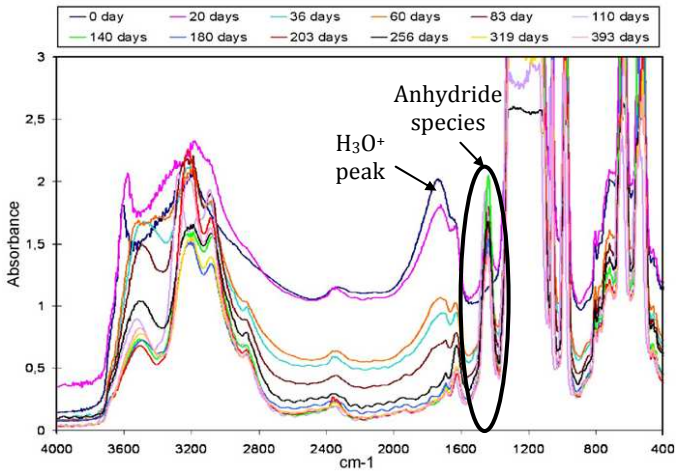

Figure 4.18: IR spectra of aged N112 (80°C and RH = 0.8 over 393 days) at 23°C, reprinted from Collette et al. [1].

The authors observed the appearance of a new absorbance band at 1440cm^{-1}. This new band was attributed to the formation of anhydride species. The absorbance band at 1710 cm^{-1} corresponds to the hydronium H_30^+, the counter ion of sulfonate groups: the authors observed a considerable decrease of this band, indicating that the sulfonic groups of the N112 membrane were affected by 393 days of aging. A possible explanation of this could be the decrease of the number of water molecules able to ionize and to solvate the ionic groups.

Based on these results, we decided to apply IR spectroscopy to an aged N115 (60°C, RH = 0.5, 484 days) and to a N115 reference sample. The measurements were performed at the SPrAM Laboratory in CEA, Grenoble. Figure 4.19 displays the results.

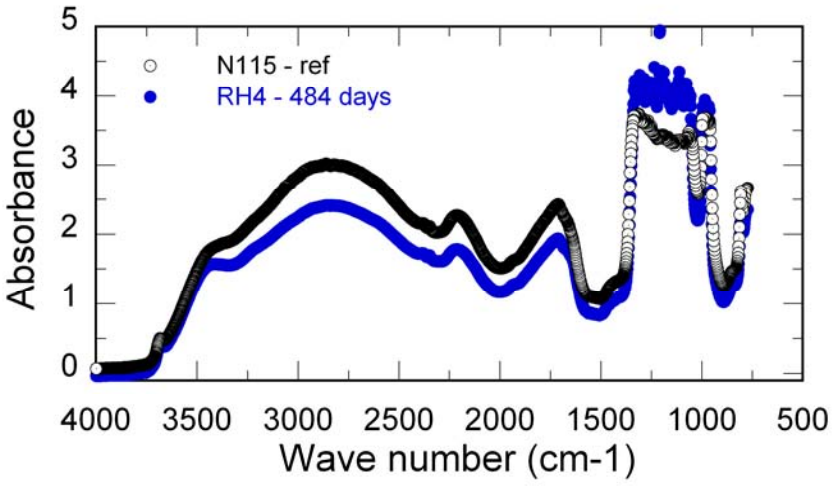

Figure 4.19: IR spectra of aged N115 (60°C and RH = 0.5 over 484 days) and the reference at 23°C. The membranes were dried before the IR measurements.

Despite the complexity of the interpretation of these IR spectra, it is possible to consider the two absorbance regions studied previously by Collette *et al*. [1]:

* At 1440cm^{-1}, we did not observe any new absorbance band; this means that no anhydride species were formed.

* At 1710 cm^{-1}, we did not observe an important decrease of the H_3O^+ band.

8 Discussion and conclusion

We studied the long-term evolution of water sorption, water transport and mechanical properties of Nafion N115 membranes exposed to constant temperature and humidity conditions.

The results obtained from the water sorption measurements show a continuous decrease of the sorption capacity of the membrane aged in vapor. However, in liquid water the loss of water sorption capacity seems to be moderate. As indicated by the IR spectra, the change in the sorption properties is not linked to a decrease of the number of H_3O^+ groups.

The tensile tests show that there is a small change in the mechanical properties of aged membranes: hydration losses in Nafion can be associated with a small increase of the rigidity of the polymer. This effect is moderate since the aging does not weaken the membrane and the structural reorganization (caused by aging) does not influence the water transport properties at the microscale.

Furthermore, the evolution of the water sorption properties is not coupled to any change in the in-plane proton conductivity; on the other hand, the test performed in the through-plane direction indicates that the conductivity could be impacted. These two different results are understandable whenever we consider that the aging is heterogeneous and does not change the surface properties of the membrane. In this case, the aging phenomena cannot be the same as the one described by Colette *et al.* since no absorption band related to the formation of anhydride species is observed on our IR spectra.

The proton conductivity results can also be clarified if we consider that a complete regeneration of the membrane properties occurred before the measurement, when cycling the humidity conditions. Moreover, we observe that the drop in water uptake of the aged samples was completely reversible after immersion in water and/or in acid solution.

In order to go further with the comparison between our results and those of Collette *et al*. [1] (see Table 4.16) we must take into account the differences between the pre-treatments applied since the impurities in the “as-received” membrane (ions and organic residues) play a role in the

aging phenomena. In our study we prepared all of our samples by strictly following the pre-treatment procedure described in Chapter 2. The main goal was to always dispose of membranes in the same reference state. This pre-treatment eliminates all (or the majority of) the impurities present in the structure after the synthesis and the casting of the membrane. In this case, the condensation of sulfonic acids and the formation of sulfonic anhydride are not catalyzed anymore, being the main reason why we do not observe any anhydride band on the IR spectra of the aged samples. This could also explain why the decline of the sorption capacity is more moderate in our study, compared to that of Collette *et al*. [1]: as we have seen in Chapter 3, not drying the membrane prior to characterization may lead to high initial values of water content and thus, to a more significant relative decrease over time.

Table 4.16: Results of hygrothermal aging in Nafion membranes from this study, compared to results obtained by Collette et al. [1].

Properties of Nafion®	**This study** *pre-treated N115 *Aging at 80°C RH = 0.8, 0.9; 402 days*		**Collette *et al*. [1]** as-received N112 *Aging at 80°C RH = 0.8; 393 days*		**Agreement**
	Protocol	**Main results**	**Protocol**	**Main results**	
Water sorption (λ)	Weighing T = 80°C RH = 0.3, 0.8, 0.9	λ: ↓ 26% (at RH = 0.8)	DVS T = 50°C RH = 0-0.9	λ: ↓ 64% (at RH = 0.8)	Yes
		λ: ↓ 8% (at RH = 0.9)		λ: ↓ 56% (at RH = 0.9)	
Proton conductivity (σ)	*in-plane mode* T = 80°C RH = 0.2-0.93	no variation (at RH = 0.9)	-	-	-
	through-plane mode T = 25°C saturated state	σ: ↓ 32% (aged at 60°C, RH = 0.74, 484 d)	*through-plane mode* T = 25°C saturated state	σ: ↓ 87%	Partial
Water self-diffusion (Ds)	PFGNMR T = 25°C	no variation	PFGNMR T = 25°C	no variation	Yes
Mechanical property (ε, σ, E)	T = 23°C RH = 0.38-0.6 500N, 50µm/s	E: ↑ 31%	T = 23°C RH = 0.5 10N, 42µm/s	E: ↑ 31%	Yes

*pre-treated: cleaned, acid washed, and dried at 60°C and 80°C; d: days.

At the end of this work, it is still difficult to understand the different experimental results as an assembly and to draw clear and definitive conclusions. Nevertheless, we can conclude the following:

- The pre-treated N115 samples may not be subjected to the so-called "hygrothermal aging" since there is not evidence about the formation of sulfonic anhydride in the membrane.
- The decrease of the sorption properties and the small changes in the mechanical properties are not coupled with any variation of the self-diffusion coefficient of water or the proton conductivity in the in-plane direction. These effects are similar in some extent to those observed when the polymer is dried at elevated temperature (Chapter 3).
- The aging phenomena that we observed were fully reversible and the membranes properties were completely recovered after immersing in hot water or in acid solution, or even after cycling the RH conditions.
- The measured changes in Nafion properties do not affect substantially the properties of MEA during fuel cell operation.
- This work shows the impact of the long-term storage of Nafion membranes and reveals the importance of following a pre-treatment procedure to avoid any degradation due to hygrothermal aging.

9 Remarks and future works

- ❖ More measurements of the proton conductivity in the through-plane direction should be made in order to confirm (or invalidate) the hypothesis that the observed aging is affecting only the volume properties of the membrane.
- ❖ Further characterization of untreated Nafion membranes is needed in order to confirm that the presence of impurities may act as catalysers of the hydrolysis reaction of sulfonic acid into sulfonic anhydride. In a more general way, the study of the effect of the pre-treatment on the hygrothermal aging is important in order to confirm that the pre-treatments may prevent the membrane from aging.

10 References

[1] Collette, F., Lorentz, C., Gebel, G., and Thominette, F., Hygrothermal aging of Nafion®, *Journal of Membrane Science*, Vol. 330, No. 1-2, 2009, pp. 21–29.

[2] Collette, F. M., Thominette, F., Escribano, S., Ravachol, A., Morin, A., and Gebel, G., Fuel cell rejuvenation of hygrothermally aged Nafion®, *Journal of Power Sources*, Vol. 202, 2012, pp. 126–133.

[3] Kawano, Y., Wang, Y., Palmer, R. A., and Aubuchon, S. R., Stress-Strain Curves of Nafion Membranes in Acid and Salt Forms, *Polímeros*, Vol. 12, 2002, pp. 96–101.

[4] Satterfield, M. B., *Mechanical and water sorption properties of Nafion and composite Nafion/titanium dioxide membranes for polymer electrolyte membrane fuel cells*, Ph.D. thesis, Princeton University, New Jersey, USA., 2007.

[5] Majsztrik, P. W., *Mechanical and Transport Properties of Nafion® for PEM Fuel Cells; Temperature and Hydration effects*, Ph.D. thesis, Princeton University, New Jersey, USA., 2008.

[6] Young, R. J. and Lovell, P. A., *Introduction to Polymers*, Chapman & Hall, London, UK., 2nd ed., 1991.

[7] Ward, I. M., *Mechanical Properties of Solid Polymers*, John Wiley & Sons, New York, USA., 2nd ed., 1983.

[8] Tschoegl, N. W., *The phenomenological theory of linear viscoelastic behavior: an introduction*, Springer-Verlag, New York, USA., 1989.

[9] Collette, F., *Vieillissement Hygrothermique du Nafion®*, Ph.D. thesis, École Nationale Supérieure d'Arts et Métiers, Paris, France., 2008.

Chapter 5

Characterization of Nafion® N115 and NRE212/zirconia composite membranes

1 Introduction

Despite the favorable properties of Nafion N115 and NRE212 membranes for fuel cell applications, as illustrated in Chapter 3, one of the major issues is the strong dependence of water sorption and proton conductivity on water content, limiting the working temperature to about 80°C. In the last years, the ability to operate fuel cells at temperatures higher than 120°C has been a goal for many fuel cell developers. At higher temperatures, the catalyst is less sensitive to carbon monoxide poisoning. In addition, working at elevated temperatures also increases the reaction kinetics and the membrane conductivity. However, this increase of membrane conductivity is observed at constant relative humidity (RH) and it is more difficult to hydrate the membrane properly at high temperature. As an example, Table 5.1 shows the molar water fractions required to reach an ionic conductivity of the order of 0.01 S/cm in a fuel cell which operates at high temperature (120°C) and/or at moderated temperature (80°C). It must be noted that the ionic conductivity values of Nafion were obtained at 120°C and RH = 0.3 (from Figure 5.1a) and at 80°C and RH = 0.3 (from Chapter 3).

Table 5.1: Saturated water vapor pressure and molar water fraction required at 120°Cand 80°C to reach an ionic conductivity in Nafion of the order of 0.01 S/cm.

Temperature (°C)	Conductivity (S/cm) at RH = 0.3	Saturated water vapor pressure (bars) - Eq 1	Molar water fraction (mol/mol) - Eq 2
120	0.01	2	0.2
80	0.01	0.46	0.04

These results show that an important increase of Nafion hydration is necessary if fuel cells operated at 120°C to avoid significant losses in Nafion proton conductivity.

$$p_{H_2O}^{sat} = \exp\left[13.669 - \frac{5096.23}{T}\right] * P_0 \qquad \text{Eq 1}$$

$$c_{H_2O} = \frac{p_{H_2O}^{sat} * RH}{R * T} \;;\; x_{H_2O} = \frac{c_{H_2O}}{c_T} \qquad \text{Eq 2}$$

To illustrate this result, Figure 5.1b shows the decrease in conductivity of a Nafion membrane at temperatures between 97°C and 143°C (Navarra *et al.* [1]).

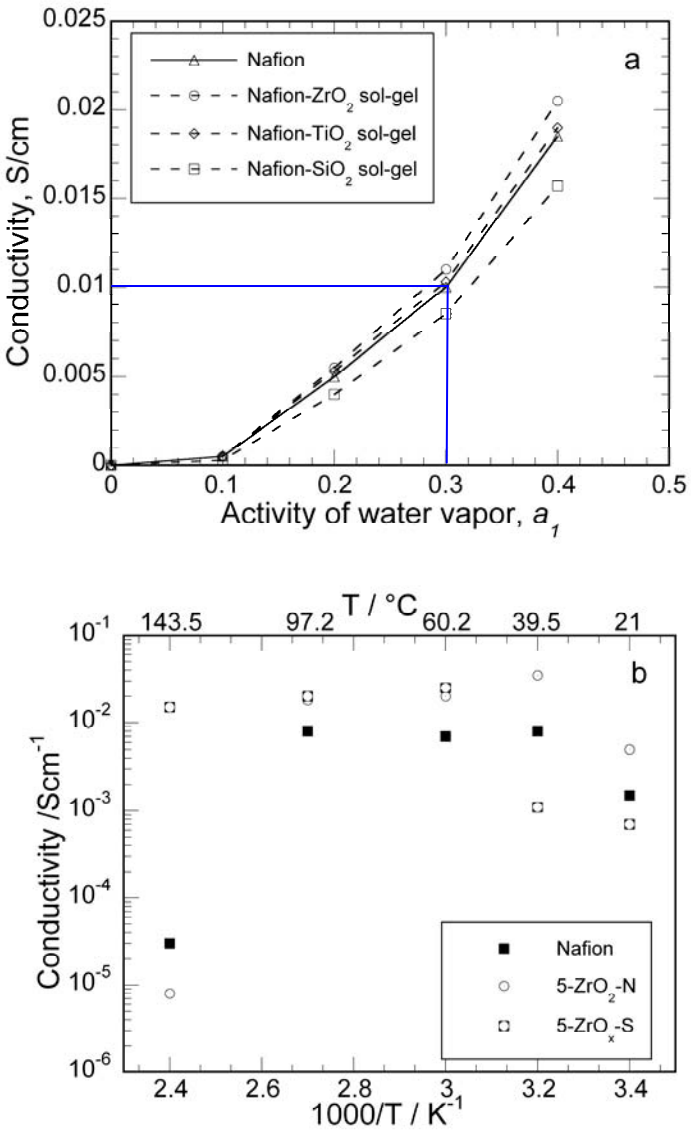

Figure 5.1: Evolution of the conductivity of (a) Nafion and modified Nafion (oxide composite) membranes at 120°C, adapted from Jalani et al. [2]; (b) Nafion and modified Nafion (ZrO_2-N and superacid ZrO_x-S) membranes as a function of temperature, adapted from Navarra et al. [1].

Moreover, for certain fuel cell applications (*e.g.* automotive), the lifetime of Nafion is shorter at high temperatures because of phenomena like shrinkage and swelling induced by hydration/dehydration cycles. As a consequence, numerous attempts have been made to develop alternative membranes operating at temperatures higher than 80°C. These membranes must demonstrate good proton conductivity, and thermo-mechanical stability, over a wide range of humidity [3, 4, 5].

Based on these considerations, we present in the first section of this chapter a survey of the literature with a special interest on water sorption, proton conductivity, mechanical properties

and fuel cell performance. Then, we characterize some properties of Nafion-zirconia composite membranes developed by the Functional Ceramics Group at West Virginia University. This laboratory had previously modified Nafion N115 and NRE212 by incorporating inorganic nanoparticles of zirconium dioxide (ZrO_2), or zirconia, improving water retention as well as providing additional acidic sites [2, 6].

The parameters selected for the previous property studies are used as reference for the characterization of Nafion-zirconia composite: temperature ranging from 30°C to 110°C and relative humidity from RH = 0.29 to RH = 0.95. It must be noted that temperatures higher than 110°C were not considered because of several experimental limitations such as difficulties to maintain high RH while avoiding condensation of water at the surface of the membrane. Furthermore, the materials used in the conductivity cell were not well adapted to pressures above 1 bar and temperatures above 110°C.

2 Literature survey

According to the literature [2, 3, 4, 5, 7, 8, 9, 10, 11, 12, 13, 14, 15, 16], one of the promising ways to develop new membranes consists in modifying Nafion® or similar materials by incorporating nanoparticles in order to enhance water retention at high operating temperature (>90°C) and low relative humidity. For a better understanding of this section, certain points are classified below.

2.1 Materials

Various materials such as inorganic oxides have been considered for the development of Nafion-based composite membranes: silicon dioxide (SiO_2), titanium dioxide (TiO_2) and zirconium dioxide (ZrO_2). These oxides exhibit high surface areas, hydrophilic natures, and a high degree of acidity (presence of Lewis acid sites), permitting to increase the water retention [2, 1]. Superacidic sulphated zirconia (S-ZrO_2) displays both Lewis (electron pair acceptor) and Brönsted (proton donor) acid sites, which should permit to increase both the water sorption and the proton transport [17], as seen in Figure 5.2.

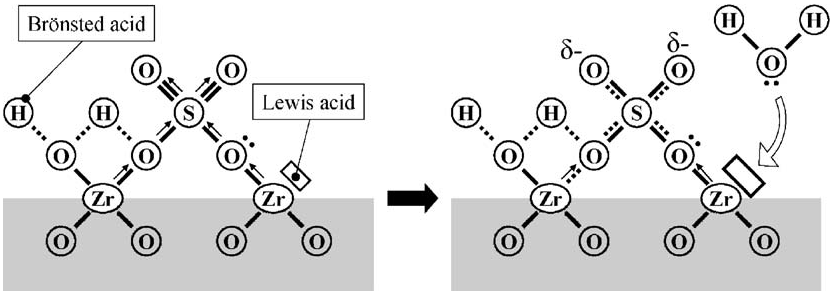

Figure 5.2: Surface model of superacidic sulphated zirconia (S-ZrO_2(p)) in the presence of water molecules, adapted from Hara and Miyayama [17].

Other examples of Nafion-based inorganic composite membranes include Nafion®/Aluminum oxide (Al_2O_3), Nafion®/Zeolite, etc [5]. Most of these oxides are present in the Nafion matrix as nano- or micro-particles, and they are apparently dispersed either into the hydrophilic channels of Nafion [18] or uniformly through the nanoporous structure of Nafion [7].

2.2 Characterization studies from the literature

Water retention

The studies presented by Hara and Miyayama [17] and Navarra et al. [1], suggested that the incorporation of ZrO_2 or superacid ZrO_2 (S-ZrO_x) nanoparticles within the Nafion membranes provide increased water retention, acidity and thermal stability at 140-150°C. In addition, Satterfield *et al*. [4] suggested that TiO_2 within Nafion membranes enhance the water sorption at 80°C.

Performance

In 1996, Watanabe *et al.* [19] demonstrated that by introducing catalyst and oxide materials in the Nafion matrix, PEMFCs could operate at 80°C under dry conditions. More recent studies [1, 2, 3, 4, 7, 20, 21, 22, 23] have shown that modified Nafion membranes could have the ability to improve the PEMFC performances (*i.e*. proton conduction, water management and thermal stability) at temperatures above 100°C and under low RH conditions. For example, Yu *et al*. [21] suggested that the incorporation of SiO_2 nanoparticles within the Nafion® membrane increases its proton conductivity and consequently the fuel cell potential at 110°C. In addition, Nicotera *et al*. [22] suggested that the incorporation of SiO_2 or TiO_2 to Nafion provides increased fuel cell potential at 90°C and 120°C at low relative humidity.

Table 5.2 reports some of the most important properties such as water uptake, proton conductivity, mechanical properties, and fuel cell potential.

Table 5.2: Properties of Nafion-oxide composite membranes according to the literature.

Author	Nafion	Oxide	Characterization of Properties	Experimental conditions			Results	
				T (°C)	RH	CD (mA/cm²)	Nafion	Modified Nafion
Deng *et al.* [24]1998	N115	SiO_2 (sol-gel)	water uptake (%)	22	-	-	15	20
			stress to failure (Mpa)	22	*u*	-	29*	26*
			strain to failure (%)	22	*u*	-	475*	325*
Miyake *et al.* [25]2001	N115	SiO_2 4-5wt% (sol-gel)	water vapor uptake (%)	25	0.16	-	3.0	2.9
				25	0.36	-	4.8	4.4
				120	0.02	-	1.4	1.0
				120	0.17-0.22	-	3.5	4.8
				120	0.34-0.38	-	5.6	8.1
			proton conductivity (S/cm)	25	0.16	-	0.0005	0.0003
				25	0.36	-	0.0070	0.0050
				120	0.29	-	0.026	0.025
				120	0.58	-	0.117	0.106
				120	0.78	-	0.210	0.185
Thampan *et al.* [3]2005	N112	ZrO_2 5wt% (sol-gel)	EW (g/mol. H^+)	25	-	-	1106	1016
			water vapor uptake (%)	120	0.1	-	3*	6*
			water vapor uptake (%)	120	0.4	-	5.7*	8.2*
			proton conductivity (S/cm)	120	0.1	-	0.0015*	0.0016*
			proton conductivity (S/cm)	120	0.4	-	0.0180*	0.0186*
			cell potential (V)	110	*d*	100	0.46*	0.48*
			resistance ohmic (Ohms)	110	*d*	135	0.056*	0.07*
Jalani *et al.* [2]2005	N112	ZrO_2 TiO_2 SiO_2 (sol-gel)	EW (g/mol. H^+)-ZrO_2	25	-	-	1100	1020
			EW (g/mol. H^+)-TiO_2	25	-	-	1100	1090
			EW (g/mol. H^+)-SiO_2	25	-	-	1100	1120
			water uptake (%)-ZrO_2	90	0.4	-	6*	8*
			water uptake (%)-TiO_2	90	0.4	-	6*	6.25*
			water uptake (%)-SiO_2	90	0.4	-	6*	7*
			water uptake (%)-ZrO_2	120	0.4	-	5.5*	8.2*
			water uptake (%)-TiO_2	120	0.4	-	5.5*	6.75*
			water uptake (%)-SiO_2	120	0.4	-	5.5*	6.5*
			conductivity (S/cm)-ZrO_2	90	0.4	-	0.023*	0.027*
			conductivity (S/cm)-TiO_2	90	0.4	-	0.023*	0.022*
			conductivity (S/cm)-SiO_2	90	0.4	-	0.023*	0.022*
			conductivity (S/cm)-ZrO_2	120	0.4	-	0.0185*	0.0205*
			conductivity (S/cm)-TiO_2	120	0.4	-	0.0185*	0.019*
			conductivity (S/cm)-SiO_2	120	0.4	-	0.0185*	0.0157*
			cell potential (V)-ZrO_2	110	*fh*	200	0.59*	0.6*
			cell potential (V)-TiO_2	110	*fh*	200	0.59*	0.57*
			cell potential (V)-SiO_2	110	*fh*	200	0.59*	0.6*

CD:current density; *u*:unknown; EW: equivalent weight; *d*: drying; *fh:* fully humidified; * values read from published curves.

Table 5.3: Properties of Nafion-oxide composite membranes according to the literature (continued).

Author	Nafion	Oxide	Characterization of Properties	Experimental conditions			Results	
				T (°C)	RH	CD (mA/cm²)	Nafion	Modified Nafion
Yu *et al.* [21]2007	N1135	SiO_2 5wt% (sol-gel)	proton conductivity (S/cm)	110	*s*	-	0.178	0.198
			tensile strength (Mpa)	*u*	*u*	-	21.63	21.35
			maximal force applied (N)	*u*	*u*	-	35.48	38.01
			cell potential (V)	80	*h*	200	0.78*	0.82*
			cell potential (V)	110	*h*	200	dropped	0.7*
Navarra *et al.* [1]2007	Nafion	ZrO_2 5wt% (recasting)	water uptake (%)	25	-	-	33.7	47.3
			IEC (meq/g)	25	-	-	0.74	0.83
			proton conductivity (S/cm)	97.2	*wd*	-	0.008*TP**	0.020*TP**
			proton conductivity (S/cm)	143.5	*wd*	-	$3x10^{-5}$*TP**	$8x10^{-6}$*TP**

CD: current density; *u*: unknown; *h*: humidified; IEC: ion exchange capacity; *wd*: water drops; *TP*: through-plane direction; * values read from published curves.

2.3 Fabrication method

As an example, Nafion/silicon dioxide membranes were synthesized by Deng *et al.* [24] using the acid-catalyzed sol-gel reaction of tetraethoxysilane (TEOS) to form silicon dioxide (SiO_2) inside Nafion (see Figure 5.3). This method consists in exposing a Nafion membrane to a solution containing water, alcohol (MeOH), and hydrolized alkoxides (tetraethoxysilane, TEOS = $Si(OC_2H_5)_4$). These polar molecules tend to migrate to the polar clusters inside the membrane. Subsequent hydrolysis and polymerisation of sorbed alkoxides are confined to these clusters, which results in the formation of nano- or macro-sized particles.

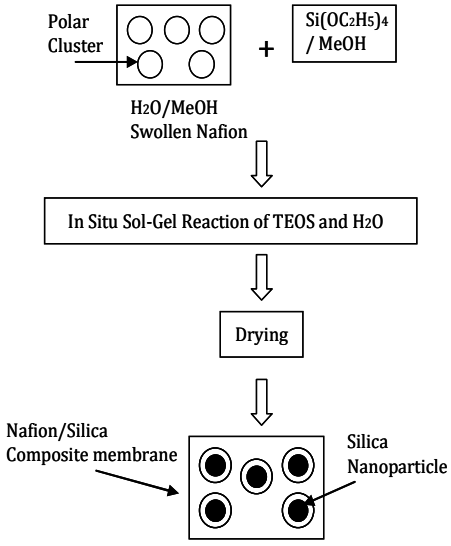

Figure 5.3: Diagram of Nafion/silica composite membrane preparation via sol-gel, adapted from Deng et al. [24].

According to these authors, inserting silica (silicon dioxide) should not alter the morphological structure of Nafion. Furthermore, these particles should improve the water retention (hydration) and the proton transport in Nafion membranes thanks to the following effects:

- Water retention: inserted silica may enhance the hydrophilicity of clusters groups (SO_3H) in Nafion. This effect was attributed to the presence of numerous groups (≡Si-OH), due to the strong hydrogen bond of H_2O molecules on the surface of the silica particles. However, some studies suggested that the physically sorbed water (*i.e.* H_2O molecules bound to the surface ≡SiOH groups) should be driven off at a higher temperature, around 170°C, as compared to H_2O molecules bounded to the SO_3H groups [24, 25] .
- Proton transport: the improvement was attributed to the proton hopping mechanism along the large hydrative silica surface. Consequently, these experimental findings suggested that proton conductivity in a Nafion/silica composite membrane will be higher that in plain Nafion, especially at high temperature when the water content is low.

Nafion N115 and NRE212/zirconia membranes fabrication (West Virginia University)

These composite membranes are prepared using sol-gel method, that is to say by *in-situ* growth of inorganic oxide particles in membranes [2, 26], at the Ceramic Centre at West Virginia University.

Nafion® N115 and NRE-212 membranes are:

- boiled in 3 wt% H_2O_2 for 1h,
- heated in 1 M sodium hydroxide (NaOH) for 6 h,
- dried for 12 h in a vacuum oven,
- immersed in ethanol (EtOH) for 1 h, for swelling the pores of the membrane to maximize absorption of the precursor solution,
- removed and immersed in 0.15/0.3M 70wt% zirconia(IV) n-propoxide ($C_{12}H_{28}O_4Zr$) solution for 6 h,
- rinsed in acetone (C_3H_6O).

The membranes are then heated in vacuum for 24 h to complete condensation reactions and some of them are autoclaved (<150°C) in order to crystallize the formed $Zr(OH)_4$ to nano ZrO_2. After this, they are boiled in 50 % in volume of sulfuric acid (H_2SO_4) for re-acidification.

Figure 5.4 shows a transmission electron microscopy image for Nafion/ZrO_2 membrane, this image was reprinted from Pan *et al*. [11].

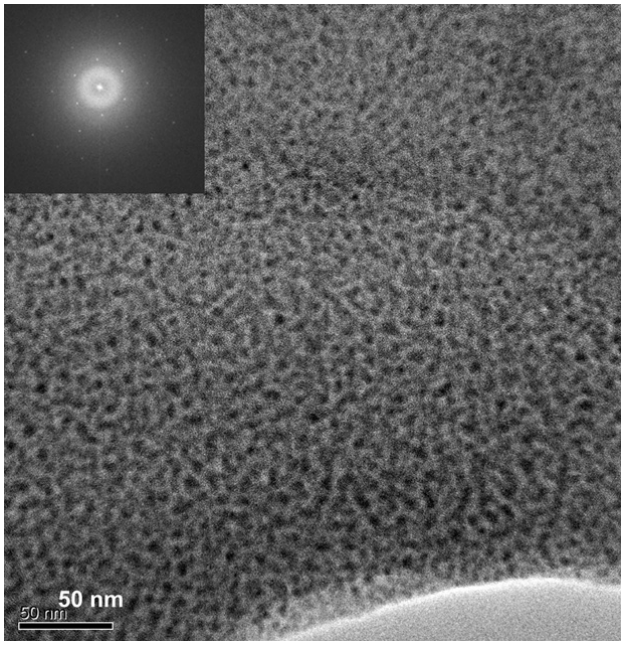

Figure 5.4: TEM image of hybrid dispersion of in-situ formed zirconia nanoparticles in 2 wt% Nafion solution, reprinted from Pan et al. [11].

2.4 Fuel cell test at West Virginia University

Once the inorganic oxide nanoparticles were incorporated in the Nafion® membranes, their performances were tested at high temperature and low relative humidity conditions.

- Electrodes were attached to modified membranes (3-7% weight when immersed in a 0.15/0.3M solution of $Zr(OH)_2$) by hot-pressing.
- The active layer had been brushed with 5% Nafion® solution before pressing.
- The fuel cell was setup and connected to a humidifier. Hydrogen and oxygen were supplied using mass flow controllers and the cell was controlled by the electronic load.

Figure 5.5 shows the polarization curves.

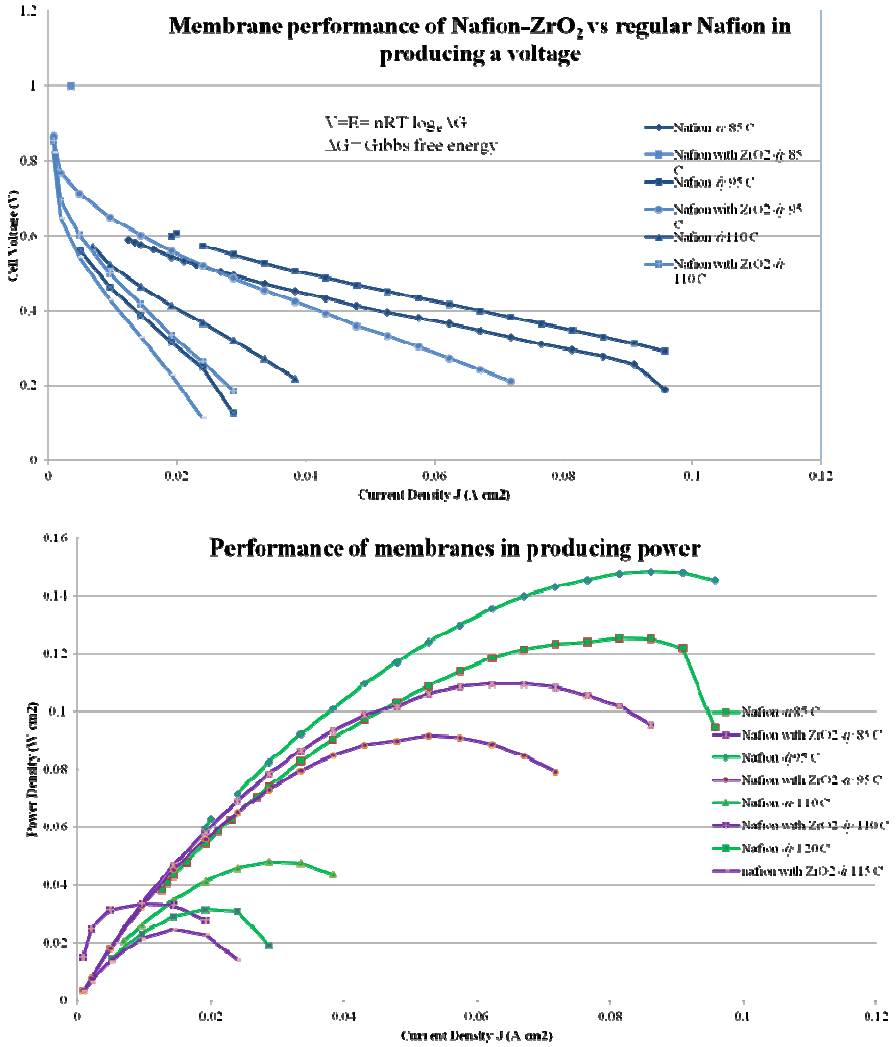

Figure 5.5: Polarization curves (top) and power curves (bottom) of Nafion/zirconia composite membranes in a fuel cell system at West Virginia University.

These preliminary results show that incorporating nanoparticles of zirconia (ZrO_2) does not improve the fuel cell voltage nor the conductivity of the membranes. The modified membrane seems to present high resistance even if their water contents were (presumably) higher than those of plain Nafion.

Based on these statements, we performed systematic water sorption, proton conductivity, and stress-strain measurements on Nafion/zirconia composite membranes. Our primary objective is to understand why these Nafion composite membranes do not perform much better than the original ones, especially at high temperature and low relative humidity.

3 Characterization of Nafion® N115 and NRE212/zirconia composite membranes

The composite membranes were classified in accordance with their fabrication conditions (at West Virginia University) as described in the following table:

Nafion composite	Oxide	Concentration [M]
N115-I	ZrO_2 + $Zr(OH)_4$	0.15
N115-II	ZrO_2	0.15
N115-III	ZrO_2	0.3
N212-I	ZrO_2 + $Zr(OH)_4$	0.1
N212-III	ZrO_2	0.3

It must be noted that N115-I and N212-I were not autoclaved, thus the final reactants were a mixture of oxides and hydroxides.

3.1 Water sorption

3.1.1 In vapor

The water sorption of Nafion composites were measured at 30°C, 60°C and 80°C over a wide relative humidity range (RH2 - RH9). Figure 5.6 shows the isotherms.

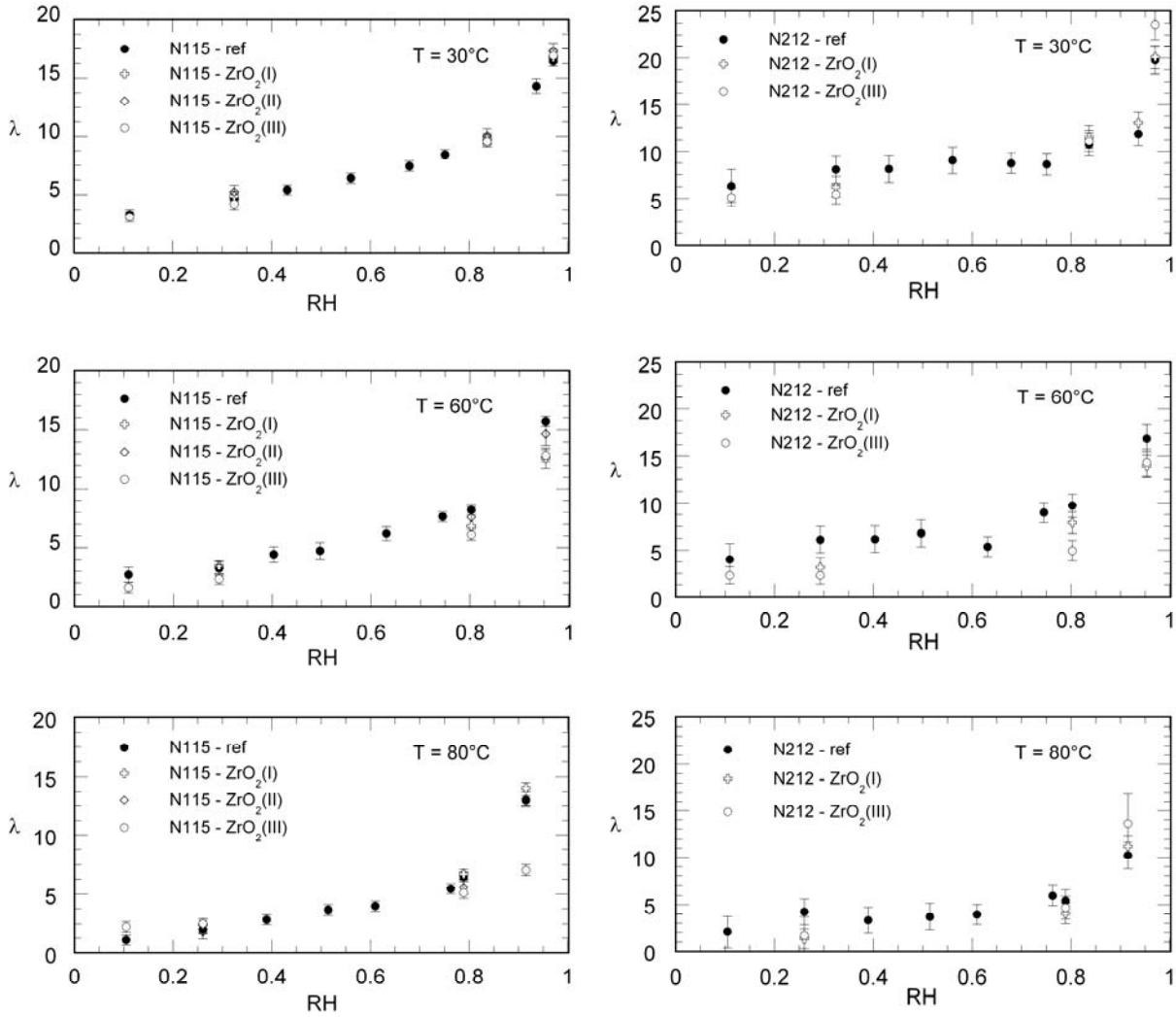

Figure 5.6: Water sorption in modified Nafion at 30°C, 60°C and 80°C. Left column: composite N115. Right column: composite NRE212.

We did not observe any increase of the water sorption of composite membranes compared to the original Nafion.

3.1.2 In liquid

Figure 5.7 displays sorption in Nafion N115- and NRE212-zirconia composite membranes, measured at 30°C, 60°C and 80°C. The λ values are listed in Table 5.4.

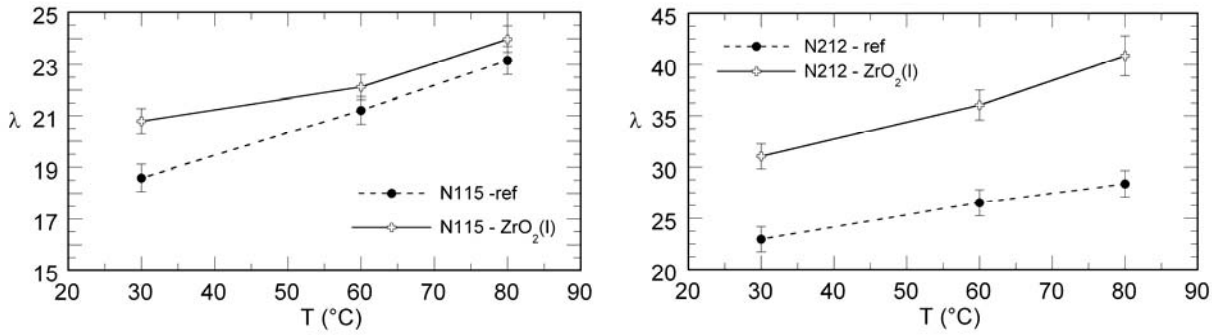

Figure 5.7: Water sorption in composite N115 (left column) and composite NRE212 (right column) measured at 30°C, 60°C and 80°C.

We observed an increase of the water content of composite membranes. The sorption is higher in NRE212 composite membranes, as shown in the table below.

Table 5.4: Water sorption (λ) as a function of temperature T.

	T = 30°C	T = 60°C	T = 80°C
N115	18.6±0.5	21.2±0.5	23.2±0.6
N115-ZrO_2 (I)	20.8±0.5	22.1±0.5	24±0.5
NRE212	23±1.2	26.5±1.3	28.4±1.3
NRE212-ZrO_2 (I)	31.1±1.2	36.1±1.5	40.9±1.9

3.2 Proton conductivity

Figure 5.8 presents proton conductivity measurements carried out on Nafion N115- and NRE212-zirconia composite membranes in equilibrium with water vapor at temperatures ranging from 30°C to 110°C.

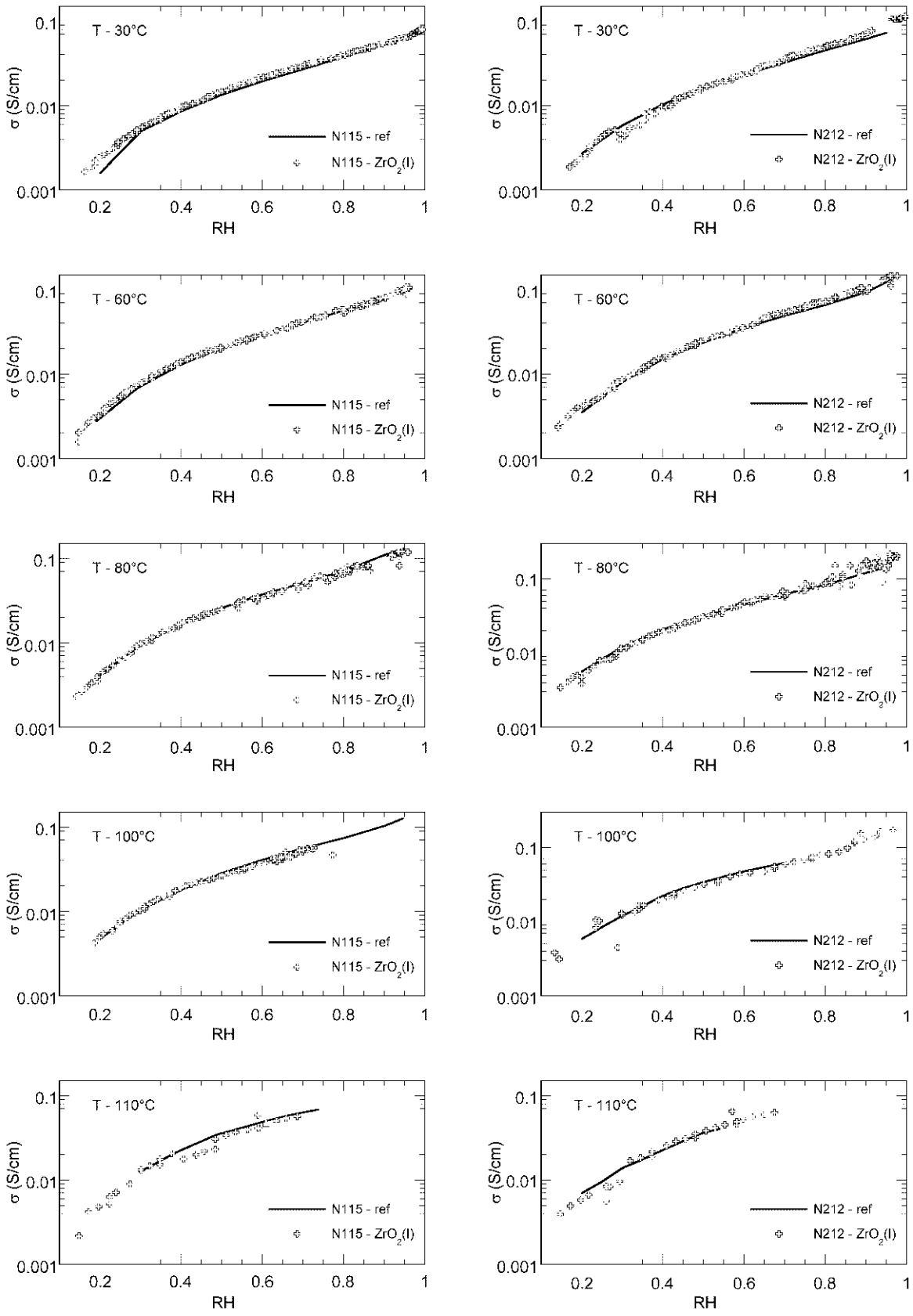

Figure 5.8: Proton conductivity in composite N115 (left column) and composite NRE212 (right column) measured from 30°C to 110°C.

We can observe from Figure 5.8 that the ionic conductivity of the composite membranes did not vary. This observation is valid for the different RH conditions and for the temperatures considered.

3.3 Strain-stress and Young modulus

Figure 5.9 shows the stress-strain curves of Nafion N115-zirconia composite membranes measured at 23°C and RH = 0.38. An average of four tests was made in order to minimize the experimental errors; the graphic shows the mean values.

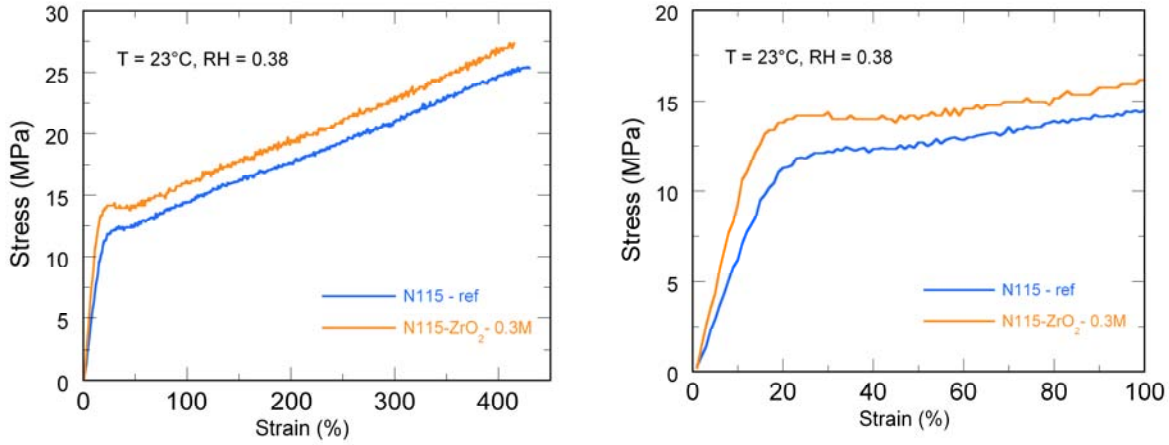

Figure 5.9: Stress-strain curves of composite N115 measured at 23°C and RH = 0.38.

As shown in Figure 5.9, the Young modulus (the slope of the stress-strain curve at small strains) of the composite membrane is higher than that of the reference membrane; however, the plastic modulus (the slope of the stress-strain curve beyond the yield point) is similar for both. Table 5.5 shows the mechanical properties of the N115 composite and the N115 deduced from the experimental stress-strain curves.

Table 5.5: Mechanical parameters of N115 and N115 composite.

Mechanical parameters of N115 at T = 23°C, RH = 0.38			
Nafion	Strain to failure (%)	Stress to failure (MPa)	E (MPa) curve
N115-ref	433±27	26±2	67±3
N115-ZrO_2	415±21	27±1	98±9

4 Conclusion

The composite membranes present higher water sorption in liquid water and better mechanical property in term of toughness, with respect to plain Nafion. However, no difference was observed in term of water sorption in vapor and proton conductivity. These results are not surprising since the fuel cell characterization realized in West Virginia University demonstrated a decrease in the fuel cell performance compared to plain Nafion. A possible explanation to this can come from composite membrane fabrication process: because of a possible non-uniform dispersion of nanoparticles within Nafion, the samples used for characterization could be non representative in term of zirconia concentration. Insufficient or saturated concentration of zirconia nanoparticles in the membrane could limit their performance.
On the other hand, the low performance of the fuel cells tested at West Virginia University could be due to the MEA fabrication process: difficulties in the preparation of the active layers or a possible weak contact between the electrodes.

Although the results are disappointing in term of membrane performance, the characterization of the physical properties of composite membranes helped us to interpret their performance during fuel cell operation.
Finally, the results presented in this study illustrated the difficulty to elaborate better membranes than Nafion or PFSA for new generations of PEMFC systems able to work at high temperature and under low humidity conditions.

5 References

[1] Navarra, M. A., Croce, F., and Scrosati, B., New, high temperature superacid zirconia-doped Nafion (TM) composite membranes, *Journal of Materials Chemistry*, Vol. 17, No. 30, 2007, pp. 3210–3215.

[2] Jalani, N., Dunn, K., and Datta, R., Synthesis and characterization of Nafion®-MO2 (M = Zr, Si, Ti) nanocomposite membranes for higher temperature PEM fuel cells, *Electrochimica Acta*, Vol. 51, No. 3, 2005, pp. 553–560.

[3] Thampan, T., Jalani, N., Choi, P., and Datta, R., Systematic approach to design higher temperature composite PEMs, *Journal of the Electrochemical Society*, Vol. 152, 2005, pp. A316–A325.

[4] Satterfield, M. B., Majsztrik, P. W., Ota, H., Benziger, J. B., and Bocarsly, A. B., Mechanical properties of Nafion and titania/Nafion composite membranes for polymer electrolyte membrane fuel cells, *Journal of Polymer Science Part B: Polymer Physics*, Vol. 44, No. 16, 2006, pp. 2327–2345.

[5] Dupuis, A.-C., Proton exchange membranes for fuel cells operated at medium temperatures: Materials and experimental techniques, *Progress in Materials Science*, Vol. 56, No. 3, 2011, pp. 289–327.

[6] Malhotra, S. and Datta, R., Membrane-Supported Nonvolatile Acidic Electrolytes Allow Higher Temperature Operation of Proton-Exchange Membrane Fuel Cells, *Journal of The Electrochemical Society*, Vol. 144, No. 2, 1997, pp. L23–L26.

[7] Adjemian, K. T., Srinivasan, S., Benziger, J., and Bocarsly, A. B., Investigation of PEMFC operation above 100 °C employing perfluorosulfonic acid silicon oxide composite membranes, *Journal of Power Sources*, Vol. 109, No. 2, 2002, pp. 356–364.

[8] Yang, C., Srinivasan, S., Bocarsly, A., Tulyani, S., and Benziger, J., A comparison of physical properties and fuel cell performance of Nafion and zirconium phosphate/Nafion composite membranes, *Journal of Membrane Science*, Vol. 237, 2004, pp. 145–161.

[9] Sacca , A., Carbone, A., Passalacqua, E., D'Epifanio, A., Licoccia, S., Traversa, E., Sala, E., Traini, F., and Ornelas, R., Nafion-TiO2 hybrid membranes for medium temperature polymer electrolyte fuel cells (PEFCs), *Journal of Power Sources*, Vol. 152, No. 1-2, 2005, pp. 16–21.

[10] Jones, D. J. and Rozière, J., Advances in the Development of Inorganic-Organic Membranes for Fuel Cell Applications, *Advances in Polymer Science*, Vol. 215, Springer Berlin Heidelberg, 2008, pp. 219–264.

[11] Pan, J., Zhang, H., Chen, W., and Pan, M., Nafion-zirconia nanocomposite membranes formed via in situ sol-gel process, *International Journal of Hydrogen Energy*, Vol. 35, No. 7, 2010, pp. 2796–2801.

[12] Alvarez, A., Guzman, C., Carbone, A., Saccà , A., Gatto, I., Passalacqua, E., Nava, R., Ornelas, R., Ledesma Garcia, J., and Arriaga, L., Influence of silica morphology in composite Nafion membranes properties, *International Journal of Hydrogen Energy*, Vol. 36, No. 22, 2011, pp. 14725–14733.

[13] Wang, Z., Tang, H., Zhang, H., Lei, M., Chen, R., Xiao, P., and Pan, M., Synthesis of Nafion/CeO2 hybrid for chemically durable proton exchange membrane of fuel cell, *Journal of Membrane Science*, Vol. 421-422, 2012, pp. 201–210.

[14] Damay, F. and Klein, L. C., Transport properties of NafionTM composite membranes for proton-exchange membranes fuel cells, *Solid State Ionics*, Vol. 162-163, 2003, pp. 261–267.

[15] Bauer, F. and Willert Porada, M., Zirconium phosphate Nafion® composites - a microstructure-based explanation of mechanical and conductivity properties, *Solid State Ionics*, Vol. 177, 2006, pp. 2391–2396.

[16] Uchida, H., Ueno, Y., Hagihara, H., and Watanabe, M., Self-humidifying electrolyte membranes for fuel cells. Preparation of highly dispersed TiO2 particles in Nafion 112, *Journal of the Electrochemical Society*, Vol. 150, No. 1, 2003, pp. A57–A62.

[17] Hara, S. and Miyayama, M., Proton conductivity of superacidic sulfated zirconia, *Solid State Ionics*, Vol. 168, 2004, pp. 111–116.

[18] Mauritz, K. A., Stefanithis, I. D., Davis, S. V., Scheetz, R. W., Pope, R. K., Wilkes, G. L., and Huang, H.-H., Microstructural evolution of a silicon oxide phase in a perfluorosulfonic acid ionomer by an in situ sol-gel reaction, *Journal of Applied Polymer Science*, Vol. 55, No. 1, 1995, pp. 181–190.

[19] Watanabe, M., Uchida, H., Seki, Y., Emori, M., and Stonehart, P., Self-Humidifying Polymer Electrolyte Membranes for Fuel Cells, *Journal of the Electrochemical Society*, Vol. 143, No. 12, 1996, pp. 3847–3852.

[20] Jalani, N. and Datta, R., The effect of equivalent weight, temperature, cationic forms, sorbates, and nanoinorganic additives on the sorption behavior of Nafion®, *Journal of Membrane Science*, Vol. 264, No. 1-2, 2005, pp. 167–175.

[21] Yu, J., Pan, M., and Yuan, R., Nafion/Silicon oxide composite membrane for high temperature proton exchange membrane fuel cell, *Journal Wuhan University of Technology, Materials Science Edition*, Vol. 22, No. 3, 2007, pp. 478–481.

[22] Nicotera, I., Zhang, T., Bocarsly, A., and Greenbaum, S., NMR Characterization of Composite Polymer Membranes for Low-Humidity PEM Fuel Cells, *Journal of The Electrochemical Society*, Vol. 154, No. 5, 2007, pp. B466–B473.

[23] D'Epifanio, A., Navarra, M. A., Weise, F. C., Mecheri, B., Farrington, J., Licoccia, S., and Greenbaum, S., Composite Nafion/Sulfated Zirconia Membranes: Effect of the Filler Surface

Properties on Proton Transport Characteristics, *Chemistry of Materials*, Vol. 22, No. 3, 2010, pp. 813–821.

[24] Deng, Q., Moore, R. B., and Mauritz, K. A., Nafion®/(SiO2, ORMOSIL, and dimethylsiloxane) hybrids via in situ sol-gel reactions: Characterization of fundamental properties, *Journal of Applied Polymer Science*, Vol. 68, No. 5, 1998, pp. 747–763.

[25] Miyake, N., Wainright, J. S., and Savinell, R. F., Evaluation of a Sol-Gel Derived Nafion/Silica Hybrid Membrane for Proton Electrolyte Membrane Fuel Cell Applications: I. Proton Conductivity and Water Content, *Journal of The Electrochemical Society*, Vol. 148, No. 8, 2001, pp. A898–A904.

[26] Choi, P., Jalani, N. H., and Datta, R., Thermodynamics and Proton Transport in Nafion III. Proton Transport in Nafion/Sulfated ZrO2 Nanocomposite Membranes, *Journal of The Electrochemical Society*, Vol. 152, No. 8, 2005, pp. A1548–A1554.

Conclusions and perspectives

We performed systematic sorption, transport and mechanical measurements in commercial Nafion N115 and NRE212 membranes. Simple and reproducible experimental protocols allowed us to measure these membrane properties over a wide range of conditions. The primary emphasis was put on the measurement of the effects of the drying temperature (thermal history) on the water content of the membrane, its proton conductivity, the value of the water self-diffusion coefficient, and its correlation with the Young modulus.

We have found from literature that Nafion membranes are treated differently prior to their use in sorption, transport and mechanical studies. Consequently the results showed discrepancies. The most commonly used pre-treatment consists in boiling the membrane in aqueous solutions and drying from room temperature to very high temperatures. These pre-treatments can alter the physical structure of the membrane and consequently the manner in which the ionic groups are ordered, which can lead to variation in water sorption and other properties.

In order to understand the effect of such pre-treatments and the heterogeneity of results in the literature, Nafion N115 and NRE212 membranes were heat-treated (in term of drying) at different temperatures. We come with the following conclusions:

- When the membrane samples were heat-treated at moderate temperature (60°C < T_{dry} < 100°C) some residual water stayed strongly attached to the structure of the polymer (λ = 1.5 ± 0.5 in Nafion N115).
- In heat-treated membranes, the sorption capacity was reduced due to the shrinkage of the polymeric structure. This effect was visible in both liquid and vapor phase, increases with the drying temperature, and decreases with the measuring temperature. Consequently, proton conductivity, water self-diffusion coefficient and mechanical properties were also altered in heat-treated samples due to this drop in sorption capacity. For transport properties these differences vanished when increasing the temperature. When the samples were not heat-treated, the sorption capacity was not a function of temperature.

The effects of the temperature at which the measurements are performed are also sometimes not well documented and understood. Thus, the effects of temperature should be carefully considered when comparing sorption, transport and mechanical properties. For instance, we have seem from the literature review that there exists controversy in the literature about these effects: several researchers found that for a certain relative humidity, water uptake decreases when temperature increases [1, 2, 3, 4] while others reported the

opposite trend [5, 6, 7]. Our study allows to separate the pre-treatment effects from the effective effect of temperature. We come with the following conclusions:

- The measurement of sorption isotherms between 30°C and 80°C showed a decrease in sorption capacity in the vapor phase with the temperature. The decrease of the Young modulus of the polymer with temperature cannot explain this behavior. Other properties of the membrane, such as changes of its hydrophilicity with temperature, have then to be considered to gain a deeper understanding of sorption in this system.
- The proton conductivity, measured over a wide range of temperatures, followed a polynomial law when plotted as a function of relative humidity. When expressed as a function of water content, a threshold above which proton transport becomes efficient was put forward. Our measurements showed that the water content corresponding to this threshold decreased with temperature.

The characterization of the properties of Nafion exposed to constant temperature and relative humidity for long periods of time was needed to evaluate their stability. We studied the long-term evolution of water sorption, water transport and mechanical properties of Nafion N115 membranes exposed to constant temperatures (60°C and 80°C) and relative humidity (from RH = 0.2 to RH = 0.9) conditions. We obtained the following results:

- The water sorption decreased continuously for membranes aged in vapor. In liquid water, the loss of water sorption capacity was, much more moderate. As indicated by the IR spectra, the change in the sorption properties was not linked to a decrease of the number of hydronium (H_3O^+) groups. The tensile tests showed that this was rather due to a small increase of the rigidity of the polymer. This effect was very moderate since the aging did not weaken the membrane and the structural reorganization did not influence the water transport properties at the micrometer scale.
- The evolution of the water sorption properties was not coupled to any change in the in-plane proton conductivity; on the other hand, a test performed in the normal direction indicated that the normal conductivity could be impacted.

In summary, we observed a decrease of certain Nafion properties with time. The results were relatively unstable and less pronounced than those of Collette *et al*. [8]. Furthermore, the observed aging phenomena were fully reversible: the membranes properties were completely recovered when immersed in hot water, in acid, or even after cycling the RH conditions. Our aging protocols, however, were different from those described by Collette *et al.* since there existed differences in the applied pre-treatments. Indeed, the impurities (ions and inorganic residues) that are always present in the "as-received" membranes may play the role of a catalyst of the aging phenomena. In our study, we prepared all of our samples by following a pre-

treatment procedure that removes a good proportion of the impurities and therefore can slow down or limit the aging.
Finally, this study showed the impact of the long-term storage of Nafion membranes at constant T and RH, and reveals that it is important to follow a pre-treatment procedure in order to avoid any degradation due to hygrothermal aging.

At the end of this thesis work, we characterized Nafion/zirconia (ZrO_2) composite membranes developed by the Functional Ceramics Group at West Virginia University, USA. The conclusions of this study were the following:

- The composite membranes present higher water sorption in liquid water and better mechanical property in term of toughness, with respect to unmodified Nafion. However, no difference was observed in term of water sorption in vapor and proton conductivity. These results are not surprising since the fuel cell characterization realized in West Virginia University demonstrated a decrease in the fuel cell performance compared to unmodified Nafion.
- A possible explanation to this can come from the fabrication process: because of a possible non-uniform dispersion of nanoparticles within Nafion, the samples used for characterization could be non representative in term of zirconia concentration. Insufficient or saturated concentration of zirconia nanoparticles in the membrane could limit their performance.
- On the other hand, the low performance of the fuel cells tested at West Virginia University could be due to the MEA fabrication process: difficulties in the preparation of the active layers or a possible weak contact between the electrodes.

Although the results are disappointing in term of membrane performance, the characterization of the physical properties of composite membranes helped us to interpret their performance during fuel cell operation.
The results presented in this study illustrated the difficulty to elaborate better membranes than Nafion or PFSA for new generations of PEMFC systems able to work at high temperature and under low humidity conditions.

Finally, the experimental results presented during this thesis work can be used in studies involving water transport, water management and durability, especially for numerical simulation or modelling. More fundamentally, they can help understanding the thermodynamics of sorption and transport phenomena in PFSA membranes

References

[1] Rieke, P. and Vanderborgh, N., Temperature dependence of water content and proton conductivity in polyperfluorosulfonic acid membranes, *Journal of Membrane Science*, Vol. 32, No. 2-3, 1987, pp. 313–328.

[2] Broka, K. and Ekdunge, P., Oxygen and hydrogen permeation properties and water uptake of Nafion® 117 membrane and recast film for PEM fuel cell, *Journal of Applied Electrochemistry*, Vol. 27, 1997, pp. 117–123.

[3] Takata, H., Mizuno, N., Nishikawa, M., Fukada, S., and Yoshitake, M., Adsorption properties of water vapor on sulfonated perfluoropolymer membranes, *International Journal of Hydrogen Energy*, Vol. 32, No. 3, 2007, pp. 371–379.

[4] Maldonado, L., Perrin, J.-C., Dillet, J., and Lottin, O., Characterization of polymer electrolyte Nafion membranes: Influence of temperature, heat treatment and drying protocol on sorption and transport properties, *Journal of Membrane Science*, Vol. 389, No. 0, 2012, pp. 43–56.

[5] Morris, D. R. and Sun, X., Water-sorption and transport properties of Nafion 117 H, *Journal of Applied Polymer Science*, Vol. 50, No. 8, 1993, pp. 1445–1452.

[6] Jalani, N. and Datta, R., The effect of equivalent weight, temperature, cationic forms, sorbates, and nanoinorganic additives on the sorption behavior of Nafion®, *Journal of Membrane Science*, Vol. 264, No. 1-2, 2005, pp. 167–175.

[7] Jalani, N., Choi, P., and Datta, R., TEOM: A novel technique for investigating sorption in proton-exchange membranes, *Journal of Membrane Science*, Vol. 254, No. 1-2, 2005, pp. 31–38.

[8] Collette, F. M., Thominette, F., Escribano, S., Ravachol, A., Morin, A., and Gebel, G., Fuel cell rejuvenation of hygrothermally aged Nafion®, *Journal of Power Sources*, Vol. 202, 2012, pp. 126–133.

Abstract

The overall aim of this PhD thesis was to characterize the properties of commercial Nafion N115 and Nafion NRE212 membranes in term of water sorption, transport, and mechanical properties over a wide range of experimental conditions. Because of the high dispersion of the data in the literature, our primary objective was to gather a comprehensive set of experimental measurements and to compare them with published results. Simple and reproducible protocols allowed us to measure the membrane properties over a wide range of experimental conditions and to study the influence of certain parameters on their evolution. For example, the samples were heat-treated at different temperatures and the effect of thermal history on water sorption, transport and mechanical properties was investigated. Nafion membranes were also exposed to moderate temperature (60°C – 80°C) and constant relative humidity (RH = 0.3 to 0.95) for long periods of time, which is known to cause a so-called "hygrothermal aging" resulting in a decrease in their sorption capacity and proton conductivity. Such effects were observed but they appeared to be reversible and without noticeable consequences in term of fuel cell performance.
Our experimental results can be used in studies involving water transport, water management and durability of fuel cells, especially for numerical simulation or modelling. More fundamentally, they can help understanding the thermodynamics of sorption and transport phenomena in PFSA membranes.

Keywords
Nafion, pre-treatment, thermal history, sorption, proton conductivity, water diffusion, Young modulus, temperature, relative humidity, fuel cell, PEMFC.

Résumé

L'objectif général de cette thèse de doctorat est de caractériser les propriétés de membranes PFSA de type Nafion N115 et Nafion NRE212 en termes de sorption d'eau, de propriétés de transport et de propriétés mécaniques, sur une large gamme de conditions expérimentales. Nous avons réalisé de très nombreuses mesures afin de comparer les résultats avec les données de la littérature, souvent dispersées. Des protocoles simples et reproductibles nous ont permis de mesurer les propriétés des membranes et d'étudier l'influence de certains paramètres sur leur variation. Les échantillons ont par exemple été séchés à différentes températures et nous avons étudié l'effet de ce prétraitement thermique sur la capacité de sorption, les propriétés de transport et les propriétés mécaniques. Les membranes Nafion ont également été exposées à une température modérée (60°C – 80°C) et à une humidité relative constante (RH = 0.3 à 0.95) pendant plusieurs semaines, conditions à l'origine d'un phénomène dit de "vieillissement hygrothermique" qui affecte leur capacité de sorption et leur conductivité protonique. De tels effets ont été observés mais ils se sont révélés réversibles et sans conséquences notables en terme de performances une fois les membranes utilisées en pile à combustible.
Nos résultats peuvent être utilisés dans des études impliquant le transport et la gestion de l'eau dans les piles à combustible ainsi que leur durabilité, en particulier pour de la simulation numérique ou de la modélisation. Plus fondamentalement, ils peuvent aider à comprendre la thermodynamique de sorption et les phénomènes de transport dans les membranes PFSA.

Mots-clés
Nafion, prétraitement, mémoire thermique, sorption, conductivité protonique, diffusion de l'eau, module d'Young, température, humidité relative, piles à combustible, PEMFC.